The Dissertation Committee for Lisa Lyn Malachowski Certifies that this is the approved version of the following dissertation:

Investigation of Immobilized Biopolymers for Metal Binding

Committee:

James A. Holcombe, Supervisor

Jennifer S. Brodbelt

Karen S. Browning

Howard M. Liljestrand

John T. McDevitt

Investigation of Immobilized Biopolymers for Metal Binding

by

Lisa Lyn Malachowski, B.S.

Dissertation

Presented to the Faculty of the Graduate School of

The University of Texas at Austin

in Partial Fulfillment

of the Requirements

for the Degree of

Doctor of Philosophy

The University of Texas at Austin

August, 2004

Dedication

To my parents, for teaching me that I can accomplish anything I put my mind to and to Casey, Cortney and Ann Lea so they know that they can too.

Acknowledgements

First off, I would like to express my gratitude to Dr. James A. Holcombe for his leadership, guidance, and especially his patience. His constant demand for the best from his students helped me develop into a better scientist.

I would also like to acknowledge several past and present Holcombe group members. A special thanks goes to Thomasin Miller, Ph.D. for getting me started and for always being available to answer my questions (even when it meant going back through those old lab notebooks.) Tommi, along with George Havrilla of Los Alamos National Labs, also provided the background research and collaboration on the combinatorial chemistry project. Thanks to Jacqueline Stair for collaborating on the literature review, Thomas Kreschollek for his electronics expertise and his assistance in designing the bubble meter (where were you when I electrocuted myself?) and to Bill Balsanek for his help with the ICP. Thanks to Ashley Johnson for being such a good friend and understanding my frustrations during the job search. Thanks to Gulay (our crazy Turk) for coming back to work here and bringing new energy and ideas to the lab. Also, thanks to the rest of the Holcombe group, Brianna, Carina, John, and Nikhilesh for being such supportive group members.

Finally, my family and friends deserve special recognition. Thanks to my mom and dad, my grandparents and Jill and Mike for being such an amazing family and for

their love and support over the years; to Heidi, Karen and Ann for the great conversations and everlasting friendship; and to Brent for his unconditional love and for making these past four years so amazing. Each of them always had the faith that I could do this, even when I didn't. They all supplied endless amounts of encouragement and I will always be grateful to them for that.

Investigation of Immobilized Biopolymers for Metal Binding

Publication No._____

Lisa Lyn Malachowski, Ph.D.

The University of Texas at Austin, 2004

Supervisor: James A. Holcombe

This research focuses on the utility of immobilized poly amino acids for metal remediation and preconcentration. The biohomopolymer poly-L-histidine (PLHis) was immobilized onto controlled pore glass (CPG) and its metal binding capabilities evaluated through the use of a flow injection analysis - flame atomic absorption system (FIA-FAAS). The metal binding capability of PLHis-CPG was determined through the analysis of the generated breakthrough curves. The polymer likely coordinates cationic metals through the imidazole side chain ($pK_a \approx 6$) present on each histidine residue with both strong and weak binding sites for Cu^{2+}, Cd^{2+}, Co^{2+}, and Ni^{2+}. It has also been shown that the protonated imidazole side chain present in acidic conditions is capable of binding metal oxyanions such as chromates, arsenates, and selenites; although oxyanion binding currently exhibits interferences from competing anions in solution, such as sulfate and nitrate.

Poly-L-Aspartic Acid (PLAsp) and Poly-L-Glutamic Acid (PLGlu) were also individually immobilized onto controlled pore glass (CPG) and compared using their

metal binding capabilities. Elemental combustion analysis was used to yield polymer coverage approximations. Formation constants and site capacities of both polymers for Cd^{2+} were determined through equilibrium and breakthrough studies. Additionally, the metal selectivity of PLAsp and PLGlu was evaluated when breakthrough curves were run with several metals present in solution at one time. Both polymers exhibited similar binding trends and binding strengths for all of the metals studied. This likely reflects the absence of a predetermined tertiary structure of the polymers on the surface and the relatively high residue-per-metal ratio (~20:1), which places less stringent requirements on the steric hindrance between the side chains and the resultant "wrapping" of the peptide around the metal.

Initial attempts at determining formation constants of PLAsp and PLGlu through competitive binding experiments with either EDTA or oxalate present were unsuccessful due to complications caused by the current immobilization procedure. Therefore, alternate immobilization procedures were investigated utilizing an epoxide linker. These methods eliminate the formation of an amine functionality on the surface.

Additionally, a combinatorial approach was used in an attempt to elucidate an optimal copolymer primary structure for successful binding of a target metal. This approach included screening the library for successful binding with micro x-ray fluorescence (MXRF) and obtaining the sequence of the successful copolymer through Edman Degradation.

A considerable amount of the metal binding experiments conducted in this research used the analysis of breakthrough curves generated through flow injection-flame atomic absorption spectrometry. Solution flow rate is a critical parameter in

breakthrough analysis. Due to the absence of an inexpensive, on-line flow meter for flow injection analysis systems, an electronic flow meter was constructed to measure the flow rate during the FIAAS measurements. Thus, flow rates can be measured while collecting breakthrough data, and continuous monitoring of flow rates is possible.

Table of Contents

List of Tables

List of Figures

Chapter 1: Introduction

1.1 HEAVY METALS IN THE ENVIRONMENT

Heavy metals are introduced into the environment through a number of industrial processes [1]. Depending on the chemical form and exposure level; heavy metals can potentially be very harmful to humans and have a negative impact on the environment (Table 1.1).

Table 1.1 Maximum Contaminant Level (MCL) of Various Metal Contaminants in Water [2]

Metal	MCL (mg/L)	Potential Health Effects from Ingestion of Water	Source of Contamination (man-made)
As	0.01	Skin damage Problems with circulatory systems Increased risk of getting cancer	Erosion of natural deposits; runoff from glass & electronics production wastes
Cd	0.005	Kidney damage	Corrosion of galvanized pipes; erosion of natural deposits; batteries and paints
Cr	0.1	Allergic dermatitis	Discharge from steel and pulp mills; erosion of natural deposits
Cu	1.3	Short term exposure: Gastrointestinal distress Long term exposure: Liver or kidney damage	Corrosion of household plumbing systems; erosion of natural deposits
Hg Inorganic	0.002	Kidney damage	Erosion of natural deposits; discharge from refineries and factories; runoff from landfills and cropland
Pb	0.015	Infants and children: Delays in physical or mental development Adults: Kidney problems; high blood pressure	Corrosion of household plumbing systems; erosion of natural deposits
Se	0.05	Hair or fingernail loss; numbness in fingers or toes; circulatory problems	Discharge from petroleum refineries; erosion of natural deposits; discharge from mines

Unlike organic pollutants, metal contamination is exacerbated by the fact that metals are a non-degradable, recirculating contaminant and accumulate in the environment [3, 4]. As a direct result of this fact, it is necessary to remediate heavily contaminated sites. This can only be accomplished by isolation and recovery of heavy metals since degradation is not an option. As a first attempt at remediation, bulk techniques, such as simple filtration or precipitation are often utilized [3, 5]. Although these techniques are useful in removing a significant fraction of the contaminant, they are unable to reduce the contaminant levels to meet environmental agency regulations for many of the more toxic metals. As a result, a polishing or finishing step must be employed. This finishing step is often in the form of a chemical extraction. The ideal metal extraction and reclamation technique must have the following attributes:

Selectivity – binding only to the metal of interest, thus allowing for separation from metals that are harmless or beneficial that could overwhelm the available binding sites and significantly reduce the efficiency or capacity of the extracting media.

Strong binding – necessary if effective removal from contaminated areas to an allowable level is to be realized.

Easy release – allowing for efficient preconcentration of the contaminant and rejuvenation or reuse of the media.

Environmental innocuity – preventing further contamination when the media is ultimately discarded.

Stability – ability to be reused with an extended lifetime, ensuring cost effectiveness.

In many instances, the attributes sited for remediation are identical to those desired if preconcentration methodologies are sought as a means of assisting analytical detection methods. With the need to establish concentration levels in the low to sub-ppb levels, validation of the remediation procedure requires sensitive analytical tools. While techniques exist for all regulated contaminant levels, many labs must resort to less sensitive instrumental capabilities and must employ preconcentration tools to detect regulatory levels.

1.2 CURRENT TECHNOLOGY

Currently, the most common chemical modes of metal removal include ion exchangers or removal by chelation with synthetic crown ethers or other macrocylic cage molecules (e.g., [6-10]). The most significant drawback associated with typical ion exchangers is the lack of selectivity in metal binding and/or weak binding characteristics. While crown ethers are both selective and strong binders, due to polydentate chelation within a sized cavity, they often exhibit slow release kinetics [6]. This is a potential problem when metal reclamation is required. In addition, many crown ethers are also very toxic, so using them may simply add to the problem of contamination.

1.3 THE USE OF NATURAL SYSTEMS IN METALS REMEDIATION

As a result of the inherent problems with most of the current metal remediation strategies, researchers are now turning toward natural systems. Phytoremediation is a

very actively pursued and effective approach to remediation for both natural waters and soils (e.g., [11-14]). Similarly, the use of immobilized unicellular algae and other micro-organisms in metal preconcentration and remediation has a long history with encouraging results (e.g., [15-21]). The likely source of binding in these unicellular organisms are the chemicals that make up the organism. While these can range in character from simple cellulose to more elaborate proteins, isolation of these particular biocompounds and direct utilization of only those cellular components that are directly involved in metal binding is an interesting approach. In fact, the potential utility of amino acids, peptides and proteins that have been immobilized on a substrate for general use in column applications has been investigated.

1.3.1 Metallothioneins

A well known class of metal binding proteins, the metallothioneins, is an example of such biomolecules that are characterized as having a high degree of metal binding specificity and have been isolated in a wide variety of organisms (e.g., [22-25]). Their strong binding characteristics and selectivity seem to fit the criteria of the ideal metal chelator. Upon immobilization these proteins seemed to lose their metal binding capabilities outside of the pristine cellular environment where they typically function in nature [26]. In this particular instance, closer examination of several metallothioneins showed that their sequences contained a significantly high percentage of cysteine residues and that sulfhydryl groups present on these residues are primarily responsible for metal binding [24, 25]. This suggests the possibility of using simpler amino acid chains or synthetic peptides (e.g., poly-amino acids) as metal binding alternatives to natural

peptides. Considering only the natural set of amino acids, one can readily recognize a variety of functionalities that could serve as coordination sites for metal chelation. Using amino acids as building blocks with their various side chains and recognizing that peptides are simple polymers of these units using a common amide linkage, a wide variety of interesting chelators could be envisioned. More specifically, these chelators may exhibit the desired characteristics of specificity and have the added side benefit of being non-toxic when discarded.

1.3.2 Amino Acids and Short Peptides

Significant research has been conducted in the areas of metal binding by immobilized amino acids as well as short chain polypeptides. In some instances the incorporation of amino acids into short polymeric chains or evaluation of anionic compounds have also been investigated. A brief review of these studies is the focus of the following discussion. Figure 1.1 shows selected amino acids from the standard set of 21 that are relevant to these studies.

Figure 1.1 Amino acids utilized in metal binding studies

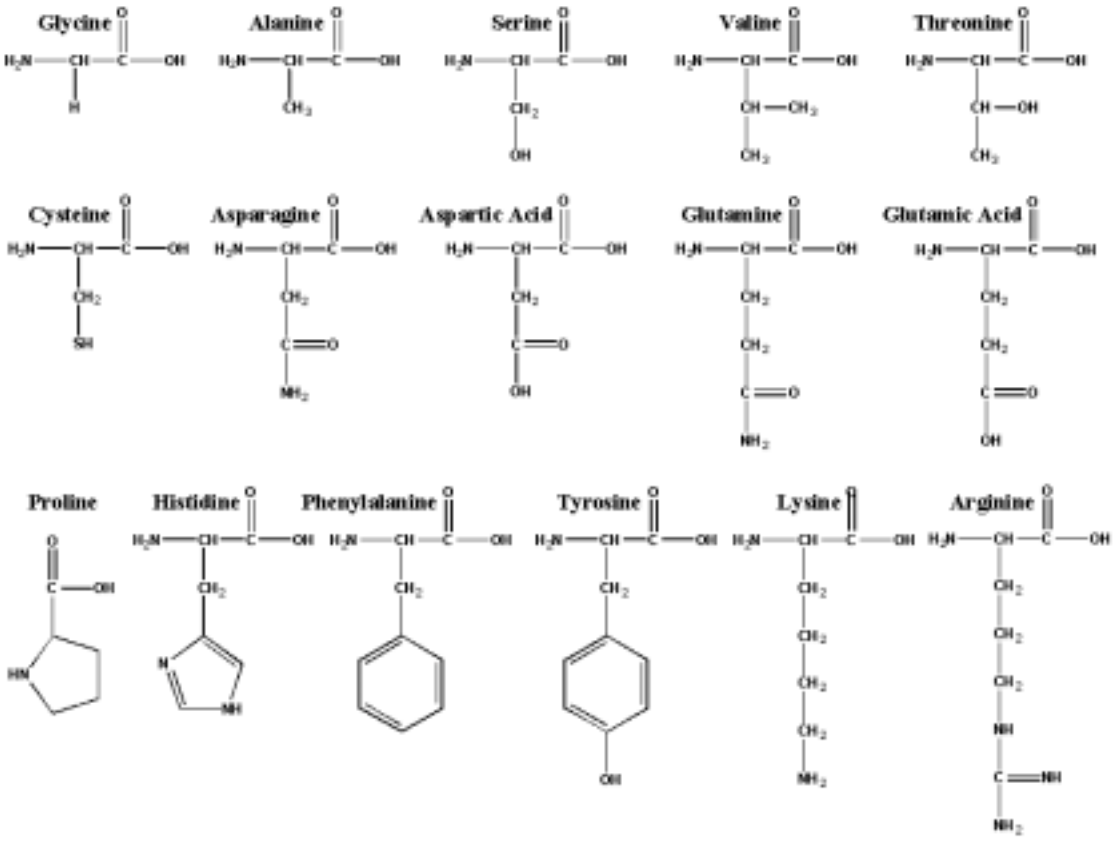

1.3.2.1 Single Amino Acids

As mentioned previously, cysteine (Cys) is a major component of a group of metal binding proteins, called metallothioneins [24]. As a result, researchers have investigated Cys immobilized onto a solid support for use as a metal chelator. Elmahadi and Greenway utilized Cys immobilized onto silanized controlled pore glass (CPG) through a gluteraldehyde linker for preconcentration of Cd^{2+}, Co^{2+}, Cu^{2+}, Hg^{2+}, Pb^{2+} and Zn^{2+} [27]. Capacities for these metals were determined through breakthrough curve

analysis and calculated at 12.48, 5.50, 7.86, 6.06, 11.66 and 7.88 mmol of metal/g of dry resin, respectively

Denizli and coworkers [28, 29] and Disbudak et al. [30] also utilized immobilized Cys for metal preconcentration and remediation. In each of these studies 2-methacryloylamindocysteine (MAC) was allowed to react with 2-hydroxyethylmethacrylate (HEMA) in an aqueous medium. The product was spherical beads, with an average size of 150 – 200 μm, of poly(2-dyroxyehylmethacrylate – methacryloylamidocysteine), [p(HEMA-MAC)]. The beads were characterized according to their swelling ratio, FTIR analysis and elemental analysis. The spectroscopic studies were conducted in the absence of metal to characterize the beads and confirm the incorporation of MAC, not to study the metal binding characteristics. In separate studies, binding characteristics were determined for As^{3+}, Cd^{2+}, Cr^{3+}, Cu^{2+}, Hg^{2+} and Pb^{2+}; and it was shown that while the pHEMA beads exhibited negligible Cd^{2+} binding, p(HEMA-MAC) beads exhibited significant Cd^{2+} capacity. The microbeads can be regenerated with an acidic solution.

Several studies have been conducted using glycine (Gly) residues supported on various crosslinked resins. George and coworkers [31], and Vinodkumar and Matthew [32] studied the metal binding capabilities and the effects of the degree of crosslinking on metal uptake using polyacrylamide crosslinked with N,N'-methylene-bis-acrylamide (NNMBA) with supported Gly. Gly was incorporated into the resin by transamidation using a solution containing an excess of the sodium salt of glycine. The metals studied include Co^{2+}, Cu^{2+}, Fe^{2+}, Fe^{3+}, Ni^{2+} and Zn^{2+}. Metal binding increased with an increase in crosslinking, until 8% crosslinking and then decreased. Interestingly, the metal

desorbed resins showed specificity toward the previously desorbed metal over other metals. This was attributed to "pockets" left by the desorbed metal or the "memory" of the ligand for the metal.

George et al. also studied the metal binding ability of divinylbenzene (DVB)-crosslinked polyacrylamide supported Gly toward Co^{2+}, Cu^{2+}, Ni^{2+} and Zn^{2+} [33]. Once again, Gly residues were introduced through transamidation with Gly. Interestingly, as the degree of crosslinking increases from 2-20%, the metal complexation decreases due to a decrease in the available carboxylate ligands for metal binding with an increase in DVB content. The resin does show enhanced specificity toward the desorbed metal over other metals in subsequent runs, and the time for rebinding of the desorbed metal is significantly less for rebinding than it is for initial binding as seen with the NNMBA crosslinked resin.

Finally, George et al. directly compared the metal-ion complexation characteristics between Gly functionalities supported on DVB-crosslinked polyacrylamide and NNMBA-crosslinked poylacrylamide toward Co^{2+}, Cu^{2+}, Ni^{2+} and Zn^{2+} [34]. DVB was chosen because it is more rigid and hydrophobic than NNMBA. The NNMBA-crosslinked polyacrylamide was shown to be more effective at metal complexation than the DVB-crosslinked resin while DVB showed increased selectivity over NNMBA. Again, metal rebinding is much faster and more specific than initial binding on both resins. Each of these resins can be regenerated by acid washing and reused.

In a procedure similar to that described previously by Denizli [28, 29] and Disbudak [30], Say et al. prepared poly(hydroxyethyl methacrylate-*co*-

methacrylamidohistidine) p(HEMA-*co*-MAH) beads for metal complexation [35]. Again, these beads were fully characterized without metals bound by swelling studies, FTIR and elemental analysis of the bead. In additional experiments, the metal binding affinity was demonstrated to be $Cu^{2+} > Cr^{3+} > Hg^{2+} > Pb^{2+} > Cd^{2+}$ and the beads could be easily regenerated with 0.1M HNO_3.

In an attempt to prepare a novel molecular imprinted adsorbent to remove heavy metals, Say et al. synthesized Cu^{2+} – imprinted poly(ethylene glycol dimethacrylate-methacryloylamidohistidine/Cu^{2+} (poly(EGDMA-MAH/Cu^{2+}) microbeads by dispersion polymerization of EGDMA and MAH/Cu^{2+} [36]. After removal of the Cu^{2+}, these beads exhibited a maximum Cu^{2+} capacity of 48 mg of Cu^{2+}/g of support and excellent selectivity of Cu^{2+} over Zn^{2+}, Ni^{2+} and Co^{2+}. Metal binding exhibited a strong dependence on pH, with increased binding at increased pH. Cu^{2+} was easily desorbed with EDTA, and the beads were reusable without a significant loss in capacity.

Phenylalanine (Phe) has also been immobilized onto spherical macroreticular styrene-divinylbenzene beads to create a chelating resin [37]. This resin was capable of separating Cu^{2+} from Co^{2+} and Ni^{2+}. Co^{2+} and Ni^{2+} are not retained on the column at pH 3 while copper is and can be eluted with 1 M HCl. The beads are also capable of removing Cu^{2+} from seawater.

1.3.2.2 Immobilized Poly-Amino Acids on Silica Supports

In addition to single amino acids, poly-amino acids and peptides have been immobilized onto solid supports for use in metal chelating systems. Jurbergs and Holcombe attached poly-L-cysteine (PLCys) (n~50 residues) to CPG via a procedure

described by Masoom and Townshend [38] and characterized PLCys according to its Cd^{2+} binding capabilities [39]. Using breakthrough analysis, it was determined that PLCys was an effective chelator for Cd^{2+}. Through competitive binding studies using ethylenediaminetetraacetate (EDTA) and ethylenediamine (en) as competing ligands, conditional stability constants were calculated at 10^{13} for the very strong binding sites, $10^{9} – 10^{11}$ for the strong binding sites and 10^{6} for the intermediate sites. Although there is very strong binding, the metal can be quantitatively recovered using 0.1M HNO_3, making the column fully regenerable and reusable. A study of Cd^{2+} capacity at various pH's revealed that the affinity of PLCys for Cd^{2+} had a significant dependence on pH. There was very little binding in acidic pHs and binding increased as pH increased. They postulated that at elevated pHs the PLCys is more hydrophilic due to the sulfhydryl groups being deprotonated. As a result, the peptide chain would be unfolded due to increased hydration from ion-dipole interactions and the side chains may be more accessible in an unfolded peptide, thus leading to an increase in metal binding capacity. They were also able to determine that the metal binding of PLCys may be mass transport limited since they observed the Cd^{2+} capacity increase as the solution flow rate was decreased. Various concentrations of hard acid metals in the influent stream (e.g., alkali and alkaline earth metals, Co^{2+} and Ni^{2+}) had very little effect on PLCys - Cd^{2+} binding.

Later, a comparison of the metal binding capabilities of PLCys (n~50 residues) and 8-hydroxyquinoline (8HQ), both immobilized onto CPG, was conducted [40]. Once again using breakthrough analysis in metal capacity determination, PLCys showed more selectivity against harder acid metals than 8HQ. While 8HQ strongly complexes a broad range of metals (Cd^{2+}, Co^{2+}, Cu^{2+}, Ni^{2+} and Pb^{2+}), PLCys isolated soft acid metals such as

Cd^{2+} and Pb^{2+} and had very little affinity for Co^{2+} or Ni^{2+}. Thus, they reasoned that PLCys should be efficient in isolating many of the heavy metals from complex matrices containing hard acid metals. The conditional stability constants, again determined through competitive binding studies with EDTA and en, agreed with the previously reported values reported by Jurbergs and Holcombe [39].

In the process of studying various supports, Miller and Holcombe evaluated Cys immobilized on porous carbon, a more inexpensive support [41]. Both PLCys (n~50 residues) and the Cys monomer were tethered to Carbopack™-X, a commercially available porous carbon, by derivitizing the carbon with carboxylate functionalities by acid activation and linking the PLCys or Cys through the use of 1-ethyl-3-[3-(dimethylamino)propyl]carbodiimide (EDC). Breakthrough analysis and competitive binding studies demonstrated that porous carbon is an effective support for immobilized ligands. In fact, the capacities for all metals tested were consistently higher on the porous carbon than on CPG. It is suggested that this may be due to the immobilization efficiency. The immobilization procedure is much simpler for porous carbon than for CPG, possibility resulting in greater coverage of the polymer onto the support. Conditional stability constants were in good agreement with previous work done on CPG.

Gutierrez et al. used the same approach as Jurbergs and Holcombe [39] by attaching poly-L-aspartic acid (PLAsp) (n~50 residues) to CPG to test its metal binding capabilities [42]. The binding affinity of PLAsp is $Cu^{2+} > La^{3+} \approx Ce^{3+} \approx Eu^{3+} > Pb^{2+} > Cd^{2+} > Ni^{2+} > Co^{2+} > Mn^{2+} > Ca^{2+} > Na^{2+}$, which is somewhat complimentary to PLCys and consistent with carboxylate functionality complexing [43].

In an attempt to find a cheaper alternative to PLAsp, Miller et al. compared immobilized PLAsp to immobilized poly-acrylic acid (PAA), a synthetic polymer [44]. The results for PLAsp-CPG are similar to those reported above. Additionally, metal binding was measured as a function of pH, and capacity again decreased with a decrease in pH due to protonation of the carboxylates and possible conformational changes at low pH (ca. <pH=4) for PLAsp-CPG. Stability studies show that PLAsp-CPG exhibited minimal loss of capacity upon exposure to 0.05M ammonium acetate buffer, 5% H_2O_2, and elevated temperature (60°C).

Miller and Holcombe also studied gold as a support for PLAsp [45]. Gold was chosen because it acts as an inert surface, acting only as an anchor for the polymer and remaining unreactive toward the metals in solution. The gold used initially was in the form of gold transmission electron microscopy (TEM) grids that were stacked in a microcolumn with thin PTFE spacers between each grid to promote mixing and flow. The immobilization of the polymer was conducted on-line with an FI system, using a modification of a procedure described by Leggett [46]. The metal binding trend remained the same as for PLAsp on CPG but the capacities were considerably higher for the PLAsp on gold for all of the metals studied: Al^{3+}, Ce^{3+}, Cu^{2+}, Eu^{3+}, Fe^{3+} and La^{3+}. This is possibly due to a more efficient immobilization procedure. The same authors also attempted to employ gold coated CPG substrates for immobilization prepared by electroless coating techniques, but the results were not encouraging due to patchy gold coverage and possible pore blockage by the deposited gold [47].

1.3.2.3 Membrane Immobilized Poly-Amino Acids

In addition to silica, gold and carbon, poly-amino acids have also been immobilized onto membranes. Membrane technology is very well developed in the area of separations and remediation (e.g., [48-50]). Often used in the passive separation of contaminants from solution, popular membrane technologies include reverse osmosis, nanofiltration and ultrafiltration. In heavy metal sorption, the membrane is often functionalized with a metal chelating group such as iminodiacetate, amidoxime, phosphoric acid or sulfonic/carboxylic groups to facilitate metal removal [51-58]. Thus, the membrane serves as a support for the metal binding material and with the attachment of these groups the membrane can be tuned to exclude specific solutes.

Recently, researchers have investigated the attachment of amino acids and poly-amino acids to membrane surfaces for metal extraction purposes. For example, Bhattacharyya and coworkers attached poly-L-glutamic acid (PLGlu) (n~93 residues) to several different microfiltration membranes (both silica and cellulose-based) to study the heavy metal sorption characteristics [59]. The polymer was attached to the membranes through an aldehyde functional group on the surface of the membrane. It was shown that the PLGlu functionalized membrane is capable of binding heavy metals with the affinity following the order of $Pb^{2+} \geq Cu^{2+} > Ni^{2+} \approx Cd^{2+}$. The membrane also exhibited preferential binding of Pb^{2+} and Ni^{2+} over Ca^{2+}. The binding characteristics were dependant upon the type of membrane used, the degree of PLGlu functionalization, pH, and metals present.

Poly-D-aspartic acid (PDAsp) and poly-L-aspartic acid (PLAsp) have also been successfully immobilized onto both cellulose and silica based microfiltration membranes [60]. These functionalized membranes show capacities for Cu^{2+}, Cd^{2+} and Pb^{2+} that are consistently higher than conventional ion exchange and chelation resins, in the range of mmol of metal/g of sorbant. Not unexpectedly, little difference was seen in the performance in PDAsp and PLAsp. Ritchie and coworkers outlined the three primary mechanisms for metal sorption to include ion exchange, chelation and electrostatic interactions [60]. Due to the polymeric nature of these ligands attached to a membrane, electrostatic interactions take the form of counterion condensation. Condensation zone binding is an important factor in the increase in binding capacity of functionalized membranes over conventional ion exchange systems due to the high charge density within the membrane pores.

In similar studies, Hestekin et al. show the differences that result from PLGlu and PLAsp bound to either pure cellulose or cellulose acetate based membranes [61]. Counterion condensation was more closely evaluated and a continuous flow system was employed with the membrane system. Results indicate that pure cellulose membranes with a higher surface area provide more aldehyde linkage groups for greater polymer attachment and that counterion condensation is an important mechanism for metal ion sorption in membrane systems.

Ritchie et al. have also immobilized PLCys onto both silica and cellulose based membranes and evaluated it according to its metal binding capabilities. PLCys was shown to be an effective chelator for heavy metals such as Hg^{2+}, Pb^{2+}, and Cd^{2+} [62]. Other parameters examined in this study included the efficiency of PLCys deprotection,

the efficiency of PLCys functionalization, effects of flow rate and metal concentration, and the effects of the presence of mercury counterions on PLCys metal binding. Also investigated was the metal selectivity of membrane immobilized PLGlu in the presence of a multi-metal solution containing both Cd^{2+} and Pb^{2+}.

Denizli et al. synthesized a poly (2-hydroxyethylmethacrylate-co-methacrylamindophenylalanine) membrane for copper adsorption [63, 64]. The membranes were prepared through UV-initiated photopolymerization of 2-methacrylamidophenylalanine (MAPA) and 2-hydroxyethylmethacrylate (HEMA) with azobisisobutyronitrile present as an initiator. Characterization of this membrane revealed the order of metal affinity to be $Hg^{2+} > Ni^{2+} > Cu^{2+}$, with metal adsorption increasing with increased pH, leveling off at pH 5.0. The capacities of these membranes were reported as mmol of metal/m^2 of membrane. The membranes can be regenerated with 0.1M HNO_3 and reused without significant loss of capacity.

Researchers have also attached phenylalanine (Phe) to a polyethylene membrane, in the form of a hollow fiber, through radiation-induced graft polymerization [65]. The attachment of the polymer was conducted using two different reaction schemes in an effort to determine which method would produce the highest density of functional groups. The first method involved grafting glycidyl methacrylate (GMA) to the fiber and then coupling the Phe to the GMA. The second method involved attaching the Phe to the GMA first and then grafting the Phe-GMA to the fiber. Although the fiber was not fully characterized for metal binding capacity, the Cu^{2+} binding along the cross section was monitored and a uniform distribution of Cu^{2+} through the fiber was found. This demonstrated a homogeneous distribution of Phe through the fiber. It was also concluded

that the second reaction scheme (grafting the Phe-GMA complex to the fiber) occurred at a rate 180-fold less than grafting the GMA alone. The preliminary results from this study indicate that with further investigation, this technology may be applicable to heavy metal remediation.

1.3.2.4 Immobilized Peptides

Peptides and short chains of amino acids have also been immobilized for metal extraction. Terashima et al. immobilized a fusion protein synthesized from maltose binding protein (pmal) and human metallothionein (MT) onto Chitopearl resin [66]. This resin was evaluated for its Cd^{2+} and Ga^{2+} binding capabilities. Interestingly, the optimal pH for Cd^{2+} binding was determined to be 5.2 while for Ga^{2+} it was 6.5. Based on the hard and soft acid-base theory and the analysis of the adsorption isotherms of these metals, the results indicate that the cysteine residues of the MT moiety of the immobilized protein are responsible for Cd^{2+} binding. Other negatively charged residues such as Asp, Glu, lysine (Lys), serine (Ser), threonine (Thr), glutamine (Gln) and asparagines (Asn) bind Ga^{2+}. As a result of this strong metal binding dependence on pH, this system can distinguish between these two metals.

Another class of metal binding proteins, synthetic phytochelatins, has shown improved Cd^{2+} binding over metallothioneins [67]. Xu et al. used a novel approach by attaching a cellulose-binding domain (CBD) to a synthetic phytochelatin (EC20). The CBD attached itself to a cellulose support thus immobilizing the phytochelatin [68]. Upon addition of Cd^{2+} the CBD-EC20 membrane bound the metal at a ratio of ~10 Cd^{2+}/ immobilized CBD-EC20 while the membrane with only the CBD attached did not bind

any Cd^{2+}. Upon addition of EDTA, Cd^{2+} was removed and the membrane capacity was restored.

1.3.2.5 Immobilized Amino Acid for use in Ion-Exchange Chromatography

In contrast to remediation applications where it is desirable to have extremely strong binding, other applications have interest in moderate binding so that the substrate can be used in chromatographic separations via partitioning. Single amino acids immobilized onto silica surfaces have been used extensively for ligand-exchange [69], metal chelation [70] and affinity chromatography [71]. The use of these materials for ion-exchange chromatography has not been as widely explored. Amino acids by nature are zwitterions, meaning they posses both positively and negatively charged sites. Zwitterion-exchangers are of particular interest as new stationary phases for high performance liquid chromatography (HPLC) as they may separate both anionic and cationic species in a single solution. These materials also show increases in mass transport and ion selectivity. Attachment of amino acids to silica is a simple way to achieve a variety of zwitterionic stationary phases.

In the last decade, research in this area has been advanced by Nesterenko [72] who initially explored L-hydroxyproline (Hypro) bonded silica as an anion-exchange material. The amino acid was attached to silica particles through the secondary amine via 3-glycidoxypropyltriethoxysilane. Separation of nine anions (SCN^-, ClO_4^-, I^-, NO_3^-, Br^-, Cl^-, IO_3^-, $H_2PO_4^-$ and NO_2^-) was observed at pH 3.13 with citric acid as the eluent. Significant changes in retention times were observed for different eluents and small adjustments in pH.

Nesterenko expanded his investigations using L-arginine (Arg), L-valine (Val), L-tryrosine (Tyr), L-proline (Pro) and Hypro [73-75]. Amino acids were again attached to the silica through the N-terminus and the ligands acid-base properties were used to tune ion interactions. Cation and anion-exchange properties of each amino acid were determined in addition to varying effects of carboxylic acid eluent concentration and pH. Immobilized Pro and Hypro successfully separated 6-8 various anions in a single solution under acidic conditions. Immobilized Val and Tyr were characterized as pure cation exchangers as the secondary amine interactions with surface silanol groups make anion-ligand interactions negligible. Surprisingly, Arg was also characterized as a cation exchanger with poor separation of anions. The amine functionalities of Arg are also hindered as a result of interactions with surface silanol groups. Interactions between surface silanol groups and charged sites of the amino acid in these systems tend to dictate ion selectivity. It was postulated that the basicity of the amino groups enhances charge localization due to a change in the multilayer structure at the silica surface and ultimately establish the exchange properties of the attached amino acid. Asp and Glu, amino acids possessing additional carboxylate functionalities, were also studied [76]. Various solutes such as alkali and alkaline earth metal cations were used in the study along with six benzene derivatives for sorbent evaluation. Asp and Glu were shown to be efficient cation exchangers.

Investigations of bound amino acid-metal cation interactions (i.e., complex forming or ion-exchange) were done using Glu [77]. Glu was chosen because of the relatively stable complexes it forms with metal cations and was evaluated using alkali, alkaline earth and transition metals. Conditions such as pH, ionic strength, organic

solvent, and temperature were varied. An increase in the non-polar and also the proton accepting character of organic solvents showed marked increases in capacities and changes in the metal binding character. Also, at both high ionic strength and pH, the chelate effect was shown to prevail over ion-exchange mechanisms.

In recent studies, Kiseleva et al. examine the zwitterionic-exchange properties of commercially available silica bound poly-aspartic acid (PAsp) [78]. PAsp is attached to surface amine groups through the carboxylate functionalities and thus aligns parallel to the silica surface. The stationary phase contains neutral amide groups along with residual aminopropyl and unreacted carboxylate groups. The poly-amino acid was able to simultaneously separate anions and alkali and alkaline earth metal cations showing the utility of using zwitterionic-exchange column for both cation and anion separations. The optimal pH range for PAsp bound silica is 3.0-3.5 due to the zwitterionic character of the various surface groups.

Additionally, Liu and Sun have shown that Cys immobilized onto a polyacrylonitrile-divinylbenzene resin has a significant affinity for Ag^{+}, Hg^{2+}, Au^{3+} and Pt^{4+} with capacities in the range of 0.39 – 1.22 mmol of metal/g of resin [79]. It was also shown that the immobilized Cys resin is capable of separating these metals chromatographically. In a mixed solution Pt^{4+}, Hg^{2+} and Ag^{+} were eluted sequentially, and Au^{3+} was retained by the column and eluted off with 0.1% thiourea in 0.1 M hydrochloric acid.

These researchers also conducted a comparison of the ability of three chelating ion-exchange resins to separate Mo^{6+} and W^{6+} [80]. The three functionalities immobilized onto the polyacrylonitrile-divinylbenzene resins were thioglycollic acid

linked by 1,6-hexanediol, thioglycollic acid linked by ethylene glycol, and Cys linked by 1,6-hexanediol. The initial run of Mo^{6+} and W^{6+}, was unsuccessful in the separation. Therefore, the Cys resin was not investigated further.

1.3.2.6 Immobilized Amino Acid/Peptide for Cd^{2+} Removal from Human Plasma

Removal of heavy metals from water is certainly a significant environmental problem. If water supplies were contaminant free, heavy metal poisoning would not be a concern. Unfortunately, this is not the case and there is currently no specific affinity adsorbent treatment for Cd^{2+} poisoning [29]. Bektas and co workers immobilized cysteine onto poly(2-hydroxyehylmethacrylate) (PHEMA) microspheres. The PHEMA microspheres were synthesized from a suspension of HEMA and EGDMA [81]. They demonstrated that these microspheres were capable of binding 0.065 mmol Cd^{2+}/g of support from human plasma. Additionally, they can be reused without significant loss of capacity.

In another attempt to develop a method for removal of Cd^{2+} from human plasma Denizli et al. immobilized cysteinylhexapeptide (CysHP) to poly(2-hydroxyethyl methacrylate) beads [29]. The sequence of the hexapeptide was Lys-Cys-Thr-Cys-Cys-Ala (alanine) and it was immobilized to the beads through a monochlorotriazinyl dye ligand, Cibacron Blue F3GA. The maximum Cd^{2+} bound from human plasma onto these beads in a packed-bed column-based system was determined to be 11.8 mg of Cd^{2+}/g of support.

1.3.2.7 Related Studies

Several researchers have focused on more in-depth studies pertaining to the metal binding capabilities of these systems. These include the effects of oxidation on Cys chelation and preconcentration [82], the effects of temperature on Lys and Glu retention of cations [83], and the effects of heats of adsorption on PLAsp cation binding [84]. Additionally, a study was conducted in which atomic force microscopy was used to examine conformational changes in immobilized PLCys in various environments [85]. By measuring the height of immobilized PLCys from the surface of a glass slide, it was confirmed that in neutral solutions the polymer chain was generally oriented perpendicular to the surface. With the addition of a metal, the height decreased ca. 15 nm. The addition of acid decreased the height another 10-15 nm, thus supporting the idea that a significant tertiary structure change had occurred. At low pHs the PLCys likely exists as a tight random coil on the surface. Raising the pH returned the structure to its original form.

1.4 THE FUTURE OF IMMOBILIZED POLY AMINO ACIDS

Research involving the use of immobilized amino acids, peptides and proteins for metal remediation and similar purposes has shown great promise. Amino acids are ideal building blocks for metal chelation systems. They provide a wide range of binding functionalities and are attached to one another through simple amide linkages. These novel binders are easily attached to silica, carbon, gold and polymeric particles; silica and cellulose based membranes; and incorporated into polymerized resins. The amino acid of interest can be immobilized through either the amine or carboxylate terminus or modified

to provide other possible linkage chemistries. Studies show that immobilized amino acids, peptides, and proteins are all capable of metal capacities in the μmole – mmole / g of resin range. Much research involving the use of amino acids as zwitterion-exchange materials has also proved fruitful. In addition, metal selectivity and specificity can be achieved by altering the amino acid functionalities and/or immobilization procedures used. There are still many directions continuing research in this area could head, including the use of peptide libraries and increased metal-template studies. This dissertation focuses on further characterization of immobilized poly amino acids for metal binding in addition to the use of combinatorial chemistry for the indentification of a successful metal binding copolymer.

Chapter 2: Immobilized Poly–L–Histidine for Chelation of Metal Cations

2.1 INTRODUCTION

In recent years, the investigation into methods for the removal of metals from the environment has been a major area of research due to the health risks they pose. A significant amount of research has focused on the development of novel ion exchange systems for the remediation and preconcentration of metals from natural and industrial wastewaters. These exchangers can also be combined with flow injection analysis (FIA) and atomic spectrometry for preconcentration and monitoring. A unique class of exchangers involves the use of immobilized short chain biohomopolymers (peptides) [39, 40, 42, 44, 61, 78, 86].

Previous work with immobilized biohomopolymers used for cation exchange has demonstrated that quantitative release can be achieved by simply lowering the pH of the column [39, 40, 42, 44, 87, 88]. It was suggested [44] and later shown [85] that acid caused a reversible change in the tertiary structure to provide efficient and rapid release of the metal from the binding cavity. It was also demonstrated that these biohomopolymeric systems remain functional, with minimal loss of capacity, despite repeated exposure to harsh and varied chemical conditions over extended periods of time [44].

The amino acid histidine, as seen in Figure 2.1, has an imidazole side chain available for metal binding. Sahni et al. [89] have shown the utility of imidazole or poly-

imidazole derivatives in chelation systems. Additionally, Moreira and Gushikem used silica gel functionalized with 3(1-imidazolyl)propyl groups for preconcentration of Cu, Ni, Fe, Zn and Cd from ethanol [90]. It is also well known that histidine is one of the primary metal binding sites in proteins and that the imidazole side chain is responsible for metal complexation [91-94]. In fact, a sequence of 4 - 6 histidines is frequently utilized as a "His-tag" in protein purification on a metal column in such techniques as immobilized metal ion affinity chromatography (IMAC).

Figure 2.1 Poly-L-Histidine as present at pH > 6 (n ≈ 90 – 100)

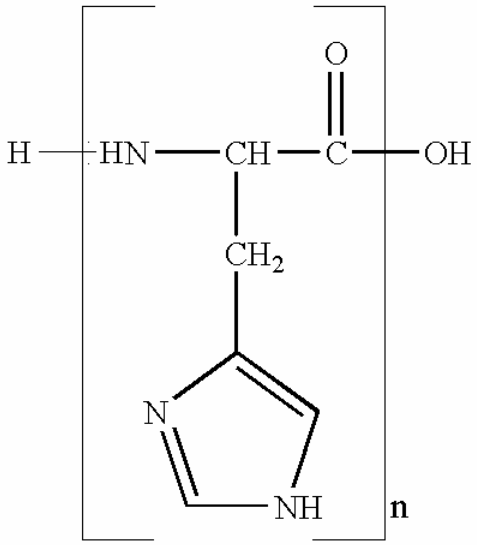

A poly-L-histidine (PLHis) (n ~90 - 100) bonded phase ion exchange system was evaluated for use in metal remediation and preconcentration of cationic metal species.

2.2 EXPERIMENTAL

2.2.1 Instrumentation

A Perkin-Elmer model 4000 atomic absorption spectrophotometer with an air/acetylene flame was used for all metal determinations. Hollow cathode lamps for the metals of interest were operated at the currents recommended by their manufacturers. Wavelengths for Ca, Cd, Co, Cu, Mg, Mn, Na, Ni and Pb were 422.7, 228.8, 240.7, 324.8, 285.2, 279.5, 589.0, 232.0 and 283.3 nm, respectively. A monochromator band-pass of 0.2 nm was used for Co, Mn and Ni, 0.4 nm for Na, and 0.7 nm for Ca, Cd, Cu, Mg and Pb.

The simple flow injection manifold, shown in Figure 2.2, consisted of an eight-roller peristaltic pump (Ismatec minicartridge MS-REGLO) and two two-way, double inlet rotary valves (Rheodyne 5020). All connections were made with 0.76 mm i.d. PTFE tubing [42].

Figure 2.2 Flow injection manifold consisting of an eight-roller peristaltic pump with two-way double inlet valves.

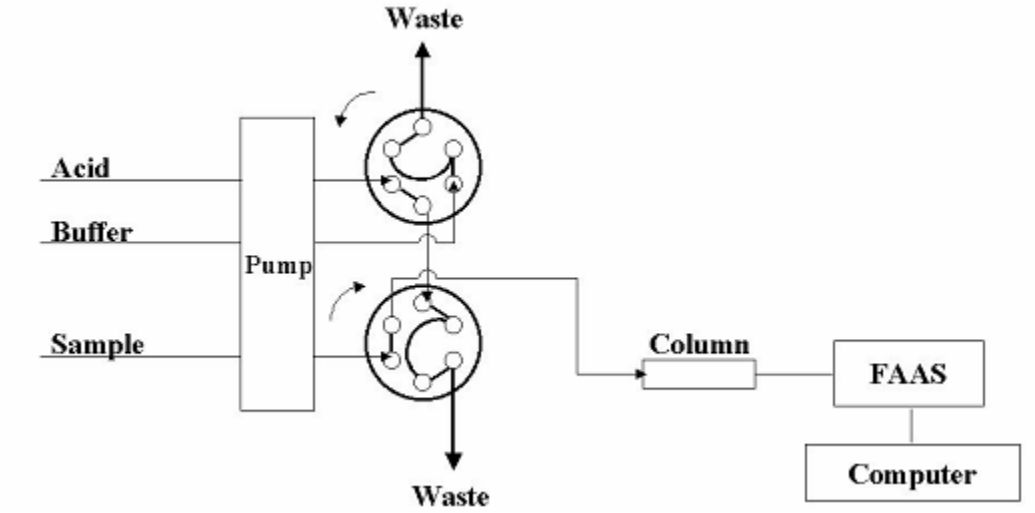

0.0727 g of immobilized PLHis-CPG was packed into a 3 mm i.d. x 25 mm long glass column with 70 mm PTFE frits (Omnifit). A Kel-F tee was placed between the column and the nebulizer to provide air compensation and to minimize noise.

2.2.2 Reagents

All chemicals were reagent grade unless noted and deionized, distilled water was used to prepare solutions. All glassware was soaked in 4 M HNO_3 overnight before use. Poly-L-Histidine (Sigma) [DP(LALLS) 104, MW(LALLS) 14,300] was used as received. The controlled pore glass (SIGMA, PG240-120) had a mean pore diameter of 22.6 nm and a mesh size of 80 - 120. Other reagents included 3-aminopropyltriethoxysilane (98%), nitric acid (Aldrich); acetic acid, sodium phosphate (Fisher Scientific); ammonium acetate, ammonium hydroxide (Mallinckrodt); gluteraldehyde (25%) (Sigma). Stock solutions of Ca^{2+} (Fisher); Cd^{2+}, Cu^{2+} and Pb^{2+} (SCP Science) atomic absorption standards were used to prepare the 10 ppm loading solutions for the metal binding experiments. For Co^{2+}, Na^{+}, Ni^{2+} (Baker), Mg^{2+}, and Mn^{2+} (Matheson, Coleman & Bell) the loading solutions were prepared from standardized solutions of the reagent grade nitrate salt. 0.5 M ammonium acetate and 0.5 M sodium acetate stock solutions were prepared and purified using a 100 - 200 mesh Chelex 100 (Bio-Rad) ion exchange column.

2.2.3 Immobilization of PLHis onto CPG

Using a modification [39] of a procedure originally described by Masoom and Townshend [38], PLHis was immobilized to the surface of the CPG as seen in Figure 2.3.

The CPG was activated by boiling ~1 g of the glass in 5% HNO_3 for 90 min. (**I**). The acid activated CPG was filtered in a medium coarse, sintered glass filter, rinsed with distilled/DI H_2O, and dried in an 80°C oven. An amine terminus was created on the surface of the glass through the use of 3-aminopropyltriethoxysilane (3-APS), a silanizing agent. The activated glass was reacted with 50 mL of 10% 3-APS, pH adjusted to pH 3.4 with HCl, at 75°C for 150 min under nitrogen (**II**). After silanization, the glass was filtered in a medium coarse, sintered glass filter, rinsed with distilled/DI H_2O, and dried in an 80°C oven. The silanization step was repeated a second time to ensure complete silanization of the glass, providing an amino terminus for linking with gluteraldehyde. Once the glass was silanized, rinsed and dried overnight at 80°C, it was allowed to react with 50 mL of 5% gluteraldehyde in a 0.01 M phosphate buffer (pH 8.0) under nitrogen for 90 min at room temperature (**III**). The gluteraldehyde serves as a linker between the amine terminus on the 3-APS and the amine terminus of the poly-amino acid. Once the gluteraldehyde was attached, the glass was filtered and rinsed with distilled/DI H_2O. 20 mg of PLHis, dissolved in 20 mL of pH 5.0, 0.01 M phosphate buffer was allowed to react with ~1 g of gluteraldehyde-CPG for 48 h at room temperature, under N_2 (**IV**). Upon completion of the immobilization the PLHis-CPG was rinsed, filtered, dried and packed in the microcolumn. The column required ca. 0.1 g of PLHis-CPG. The remainder of the PLHis-CPG was stored in a desiccator.

Figure 2.3 Immobilization procedure (**I – IV** correspond to each step of procedure as outlined in the text)

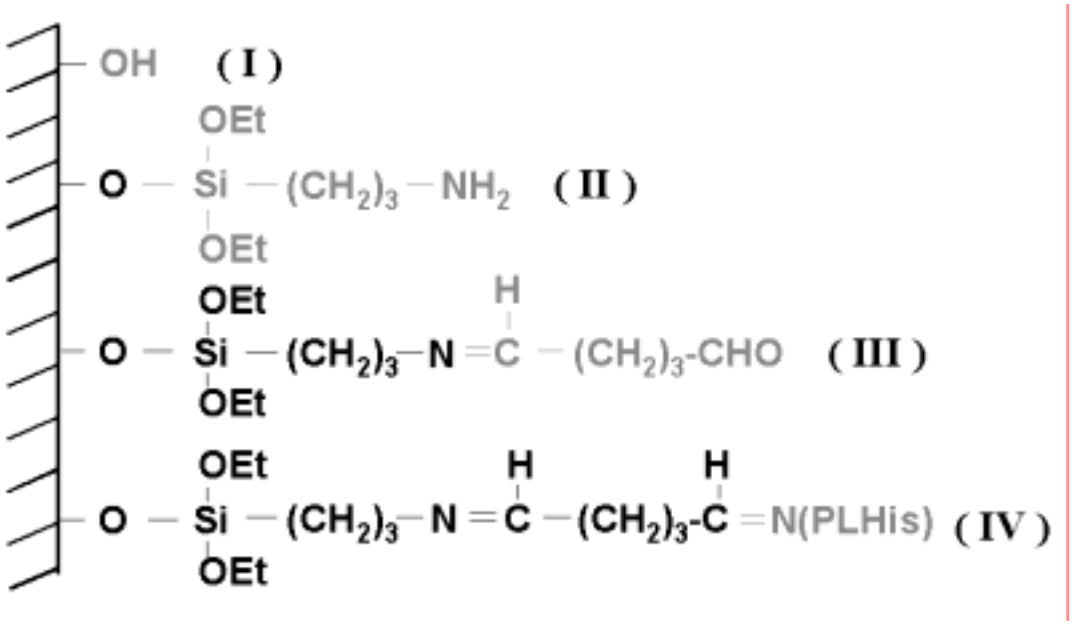

2.2.4 Binding of Metal Cations to PLHis-CPG

The previously described flow injection analysis system was utilized in all metal binding experiments. The pumps, tubing, hollow cathode lamp and flame were warmed up for at least 15 min prior to use. After conditioning the column, unretained, acidified (pH < 1.0) metal standards were run through the PLHis-CPG column and their absorbance values were used to prepare a calibration curve of the metal solution through the column.

Upon completion of the acid calibration curve, a 0.05 M ammonium acetate solution (pH 7.0) was pumped through the column for 2 min at 1 mL/min to recondition the column to the neutral pH and solution conditions. The cation metal binding solutions were prepared by dilution from the metal standards into 0.05 M ammonium acetate,

diluted from the stock, and adjusted to pH 7.0 by drop wise addition of acetic acid or ammonium hydroxide. The 10 ppm ammonium acetate-metal solution was then introduced onto the column at a flow rate of 1 mL/min and the effluent concentration was detected by flame atomic absorption spectrometry producing a breakthrough curve. By knowing the influent flow rate, the time axis can be converted to influent volume and through the calibration curve the absorbance axis can be converted to effluent concentration (Figure 2.4). Analysis of breakthrough curves results in the determination of an effective capacity of the system for the metal of interest.

Figure 2.4 Typical breakthrough curve

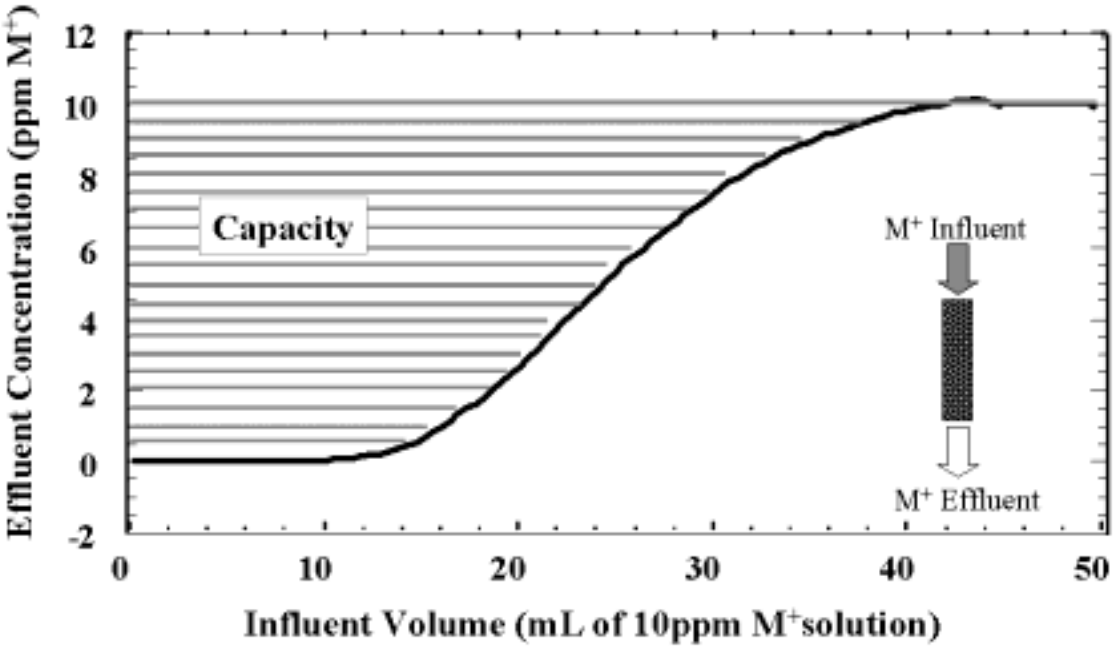

Once the effluent concentration equaled the influent concentration, the sample flow was stopped. Ammonium acetate was passed through the column and emptied into waste for ~10 s (i.e., 0.16 mL) to remove the remaining metal-containing solution from the lines

and the column dead volume. The metals were stripped from the column by flowing 0.1 M HNO_3 for 5 min at 1 mL/min through the column and collecting the effluent in a 25 mL volumetric flask for subsequent analysis by FAA. Although it has been shown in previous studies that the metals are stripped from the column in only a few hundred microliters of acid [42], 5 mL was used to ensure complete removal of the metal from the column. The strip solution was not analyzed by direct transfer from the column to the FAA because the concentrations released far exceeded the dynamic range of the detection system. Breakthrough curves and strip solution data were analyzed for each of the target cations (Ca^{2+}, Cd^{2+}, Co^{2+}, Cr^{3+}, Cu^{2+}, Mg^{2+}, Mn^{2+}, Na^{+}, Ni^{2+} and Pb^{2+}), resulting in the relative binding capacity of PLHis for each of the metals. All metal binding experiments were performed in triplicate.

2.2.5 pH Dependent Binding of Cu^{2+} to PLHis-CPG

A more detailed evaluation of the PLHis-CPG column capacity for Cu^{+2} was also undertaken for pH values ranging from 4.0 to 8.0 using a 10 ppm Cu^{2+} influent solution in 0.05 M ammonium acetate, pH adjusted with ammonium hydroxide or acetic acid, pumped through the column at a flow rate of 1.0 mL/min. Breakthrough curves and strips were collected and evaluated using the metal binding procedure described previously.

2.3 RESULTS AND DISCUSSION

2.3.1 Metal Binding Characteristics of PLHis-CPG

Breakthrough curves run on the PLHis-CPG column were analyzed by monitoring the metal concentration in the column effluent by FIAS-FAA as a function of influent volume. Figure 2.5 contains typical breakthrough curves for various metals.

Figure 2.5 Breakthrough curves of Na^+, Cd^{2+} and Cu^{2+} on PLHis-CPG; demonstrating examples of minimal binding, moderate binding, and strong binding, respectively. All solutions were 10 ppm in the respective metal and 0.05 M ammonium acetate; pH 7.

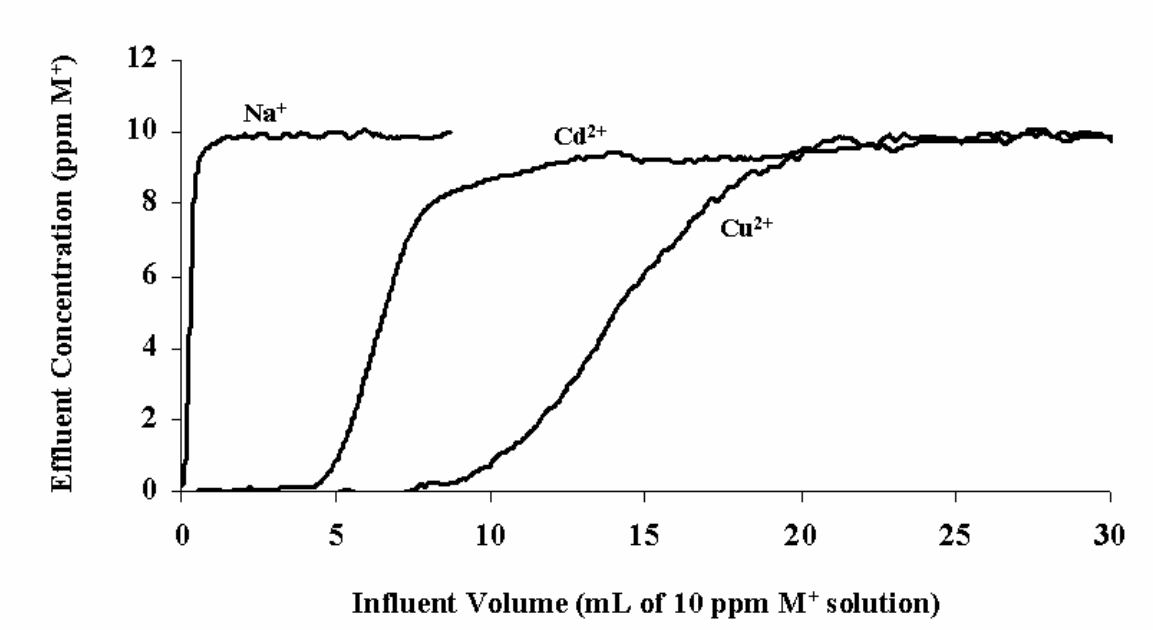

The flat baseline region present on the Cd^{2+} and Cu^{2+} curves generally represents strong metal binding sites (log $K_{effective}$ > 8). The sloped regions represent the weaker metal binding sites. The rapid rise of the effluent Na^+ concentration to that of the influent is an indication of little or no binding capacity for this cation. Breakthrough analysis of Co^{2+}

and Ni^{2+} showed both strong and weak binding sites, while Pb^{2+} demonstrated only weak sites. PLHis-CPG had very little, to no binding of Ca^{2+}, Mn^{2+}, Mg^{2+}, Na^{+} and Cr^{3+}. By integrating the breakthrough curve, the total amount of metal retained on the column can be determined. These values are validated using the results from the stripped solutions. Table 2.1 contains a summary of the cationic metal binding results for PLHis-CPG.

Table 2.1 Cationic metal binding capacity of PLHis-CPG column[a]

Metal ion	**Breakthrough data** (μmol/g CPG)	**Strip data** (μmol/g CPG)
Cu^{2+}	32.2 ± 0.3	36.7 ± 1.0
Cd^{2+}	8.4 ± 1.9	8.5 ± 0.4
Ni^{2+}	7.7 ± 0.4	8.8 ± 0.3
Co^{2+}	4.3 ± 1.3	4.9 ± 0.4
Pb^{2+}	1.7 ± 0.2	2.4 ± 0.6
Na^{+}	< 1	0.6 ± 0.2
Ca^{2+}	< 1	0.5 ± 0.1
Mg^{2+}	< 1	0.3 ± 0.2
Cr^{3+}	< 1	0.20 ± 0.02
Mn^{2+}	< 1	0.14 ± 0.04

[a]Uncertainties, expressed as sample standard deviations, reflect measurement uncertainties only, pH = 7.0, flow rate = 1 mL/min, triplicate measurements

Although the difference in capacities calculated from the breakthrough and the strip are not large, several are bigger than would be expected based on the standard deviation for triplicate analysis. In some instances the differences are slightly greater than expected

from measurement uncertainties. To ensure that the excess metal in the strip solutions could not be attributed to contamination in the buffer, blank ammonium acetate solutions were analyzed by ICPMS before and after treatment with chelex-100. The Cu^{2+}, Cd^{2+}, Ni^{2+} and Pb^{2+} concentrations in ammonium acetate were all below the detection limit by ICPMS, i.e., less than 0.4, 0.2, 1.0 and 0.4 ppb, respectively. Therefore, it must be concluded that the mass difference is not due to contamination, but may be due to systematic errors in analyzing the breakthrough data and/or collecting the strip solutions. More importantly, the relative binding trend is consistent between the breakthrough and the strip data. As a result, future comparisons of capacities are based on the breakthrough capacity values. The metal binding trend of PLHis-CPG was determined to be: $Cu^{2+} >> Cd^{2+} \approx Ni^{2+} > Co^{2+} > Pb^{2+} >> Na^{+} \approx Ca^{2+} \approx Mg^{2+} \approx Cr^{3+} \approx Mn^{2+}$. This trend is in general agreement with that reported for metal binding to nitrogen ligands such as pyridine and imidazole [43].

The main metal *cationic* binding functionality of PLHis-CPG is the imidazole ring on each histidine residue. More specifically, the lone pair of electrons on the pyridine nitrogen of the imidazole ring is active in the coordination of metals to PLHis. McCurdie and Belfiore have demonstrated that PLHis forms solid state complexes, through the imidazole side chain, with the divalent metal chlorides of cobalt, nickel, copper and zinc [95].

2.3.2 Binding of Cu^{2+} to PLHis-CPG with Varying pH

The effect of pH on the capacity of the PLHis-CPG column for Cu^{2+} was determined for pH values 4.0 to 8.0. The breakthrough curve variations with pH can be seen in Figure 2.6 and the capacity values presented in Table 2.2.

Figure 2.6 Breakthrough curves of 10 ppm Cu^{2+} on PLHis-CPG in 0.05 M ammonium acetate at various pHs.

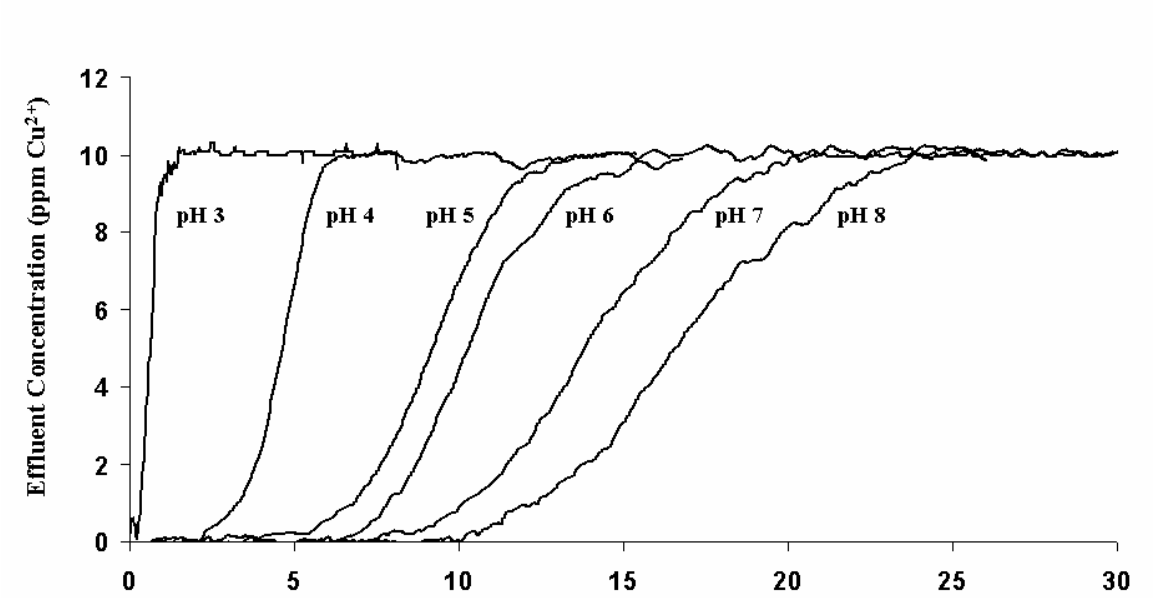

Present on each curve is a flat baseline region representative of strong binding sites and a sloped, weaker binding region. As the pH increases, there is a gain in both strong and weak site capacities.

Table 2.2 Cu^{2+} capacity dependence on pH[a]

pH	**Breakthrough Data** (μmol/g CPG)	**Strip Data** (μmol/g CPG)
3	2.28 ± 0.01	1.82 ± 0.07
4	10.5 ± 1.1	11.9 ± 0.3
5	18.1 ± 0.1	18.24 ± 0.04
6	22.5 ± 1.0	26.5 ± 0.2
7	32.2 ± 0.3	36.7 ± 1.0
8	36.4 ± 1.8	43 ± 2

[a]10 ppm Cu^{2+} in 0.05 M ammonium acetate influent, flow rate = 1 mL/min, triplicate measurements

Patchornik et al. estimated the pK_a of PLHis to be 6.15 [96], which is consistent with the reported values of 5.6 - 7.0 for the histidine residues in proteins [97] and very close to the value of 6.0 given for the imidazole side chain of histidine. However, it is important to note that it is reasonable to consider the existence of a broad range of pK_a's along the chain of the polymer and that the pK_a of 6.15 is simply a reasonable estimate. In fact, the pK_a may vary along the length of the chain with the surface as well as neighboring functional groups influencing local pK_as. At pHs greater than this, the pyridine nitrogen on the imidazole side chain is deprotonated and has an unshared lone pair of electrons capable of metal binding. Measurable binding appears between pH 3 - 4, which is consistent with studies suggesting that the PLHis-Cu^{2+} complex begins to

form at pH 3.0 [98-100]. This likely reflects the relative strength of the PLHis-Cu^{2+} coordination and its ability to displace the proton on the imidazole.

The data in Table 2.2 also indicates that there is a significant increase in metal binding capacity as the pH increases and as the percentage of deprotonated imidazoles and associated availability of lone pair electrons increases. It is interesting to note that the extent of PLHis protonation changes by ~3 orders of magnitude as the pH is lowered from 6.0 to 3.0, but the extent of Cu^{2+} binding only decreases by a factor of 10. This suggests that there must be some means of enhancing binding that offsets the significant loss of deprotonated imidazole binding sites. It is likely that a conformational change of this tethered, short-chain peptide at low pHs partially compensates for this decrease in deprotonated imidazole binding sites.

Previous studies have shown that PLHis, in solution, undergoes conformational changes with changes in pH [100-105]. It is generally agreed that a conformational transition occurs as the degree of protonation of the imidazole side chain changes, but there are differing opinions on the exact conformation of the chain, as it becomes deprotonated. Most recently, it has been concluded that at pH < 4, where the imidazole is protonated, the chain exists as a random coil; and as the imidazole deprotonates, the structure moves toward a more ordered structure, resulting in a beta-pleated sheet at pH > 5.2 [104]. Palumbo et al. studied the effects of the PLHis conformation on Cu^{+2} complexation and determined that when the chain exists as a random coil, the complexation occurs through three imidazole nitrogens and one peptide nitrogen in the square planar configuration (**complex I** [100]). In contrast, if the chain is in a more

ordered conformation, such as a beta sheet, the complexation occurs through four imidazole nitrogen in the square planar configuration (**complex II** in [100]). They also concluded that the Cu^{2+}:peptide molar ratio had an effect on which complex formed, with complex I dominating at higher metal concentrations. Therefore, the immobilized PLHis most likely forms **complex I** exclusively at low pHs, and as the pH is raised it forms **complex II** at low Cu^{2+}:peptide ratios. As the Cu^{2+} concentration increases, the beta sheet conformation gets disrupted and the coordination becomes that of **complex I**. More importantly, as both of these complexes form, the imidazole nitrogen remains as the primary binding functionality.

2.4 CONCLUSION

It has been shown that PLHis-CPG is an effective metal chelator. The metal cation binding trend is $Cu^{2+} >> Cd^{2+} \approx Ni^{2+} > Co^{2+} > Pb^{2+} >> Na^{+} \approx Ca^{2+} \approx Mg^{2+} \approx Cr^{3+} \approx Mn^{2+}$, with a capacity for Cu^{2+} calculated from breakthrough analysis of 32.2 ± 0.3 μmol Cu^{2+}/g CPG. Each of the metal cations can be quantitatively stripped from the column in several hundred microliters of 0.1 M HNO_3. The pH study conducted with metal cations showed an increase in capacity with increasing pH, most likely due to conformational changes of the polymer.

Chapter 3: Immobilized Poly–L–Histidine for Chelation of Metal Oxyanions

3.1 INTRODUCTION

It has previously been mentioned that many metals are harmful and have negative health effects (Table 1.1). However, oxyanions such as chromates and arsenates are a significant environmental concern, especially when considering the recent EPA announcement of the reduction of the maximum contaminant level of arsenic in drinking water from 50 ppb to 10 ppb [106]. All public sources of drinking water must be in compliance by January 23, 2006 [107].

Unfortunately, arsenic is a natural part of the earth's crust and therefore it is rather prevalent in rocks and soil. As a result, it is often found in high amounts in drinking water that has passed through arsenic rich soil. In fact, it has become an "environmental crisis" in a number of Asian countries [108]. Arsenic exposure has been linked to an increased risk of cancer as well as other cardiovascular, pulmonary, immunological and neurological effects [109]. Historically there are numerous methods for arsenic removal including coagulation, activated alumina, ion exchange and membrane methods such as nanofiltration and reverse osmosis [110]. However, these methods have their inherent complications or disadvantages. For example, coagulation is often not able to meet the standard set by the recent EPA regulation [111]. Ion exchangers suffer from competition with other anions in solution [110-113] and membrane methods tend to be relatively expensive [110].

In contrast, chromium is often released into the environment through industrial processes such as in steel production, leather tanning and wood impregnation with preservatives [114-116]. Although chromium as an element is necessary for human metabolism, it has very serious, negative health effects at high levels of exposure [114]. The hexavalent form of chromium is more hazardous than the trivalent form. As is the case with arsenic, numerous chromium remediation methods have been explored. Current methods include precipitation, activated alumina, ion exchange and removal with quarternary ammonium zeolites [115, 116]. Again, ion exchange resins suffer from problems with competing anions in solution as well as the possibility of being oxidized and they are susceptible to fouling [115, 117, 118]. The effectiveness of zeolites in chromium removal was shown to be dependant upon the pH and ionic strength of the solution. Additionally, regeneration and chromium recovery was also a problem [115, 116].

Bio homo-polymers have rarely been investigated for anion binding. Although, in many cases they have been shown be effective cation metal chelators. PLHis has been characterized according to its metal binding capabilities in Chapter 2. This amino acid residue is unique in that the imidazole side chain, responsible for cationic metal binding, has a pK_a of ~ 6.0 and is positively charged (deprotonated) in acidic conditions (Figure 3.1).

Figure 3.1 Poly-L-Histidine as present at pH < 6 (n ≈ 90 – 100)

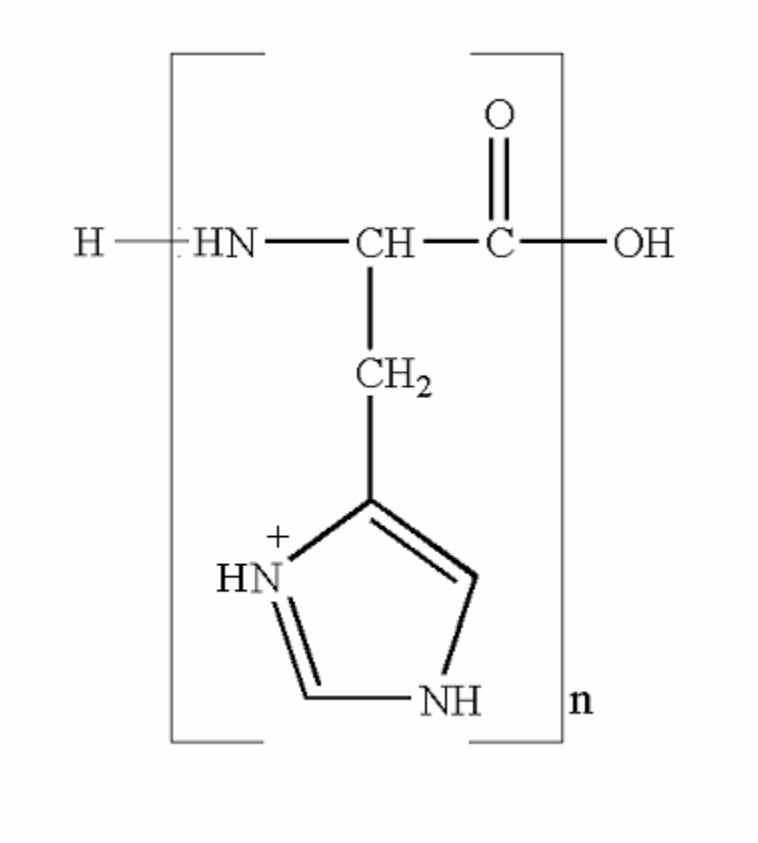

To get a better understanding of why this positively charged residue is significant in terms of oxyanion binding it is helpful to look at a chromium distribution diagram (Figure 3.2a). This diagram is based on the equilibrium constants of the various chromium species present in a 10 ppm solution. As seen in this diagram, in this relatively dilute solution, the prominent species in solution at pH < 1 is H_2CrO_4, at pH 1 - 7 the predominant species is $HCrO_4^-$, and at pH > 7 it is CrO_4^{2-}. In dilute solutions, such as 10 ppm, the chromate species dominate over the dichromate species. The three dichromate species; $H_2Cr_2O_7$, $HCr_2O_7^-$ and $Cr_2O_7^{2-}$, are present in very low concentrations compared to the chromates as can been seen in Figure 3.2b.

Figure 3.2 a) Chromium distribution diagram based on 10 ppm Cr solution b) expanded view

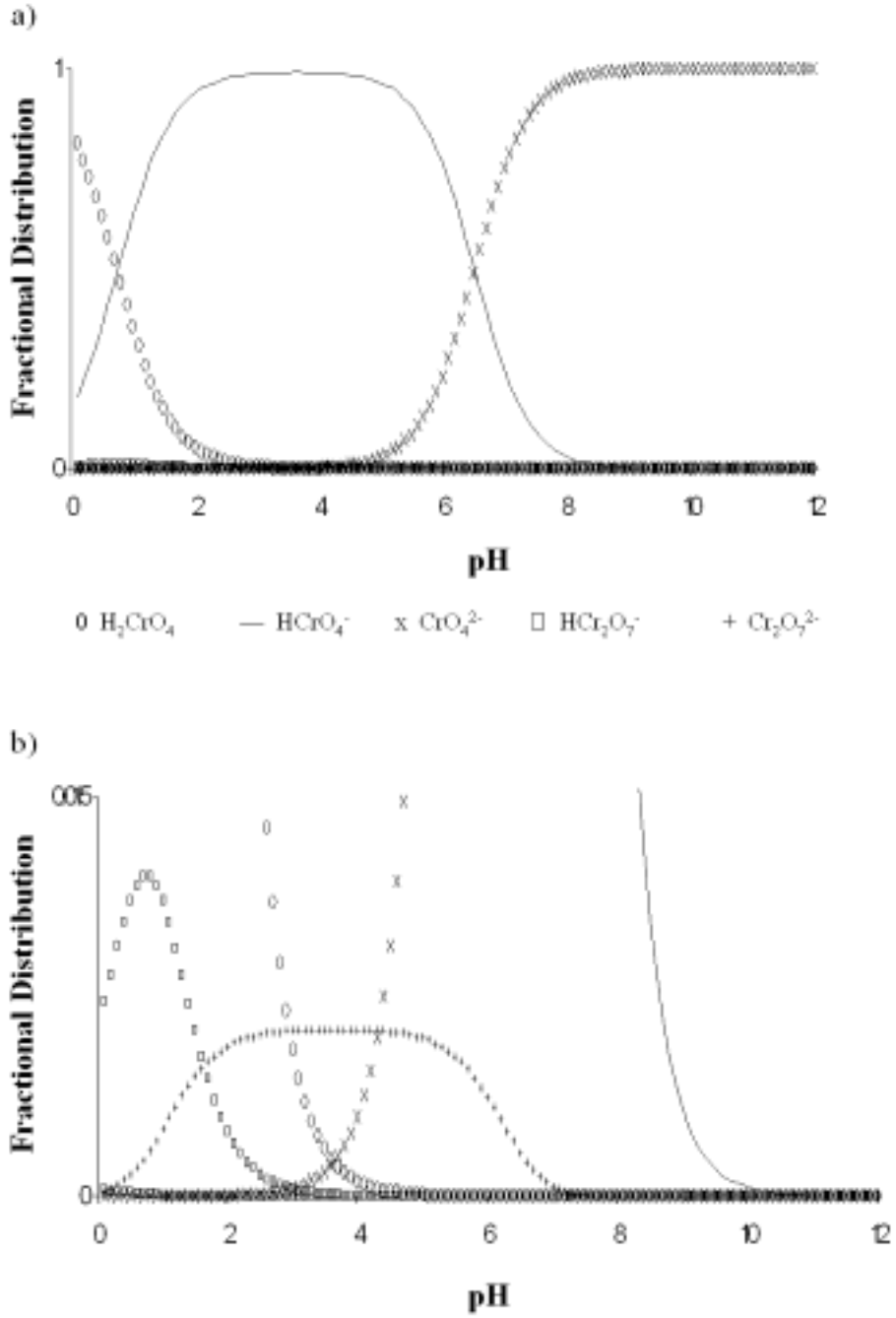

This study involves the utilization of the positively charged imidazole on immobilized PLHis-CPG for remediation of metal oxyanions such as chromates and arsenates.

3.2 EXPERIMENTAL

3.2.1 Instrumentation

A Perkin-Elmer model 4000 atomic absorption spectrophotometer with an air/acetylene flame was used for all metal determinations. Hollow cathode lamps for the metals of interest were operated at the currents recommended by their manufacturers. Wavelengths for As, Cr and Se were 193.7, 357.9 and 196.0 nm, respectively. A monochromator band-pass of 0.7 nm was used for As and Cr and 2 nm for Se.

The simple flow injection manifold consisted of an eight-roller peristaltic pump (Ismatec minicartridge MS-REGLO) and two two-way, double inlet rotary valves (Rheodyne 5020). All connections were made with 0.76 mm i.d. PTFE tubing [42].

The same immobilized PLHis-CPG column that was previously described in Chapter 2 for cation metal binding was used in all oxyanion binding studies. A Kel-F tee was placed between the column and the nebulizer to provide air compensation and to minimize noise.

A Varian VGA-76 Vapor Generation Accessory was used in conjunction with the AA and the peristaltic pump for arsenic and selenium determinations as seen in Figure 3.3. The vapor generation accessory was operated according to the manufacturer's instructions with the effluent from the column flowing into the sample line of the hydride vapor generator. Since the generator requires a flow of approximately 8 mL/min and the

effluent from the column is only 1 mL/min, a tee was added to the sample line to mix 7 M HCl at a flow of 7 mL/min with the column effluent.

Figure 3.3 Hydride generator for As and Se determinations. Pump #1 is the peristaltic pump that delivers the various solutions to the PLHis-CPG column. Pump #2 is the peristaltic pump that is responsible for delivering the $NaBH_4$ and HCl for hydride formation.

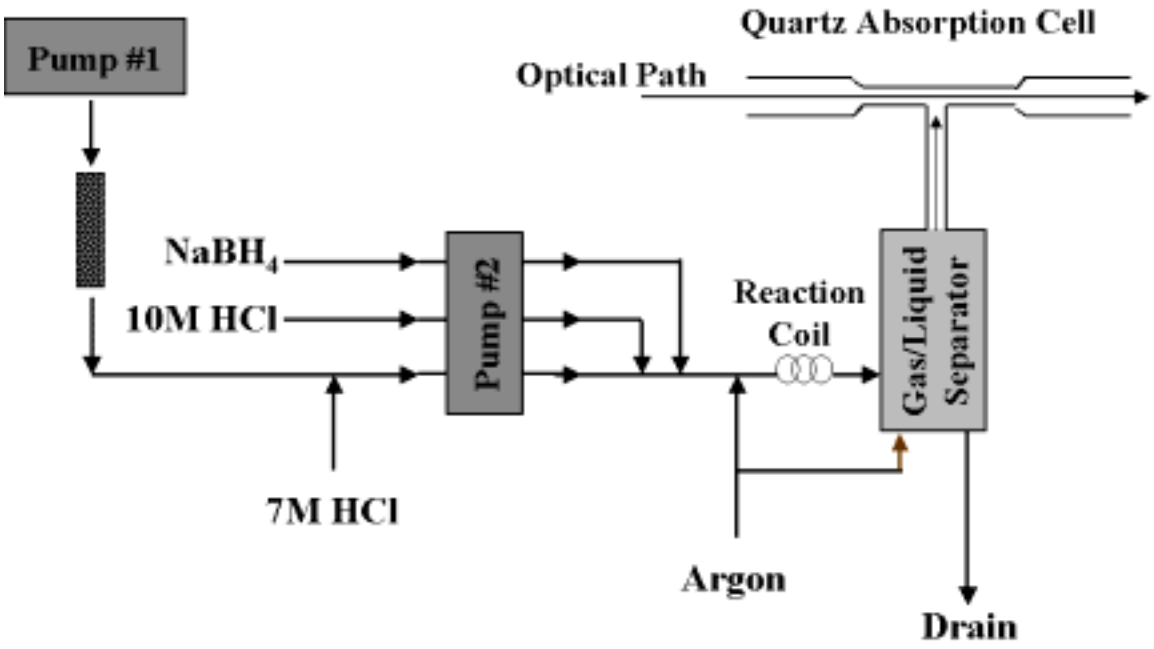

3.2.2 Reagents

All chemicals were reagent grade unless noted and deionized, distilled water was used to prepare solutions. All glassware was soaked in 4 M HNO_3 overnight before use. The previously described PLHis-CPG column was used. Other reagents included nitric acid (Aldrich); acetic acid, hydrochloric acid, perchloric acid, phosphoric acid, sodium

chloride, sodium phosphate, Tris (hydroxymethyl) aminomethane (Fisher Scientific); ammonium acetate, sodium acetate (Spectrum Chemical Mfg. Corp.); DL-dithiothreitol (Sigma); and sulfuric acid, sodium hydroxide and sodium borohydride (EM Science). Stock solutions of selenious acid (Inorganic Ventures) and potassium chromate (Ricca Chemical Company) atomic absorption standards were used to prepare the 10 ppm loading solutions for the metal binding experiments. A 1000 ppm As stock solution was prepared from sodium arsenate (Sigma) and diluted to provide the 500 ppb loading solution. 0.5 M ammonium acetate and 0.5 M sodium acetate stock solutions were prepared and purified using a 100 - 200 mesh Chelex 100 (Bio-Rad) ion exchange column.

3.2.3 pH Dependent Binding of Oxyanions of Cr(VI) to PLHis-CPG

The pH dependence of PLHis-CPG column capacity for Cr(VI) was determined under two sets of conditions. First, the Cr(VI) capacity was determined for pH values ranging from 1.0 to 6.0 using a 10 ppm Cr(VI) influent solution in 0.05 M ammonium acetate, pH adjusted with nitric acid. Second, the capacity was determined for pH values ranging from 3.0 to 6.0 with 10 ppm Cr(VI) in 0.05 M ammonium acetate, pH adjusted with acetic acid. All solutions were pumped through the column at a flow rate of 1.0 mL/min. Breakthrough curves were collected and evaluated using the procedure outlined above.

3.2.4 Anion Influence on Cr(VI) Binding to PLHis-CPG Under Acidic Conditions

In order to determine the impact of competing anions, Cr(VI) was run through the column using different acids. The FIA-FAA set-up and conditioning were the same as previously described. Prior to running the sample solution through the column for the breakthrough curve, the column was conditioned for 2 min with the metal-free acid solution that was about to be run. These solutions were: 0.1 M H_2SO_4, 0.01 M H_2SO_4, 0.1 M HNO_3, 0.01 M HNO_3, 0.1 M HCl, 0.01 M HCl, 0.1 M H_3PO_4, 0.01 M H_3PO_4, 1 M CH_3COOH, 0.1 M CH_3COOH and 0.05 M CH_3COOH. In addition, Cr(VI) was also run in 0.5 M ammonium acetate and 0.5 M sodium acetate, both pH adjusted to pH 4.0 with acetic acid, to determine the effects of different cations in solution.

After conditioning the column with a metal-free solution of the acid to be evaluated, a 10 ppm Cr(VI) solution in the respective acid was pumped through the column and breakthrough data recorded. Once breakthrough was achieved the sample flow was stopped and 0.1 M HNO_3 was passed through the column and emptied into waste for ~10 s in order to remove the remaining metal-containing solution from the lines and the column dead volume. The Cr(VI) was stripped from the column with a flow of 0.1 M HNO_3 for 10 min at 1 mL/min. The strip solution was collected into a 25 mL volumetric flask for subsequent analysis.

3.2.5 Cr Binding Studies on Modified Surfaces of CPG

To confirm that the binding observed was due to the PLHis and not unreacted surface functionalities generated during the immobilization, the uptake of Cr(VI) and Cr^{3+}, each in 0.1 M HNO_3 and in 0.05 M ammonium acetate (adjusted to pH 7.0), was

evaluated separately on three modified CPG columns: 0.0704 g of acid activated CPG, 0.0757 g of silanized CPG and 0.0653 g of gluteraldehyde CPG. The metal influent concentration was 10 ppm and the influent flow rate was 1.0 mL/min. The loading and stripping procedure was the same as that described previously.

3.2.6 Cr Speciation on PLHis-CPG

A single solution containing both 10 ppm Cr^{3+} and 10 ppm Cr(VI) in 0.1 M acetic acid was run through the PLHis-CPG column with an influent flow rate = 1.0 mL/min and breakthrough data was collected as previously described.

3.2.7 Cr(VI) Strip Efficiency

In order to determine the efficiency of the strip procedure for Cr(VI) the PLHis-CPG column was loaded with 100 μg of Cr(VI). The column was then stripped with 0.1 M nitric acid and 5 mL aliquots were collected for analysis by FAAS.

3.2.8 Binding of As(V) to PLHis-CPG

In order to determine if PLHis-CPG was able to bind arsenic, the hydride generator was positioned between the column and FAA. The FIA system, and the hydride generator were run as previously described, flowing either acid or sample through the column. After conditioning the column with 0.1 M HCl for 2 min, a 500 ppb As(V) solution in 0.1 M HCl was pumped through the column and breakthrough data was collected. Once breakthrough was achieved, 0.1 M HNO_3 was used to clear lines and strip the column as described above. To study the effects of various solution conditions on As(V) binding, 500 ppb of As(V) in a variety of solutions were run through the PLHis

column and breakthrough data was collected. These solutions include: 0.05 M ammonium acetate at pH values of 4.0, 5.0, 6.0 and 7.0, using sodium hydroxide or acetic acid to adjust the pH, distilled/deionized H_2O, 0.1 M NaCl, 0.1 M HNO_3, 0.05 M Tris, 0.05 M phosphate buffer, 0.1 M HCl, 0.01 M HCl, 1.0 mM HCl, 0.1 mM HCl, 0.1 M $HClO_4$, 0.01 M $HClO_4$ and 1.0 mM $HClO_4$.

3.2.9 Binding of Se(IV) to PLHis-CPG

The Varian VGA-76 Vapor Generation Accessory was also used in all Se determinations. The generator was positioned and run in the same manner previously described for As(V) determinations. 500 ppb Se(IV) was run on the PLHis-CPG column in various solutions: 0.1M HCl, 0.05M ammonium acetate and distilled/deionized H_2O. Column conditioning and stripping used the protocol employed for the As(V) study.

3.3 RESULTS AND DISCUSSION

3.3.1 Binding of Cr(VI) to PLHis-CPG with Varying pH

The presence of a positive, protonated imidazole under acidic conditions suggests the possible utility of PLHis for complexation of anions. More specifically, it may be useful as a chelator for metals that exist as oxyanions, such as the chromates, arsenates, etc. The pH dependence of the PLHis-CPG capacity for Cr(VI) was studied using two different means of adjusting the pH. Two 10 ppm Cr(VI) solutions were prepared in 0.05 M ammonium acetate, one was pH lowered with nitric acid the other was adjusted by acetic acid addition. Figure 3.4 shows that pH had very little effect on the binding capacity or shape of the breakthrough curves when nitric acid was used to vary the pH

between 1.0 and 6.0. Additionally, the ionic strength of the solution pH adjusted with nitric acid is increasing as more acid is added to decrease the pH, and there is no significant change in capacity.

Figure 3.4 Breakthrough curves of 10 ppm Cr(VI) on PLHis-CPG in 0.05 M ammonium acetate at various pHs. pH was adjusted with nitric acid.

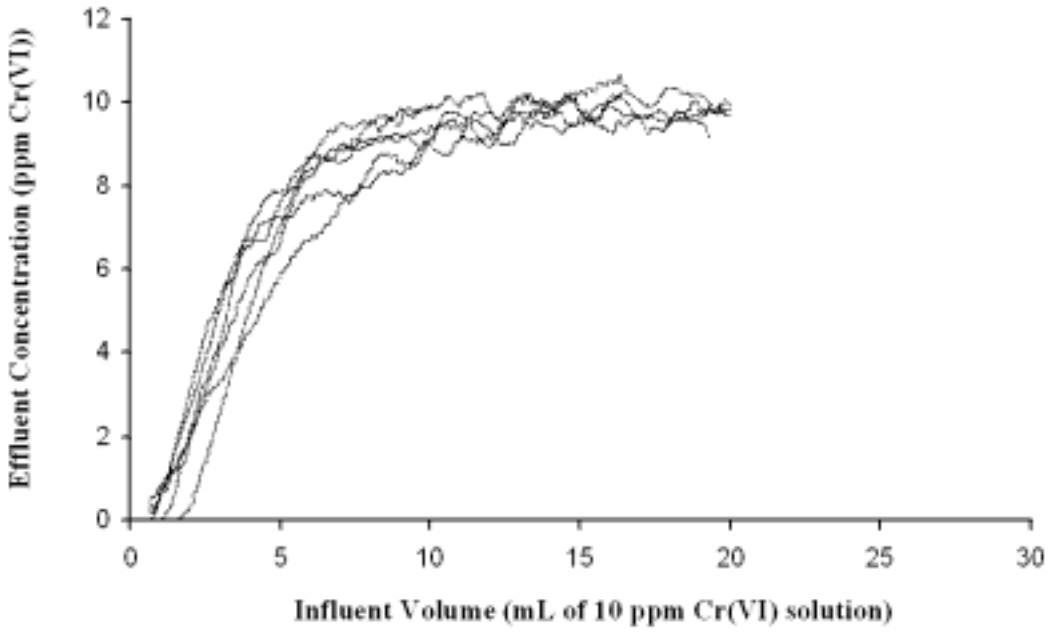

In contrast, Figure 3.5 shows that pH had a significant effect on the binding capacity when the nitrate was omitted from the solution and the pH adjusted using acetic acid.

Figure 3.5 Breakthrough curves of 10 ppm Cr(VI) on PLHis-CPG in 0.05 M ammonium acetate at various pHs. pH was adjusted with acetic acid.

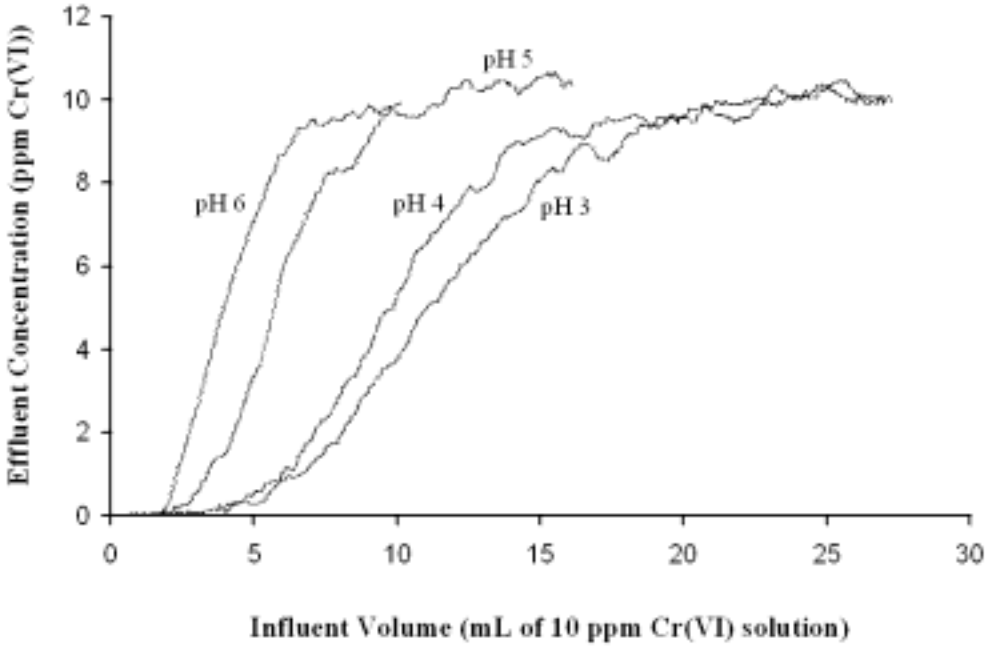

The calculated capacities are listed in Table 3.1. The acetic acid data shows a significant increase in the capacity as the pH drops from 6.0 to 5.0 and another increase as the pH drops from 5.0 to 4.0. This is consistent with a pK_a for the imidazole of PLHis of ~ 6.0 and conformation change from a beta sheet to a random coil at pH < 5.2 [104]. The column capacity for *anions* would be expected to rise as the percentage of protonated imidazoles significantly increases (i.e., pH < pK_a ~ 6.0). In this pH range (3.0 – 6.0) the distribution of chromium species remains fairly constant with the predominant species being $HCrO_4^-$. Therefore, the change in capacity is likely the result of changes in the

chelator rather than a change in the dominant chromium species present. The calculated capacities in Table 3.1 also suggest that the presence of nitrate in the solution inhibited Cr(VI) binding at all pHs. The strong influence shown by nitrate at all pHs raised the concern that other anions may also significantly impact Cr(VI) binding.

Table 3.1 Cr(VI) binding capacity dependence on pH[a]

pH	**Cr(VI) bound** Adjusted with nitric acid (μmol/g CPG)	**Cr(VI) bound** Adjusted with acetic acid (μmol/g CPG)
1	10.1 ± 0.5	-------
2	11.7 ± 1.0	-------
3	8.7 ± 0.6	25.8 ± 0.8
4	7.9 ± 0.2	23.5 ± 1.1
5	8.1 ± 0.7	16.1 ± 0.3
6	10.0 ± 1.1	10.0 ± 1.1

[a]10 ppm Cr(VI) in 0.05 M ammonium acetate influent, flow rate = 1 mL/min, triplicate measurements. (pH values < 3 were unattainable using only acetic acid to adjust pH.)

3.3.2 Binding of Cr(VI) to PLHis-CPG in the Presence of Various Anions

Since variations in the ion selectivity of ion exchangers may be caused by factors such as pH, ionic strength, competing background ligands and the nature of the exchanger [115]; the effects of CH_3COO^-, PO_4^{3-}, Cl^-, NO_3^- and SO_4^{2-}, on PLHis-CPG, were evaluated by running Cr(VI) breakthrough curves in separate solutions to which CH_3COOH, H_3PO_4, HCl, HNO_3 and H_2SO_4 were added (Figure 3.6). It should be noted that each of the solutions in Figure 3.6 has a pH of ~ 2.3 – 3 and in this range the

distribution of chromium species remains fairly constant. These pHs are also significantly below the pK_a of the imidazole so the percentage of protonated imidazoles is not changing.

Figure 3.6 Breakthrough curves of 10 ppm Cr(VI) on PLHis-CPG in solutions containing various acids.

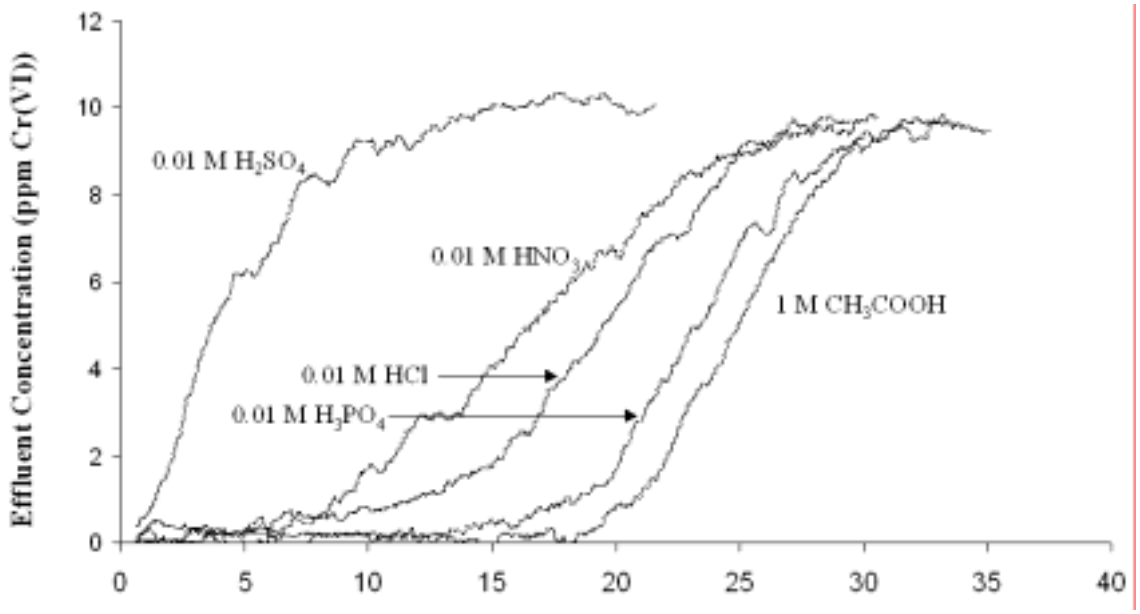

The Cr(VI) capacities calculated from these curves (Table 3.2) show that PLHis-CPG has the greatest capacity for Cr(VI) in acetic acid. It is evident from these curves that the other ions in solution (i.e., chloride, nitrate and sulfate) interfere with the binding. Also, as the concentration of the anions increases, the capacity for Cr(VI) decreases. While this appears to indicate that ionic strength may affect column capacity, a closer look at the data suggests that the impact on binding is ion specific. For example, the ionic strength of 0.1 M HNO_3 is the same as the ionic strength of 0.1 M HCl, but HNO_3 affects the capacities much more significantly. A similar effect is seen for the same acids present at

0.01 M. In summary, the presence of sulfate ions caused the greatest loss in capacity followed by nitrate, chloride and phosphate.

Additionally, comparison of the data in Table 3.2 with the data presented in Table 3.1 indicates that the presence ammonium in the ammonium acetate solutions also significantly reduces the Cr(VI) binding capacity. Due to the fact that many strong base anion exchangers contain quaternary amine functionalities it is not suprising that the presence of ammonium may interfere with Cr(VI) binding.

Table 3.2 Cr(VI) binding capacity in various acidic solutions[a]

Solution	**pH**	**Cr(VI) bound** (μmol/g CPG)
1.0 M CH_3COOH	2.9	66.2 ± 0.7
0.1 M CH_3COOH	3.8	75.5 ± 2.1
0.05 M CH_3COOH	3.95	77.2 ± 3.1
0.1 M H_3PO_4	2.1	34.8 ± 0.6
0.01 M H_3PO_4	3.0	53.8 ± 1.8
0.1 M HCl	1.0	20.3 ± 1.0
0.01 M HCl	2.4	46.6 ± 1.9
0.1 M HNO_3	1.0	9.6 ± 0.4
0.01 M HNO_3	2.3	40.7 ± 3.0
0.1 M H_2SO_4	1.4	9.8 ± 2.4
0.01 M H_2SO_4	2.3	10.1 ± 0.7

[a]10 ppm Cr(VI) influent, flow rate = 1.0 mL/min, triplicate measurements

These interferences are consistent with trends reported by Gang and coworkers [116] for Cr(VI) binding by poly(4-vinylpyridine) coated silica gel. Poly(4-

vinylpyridine) coated silica gel showed a reduction in Cr(VI) capacity in the presence of Cl^-, SO_4^{2-} and CH_3COO^-, with sulfate having the biggest impact followed by chloride and acetate. They also noted that competing anions had very little effect on capacity as long as their concentrations were less than or equal to the Cr(VI) concentration. More specifically, a 50% decrease in capacity at sulfate concentrations 250 times greater than the Cr(VI) concentration was noted [116].

Sengupta and Clifford performed extensive studies on the effects of sulfate and chloride on the removal of Cr(VI) with the styrene-divinyl-benzene (STY-DVB) anion exchange resins (IRA-900 and IRA-94) and concluded that increasing the sulfate concentration increased the selectivity of the resin for Cr(VI) while increasing the chloride concentration had no effect on the resin's selectivity for Cr(VI) [119]. Clifford also notes that there is only a slight reduction of Cr(VI) anion exchange capacity in the presence of Cl^- and SO_4^{2-} on the commercially available strong base anions exchangers: IRA 900, Dowex 11 and IRA 958 [113].

Additionally, the effects of competing anions on Cr(VI) capacity was studied on a new, polymeric ligand anion exchanger (DOW 3N-Cu) by Zhao et al. [120]. This exchanger was able to effectively remove Cr(VI) from a background of competing anions such as sulfate, chloride, bicarbonate and nitrate, which were present at concentrations much higher than Cr(VI). This exchanger was capable of a much greater capacity for Cr(VI) than IRA-900, which was used for comparison in their study. Although the effects of various concentrations of competing anions in solution was not studied by Zhao et al., breakthrough curves of HCO_3^-, NO_3^-, Cl^- and SO_4^{2-} showed that each of these ions broke through well before Cr(VI) [120]. The *weak base* (imidazole) exchange sites of the

PLHis are more susceptible to the influence of the tested anions than any of the other exchangers noted.

In order to take a closer look at the effect that the ionic strength of the solution had on Cr(VI) binding, breakthrough analysis was conducted with 10 ppm Cr(VI) solutions in different concentrations of acetic acid (1.0 M, 0.1 M and 0.05 M). The calculated capacities are listed at the top of Table 3.2. In each of these solutions the ionic strength will change with the concentration of acetic acid due to the extent of dissociation of acetic acid into acetate ions. The capacities in 0.1 M and 0.05 M are the same and there is only a slight drop in capacity in 1.0 M acetic acid. It can be concluded that pH is not a factor in these three solutions because the pH only changes from 2.0 in 1.0 M acetic acid to 3.9 in 0.05 M acetic acid. In this range, the chromium distribution remains constant with $HCrO_4^-$ still dominating; and with a pK_a of ~ 6.0 for the imidazole on the PLHis, at pH < 4 the imidazoles are >99.9% protonated. It is important to note that the Cr(VI) capacities in acetic acid are much greater than those calculated in ammonium acetate for all pH's studied. It is not obvious, however, if the presence of ammonium or the higher ionic strength is responsible for the decrease in capacity in the ammonium acetate solutions. Overall, the data indicates that the type of anion has the strongest effect on the Cr(VI) capacity. The ionic strength may play a role but its importance seems to be secondary in importance.

Upon completion of the anion studies, Cu^{2+} in ammonium acetate at pH 7 was run on the column and confirmed that the anions had not irreversibly altered the column

The PLHis-CPG results show that although PLHis has a significant capacity for Cr(VI) under certain conditions, it does have an affinity for other anions. Cr(VI)

remediation by this column may be less effective if the samples contain significant concentrations of sulfates or nitrates. However, it is apparent from the long, flat baseline seen in the breakthrough curves of Cr(VI) in the presence of chloride, phosphate or acetate in Figure 3.6 that this polymer could serve as an effective clean-up or polishing step in Cr(VI) removal.

3.3.3 Cr Binding Studies on Modified Surfaces of CPG

The immobilization procedure probably does not result in complete coverage of the CPG surface, and it has been shown previously that alkoxysilanes immobilized onto CPG are useful for oxyanion removal [121]. To evaluate the impact of non-PLHis surface binding, Cr(VI) capacities of the modified CPG were determined at each step of the immobilization: acid activated-CPG, silanized-CPG (amine terminated), gluteraldehyde-CPG and PLHis-CPG. The breakthrough capacities for the metal solutions on these four different columns are listed in Table 3.3.

Table 3.3 Cr binding capacity on CPG system at each stage of the PLHis immobilization[a]

	Capacity (μmol/g CPG)			
Metal Solution	**Acid activated CPG**	**Silanized CPG**	**Gluteraldehyde CPG**	**PLHis-CPG**
Cr(VI) acid	0.39 ± 0.07	8.3 ± 0.5	5.6 ± 0.1	11.3 ± 0.6
Cr(VI) neutral	0.23 ± 0.05	2.5 ± 0.2	0.7 ± 0.1	2.3 ± 0.2
Cr^{3+} acid	0.20 ± 0.06	0.33 ± 0.04	0.19 ± 0.01	0.28 ± 0.01
Cr^{3+} neutral	0.36 ± 0.09	1.2 ± 0.3	0.5 ± 0.2	0.35 ± 0.07

[a]10 ppm Cr influent, flow rate = 1.0 mL/min, triplicate measurements.

These results are consistent with the expectation of significant Cr(VI) anion interactions with positively charged species on the surface of the CPG, which are only present after the silanization step and the PLHis immobilization. In fact, capacity is gained with the addition of the silanizing agent after the acid activation but lost when gluteraldehyde is attached, blocking the amine terminus that was present for binding after the silanization step. The binding capacity increased again with the immobilization of the PLHis to the gluteraldehyde. This trend indicates that the metal binding capabilities of the PLHis-CPG column is due to the PLHis chelator with very little contribution from the unblocked activated glass surface, amine groups on the silanizing agent and gluteraldehyde groups. The capacities for each of these surfaces were calculated from breakthrough curves of Cr(VI) in nitric acid and in ammonium acetate at pH 7. In contrast to Cr(VI), Table 3.3 shows that each stage of the immobilization exhibited very little capacity for Cr^{3+} in either nitric acid or ammonium acetate.

3.3.4 Cr Speciation on PLHis-CPG

As seen in the previous study, PLHis-CPG does not bind Cr^{3+} while it is capable of binding Cr(VI). The Cr binding dependence on oxidation state is demonstrated in Figure 3.7 showing breakthrough curves of 10 ppm Cr^{3+} and 10 ppm Cr(VI).

Figure 3.7 Cr Breakthrough curves a) Cr^{3+} in 0.1 M acetic acid (pH 3.4), b) Cr(VI) in 0.1 M acetic acid (pH 3.4)

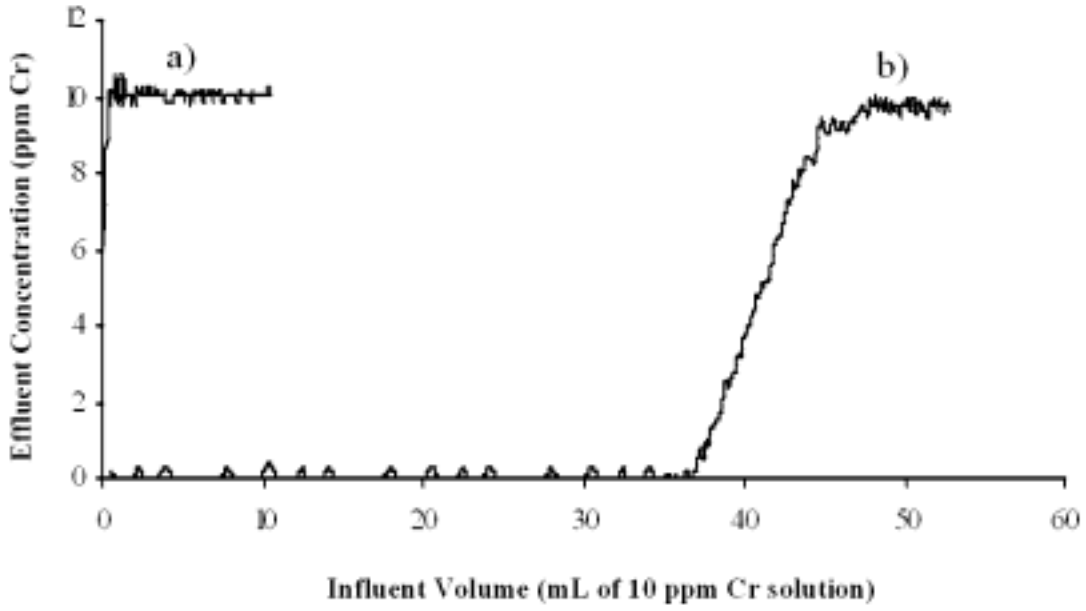

It can be seen from these two breakthrough curves that the Cr(VI) anions in solution are bound by the protonated histidine while the Cr^{3+} passes right through the column. The capacity of the column for Cr^{3+} is less than 1μmol/g of column and the capacity for Cr(VI) is approximately 75-80 μmol/g of column. With this information, a mixed solution containing both Cr^{3+} and Cr(VI) was run through the column and breakthrough data was collected (Figure 3.8).

Figure 3.8 Representative Breakthrough Curve of a single solution containing 10 ppm Cr^{3+} and 10 ppm Cr(VI) in 0.1 M acetic acid (pH 3.4).

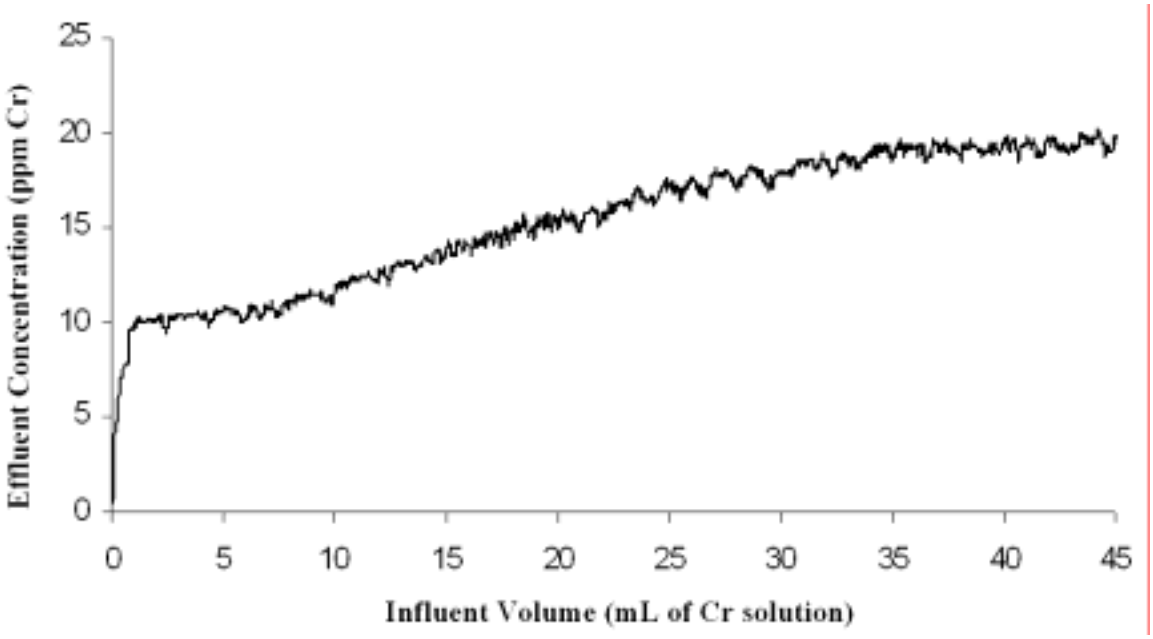

Interestingly, this curve shows the immediate breakthrough of the Cr^{3+} while the remainder of the curve resembles a Cr(VI) curve with both strong and moderate binding. This demonstrates the possible utility of this column to differentiate between the presence of Cr^{3+} and Cr(VI), with remediation being possible for Cr(VI). It should be noted that this also suggests that the interconversion of Cr(VI) to Cr^{3+} is kinetically slow in the solution being studied.

3.3.5 Cr(VI) Strip Efficiency

It has previously been shown that the metal cations can be quantitatively recovered from the peptide-immobilized columns in several microliters of acid [42]. The ability to strip into a reduced volume is a significant benefit when considering the

possibility of preconcentration or in reclaiming the metals in a concentrated form when the column is rejuvenated for reuse in remediation procedures. Initial attempts at stripping anionic Cr(VI) from the PLHis-CPG column proved more difficult than recovering the metal cations. Several strip solutions were attempted, such as 0.05 M ammonium acetate (pH 8), and the reducing agents DL-dithiothreitol (DTT) and sodium borohydride. However, it was concluded that quantitative recovery of Cr(VI) was possible with 0.1 M nitric acid. To determine the strip efficiency 100 μg of Cr(VI) was loaded onto the column. After clearing the Cr(VI) from the dead volume of the column and the lines, 0.1 M nitric acid was passed through the column at 1 mL/min and collected in 5 mL aliquots. These aliquots were individually analyzed by FAAS. The strip results are listed in Table 3.4. These results indicate that approximately 92% of the Cr(VI) is recovered in the first 10 mL and quantitative recovery is possible, but this compares poorly with the volumes of <1 mL needed to remove cationic species from the column.

Table 3.4 Cr(VI) strip efficiency[a]

Aliquot (5mL each)	**% Stripped**
1	82 ± 2
2	10 ± 1
3	5 ± 1
4	3 ± 1

[a]Stripped with 0.1 M nitric acid, flow rate = 1.0 mL/min, triplicate measurments

3.3.6 Binding of As(V) to PLHis-CPG

Similar to Cr(VI), arsenic exists as an oxyanion in solution and may effectively bind to the PLHis column. Using As(V) as the target binding species, the sensitivity of the hydride generation FAAS (HG-FAAS) detection permitted the use of a 500 ppb As(V) influent solution. 500 ppb As(V) was run through the column in a variety of solutions to evaluate the effect of the presence of competing ions on As(V) binding. Several representative breakthrough curves of As(V) in various solutions and various concentrations of HCl can be seen in Figures 3.9 and 3.10. The only solution that showed significant binding was As(V) in distilled/deionized water and As(V) in 0.1 mM HCl. The calculated capacity was determined to be 4.5 ± 0.5 μmol As/g PLHis-CPG. All of the other solutions tested: 0.05 M ammonium acetate at pH values of 4.0, 5.0, 6.0, and 7.0, using sodium hydroxide or acetic acid to adjust the pH, 0.1 M NaCl, 0.1 M HNO_3, 0.05 M Tris, 0.05 M phosphate buffer, 0.1 M HCl, 0.01 M HCl, 1.0 mM HCl, 0.1 M $HClO_4$, 0.01 M $HClO_4$ and 1.0 mM $HClO_4$ showed no capacity and their curves broke through almost immediately.

Figure 3.9 Breakthrough curves of 500 ppb As(V) on PLHis-CPG in various solutions

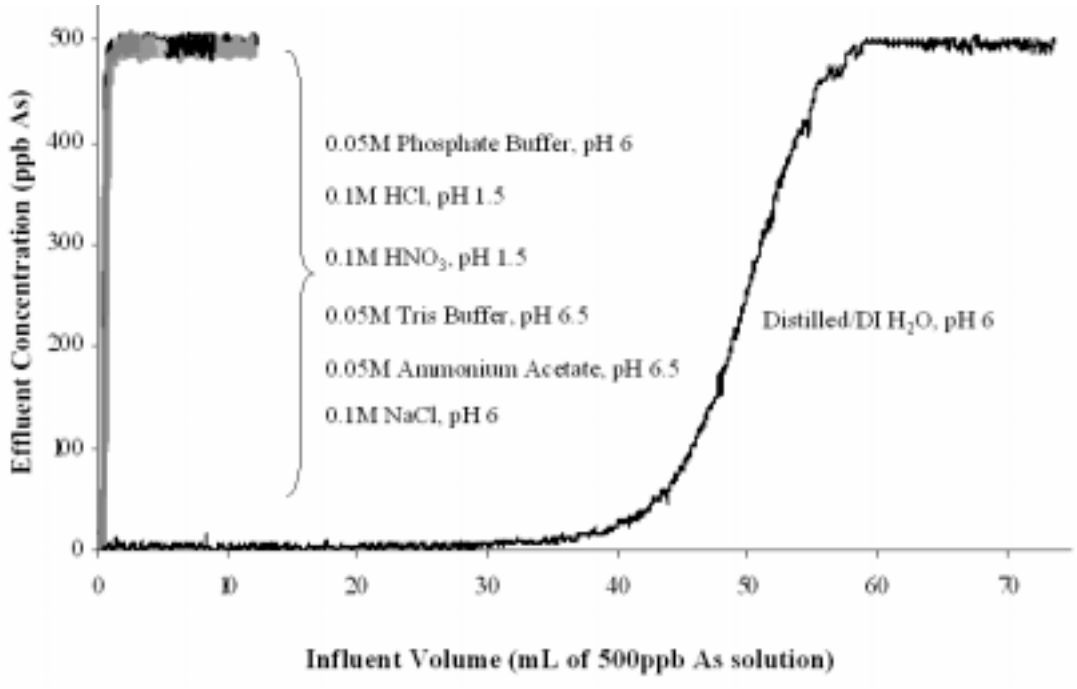

Figure 3.10 Breakthrough curves of 500 ppb As(V) on PLHis-CPG in various HCl solutions

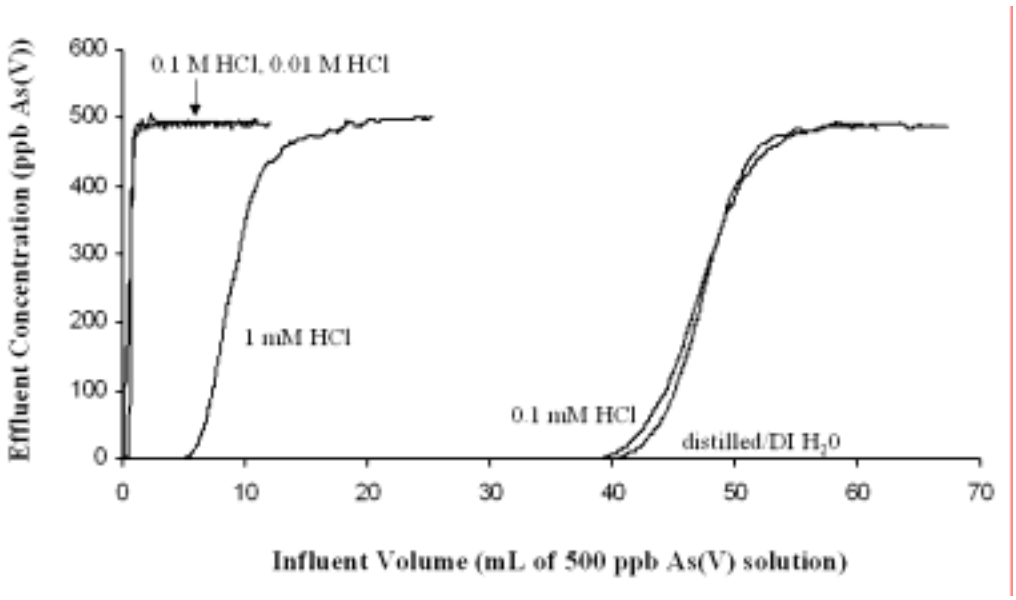

While the disruption of binding showed interferences similar to that seen for Cr(VI), they were much more severe in the case of As(V). Previous studies that demonstrated an anion exchange capacity of 106 mg As/g dry resin (poly(ethylenmercaptoacemide)) at pH 2, also experienced a reduction in capacity in the presence of other anions (Cl^- and SO_4^{2-}) [122]. It has also been shown that the As(V) capacity is very significantly reduced on the commercially available exchange resin, Dowex 11, in the presence of SO_4^{2-} [113].

Although the capacity of PLHis-CPG for As(V) is not very large, 4.5 ± 0.5 μmol As/g CPG; the extended baseline in the breakthrough curves indicates a dominance of strong binding sites ($K > 10^6$) with effluent concentrations below 8 ppb, the limit of detection for the HG-FAAS system.

3.3.7 Binding of Se(IV) to PLHis-CPG

Figure 3.11 shows several Se(IV) breakthrough curves. As these curves indicate, Se(IV) was also only retained on the PLHis-CPG column in distilled/DI H_2O. In each of the solutions tested it behaved similarly to As(V). The maximum capacity for Se(IV), in distilled/DI H_2O, was calculated to be 4.6 ± 0.4 μmol Se/g CPG. Clearly, Se(IV) suffers from the same anion interferences as As(V).

Figure 3.11 Breakthrough curves of 500 ppb Se(IV) on PLHis-CPG in various solutions

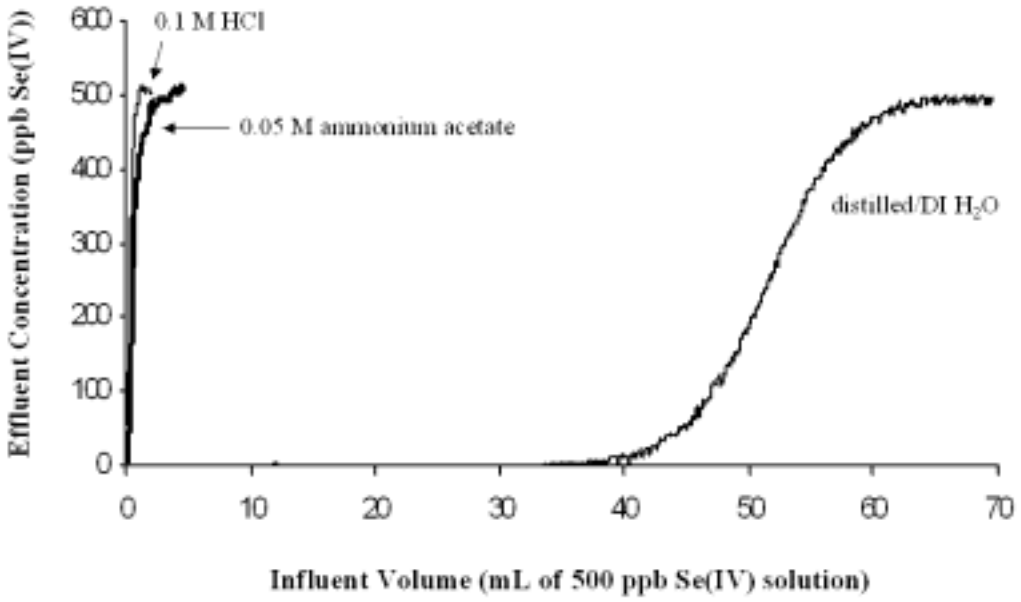

It is important to note that while the cation metals are easily stripped from the PLHis-CPG column in a few hundred microliters of acid, the oxyanions of As and Se do not come off as easily. Once again, attempts were made to strip the oxyanions (arsenates and selenites) off the column using a variety of solutions. The most effective means of stripping the oxyanions was determined to be 0.1 M HNO_3, the same solution used to remove chelated cations and Cr(VI) from PLHis-CPG. Each of the oxyanions studied can be quantitatively removed from the column in 10 mL of 0.1 M HNO_3 flowing at 1 mL/min.

3.4 CONCLUSION

In addition to binding metal cations, PLHis-CPG was also shown to bind the oxyanions of Cr(VI), As(V) and Se(IV) in acidic solution through the protonated imidazole. Oxyanion binding with PLHis-CPG suffers from a reduced capacity in the presence of competing anions in solution with interferences decreasing in the order: sulfate, nitrate, chloride, phosphate and acetate. The imidazole side chains of PLHis are weak base exchanger sites, which limits their selectivity for the metal-oxyanions investigated. Due to the fact that the oxyanions are not as easily released, PLHis-CPG is not as likely a candidate for oxyanion preconcentration as is the case for cationic metals. However, the efficient binding suggests utility as a polishing step in oxyanion remediation, although a more efficient means of column reclamation is still needed to minimize the volume of the strip solution.

Chapter 4: A Comparison of Poly-L-Aspartic Acid and Poly-L-Glutamic Acid for Chelation of Metal Cations

4.1 INTRODUCTION

Recently, a significant amount of work has focused on the development of novel systems for remediation and preconcentration of heavy metals from contaminated waste streams. An interesting focus in this development has been the use of short chain, amino acid homopolymers immobilized onto a solid support [39-42, 44, 45, 59-62]. By using amino acids as building blocks, with their various side chains, a variety of functionalities are available for coordination to metal ions. Through proper utilization of these various functionalities and the flexibility afforded by a surface-anchored linear polymer, the newly developed chelators can exhibit specificity, a highly desired characteristic in metal remediation.

In previous studies various poly amino acid chains have been immobilized onto controlled pore glass [39, 40, 42, 44, 82, 123], gold minigrids [45], porous carbon [41] and both silica and cellulose-based membranes [59-62] and their metal binding abilities were characterized. In all instances the immobilized poly amino acid chains were effective metal chelators.

Studies involving immobilized poly-L-cysteine (PLCys) with its thiol side chain functionality demonstrated its preference for soft acid metals such as Cd^{2+} and Pb^{2+} over metals such as Co^{2+} and Ni^{2+} [39-41, 62]. In contrast to PLCys, immobilized PLAsp [42, 44, 45, 60, 61] and poly-L-glutamic acid (PLGlu) [59-62] with carboxylate side chains,

showed significant Cu^{2+} and Pb^{2+} capacity. It has also been shown that poly-L-histidine (PLHis), with its imidazole side chain, is capable of binding metal cations at neutral pHs and metal oxyanions (*e.g.*, the chromates, arsenates and selenites) at acidic pHs when the imidazole is protonated [123]. The general binding trends in all of the above cases follow expected general trends based on the available cationic or anionic functionalities on the peptide.

However, it is not obvious whether more subtle changes impact metal chelation. In this study, PLAsp and PLGlu (Figure 4.1) were evaluated. The primary difference between the two amino acids is the added methylene group in the side chain of glutamic acid. The purpose of this study was to compare and evaluate the metal binding characteristics of PLAsp and PLGlu immobilized onto CPG in an attempt to determine if this slight difference in the two metal binding functional side chains has an effect on the binding strengths (i.e., formation constants) or on the number of metals binding to these polymers.

Figure 4.1 Structures of Poly-L-Aspartic Acid and Poly-L-Glutamic Acid

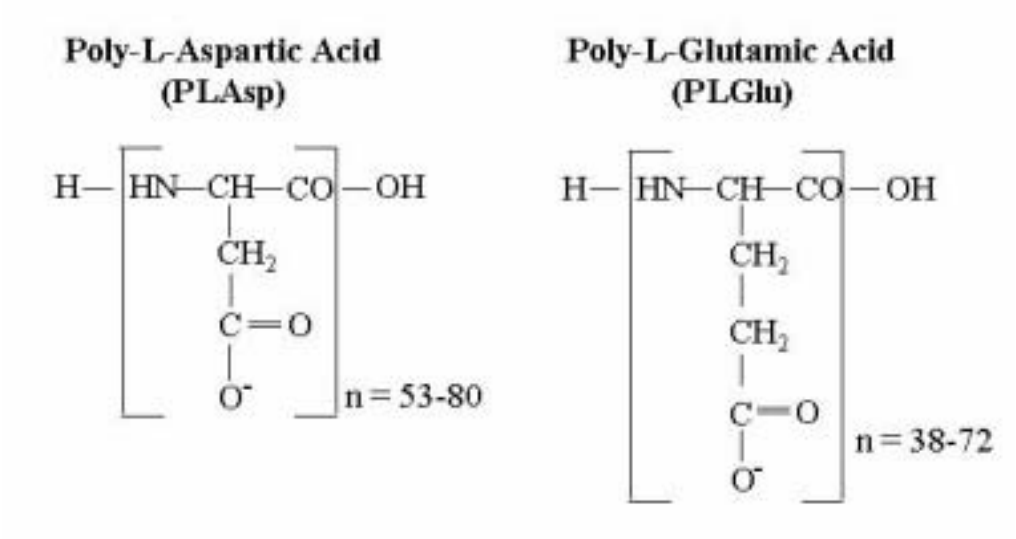

4.2 EXPERIMENTAL

4.2.1 Instrumentation

A Perkin-Elmer model 4000 flame atomic absorption (FAA) spectrophotometer with an acetylene/air flame was used for all metal determinations. Hollow cathode lamps for the metals of interest were operated at the currents recommended by their manufacturers. Wavelengths for Cd, Co, Cu, Mn, Na, Ni and Pb were 228.8, 240.7, 324.8, 279.5, 589.0, 232.0 and 283.3 nm, respectively. A monochromator bandpass of 0.2 nm was used for Co, Mn and Ni; 0.4 nm for Na; and 0.7 nm for Cd, Cu and Pb.

A simple flow injection manifold consisting of an eight-roller peristaltic pump (Ismatec minicartridge MS-REGLO) and two two-way, double inlet rotary valves (Rheodyne 5020) were used. All connections were made with 0.76 mm i.d. PTFE tubing [42].

Approximately 0.1 g of immobilized PLAsp-CPG and immobilized PLGlu-CPG were each packed into two separate 3 mm i.d. x 25 mm long glass columns with 70 mm PTFE frits (Omnifit). The empty bed volume of the column, packed with controlled pore glass is approximately 0.085 mL. A Kel-F tee was placed between the column and the nebulizer to provide air compensation and to minimize noise.

A Varian Ultramass inductively coupled argon-plasma mass spectrometer (ICPMS) was used for multi-metal analysis and analysis of breakthrough curves in the determination of formation constants. The RF power to the plasma was set at 1.2 kW, the coolant gas, auxiliary gas and nebulizer gas were set at 15 L/min, 1.05 L/min and 0.9 L/min respectively. The breakthrough curve data was collected in peak hopping scan

mode and time resolved acquisition mode with a sampling depth of 6 mm. In the multi-metal studies the following isotopes were monitored: Ni (58.6), Cu (63.65), Se (80), Cd (111) and In (115). The argon dimmer (m/z=80) was also monitored to indicate instrument drift or fluctuations. Indium was used as an internal standard and teed into the sample line after the column but prior to point where the solution entered the nebulizer.

4.2.2 Reagents

All chemicals were reagent grade unless noted, and deionized, distilled water was used to prepare solutions. All glassware was soaked in 4 M HNO_3 overnight before use. Poly-L-aspartic acid (Sigma) [DP(vis) 80, MW(vis) 11,000] and poly-L-glutamic acid (Sigma) [DP(vis) 72, MW(vis) 10,900] were used as received. The controlled pore glass (SIGMA, PG240-120) had a mean pore diameter of 22.6 nm and a mesh size of 80 - 120. Other reagents included 3-aminopropyltriethoxysilane (98%), nitric acid (Aldrich); acetic acid, sodium phosphate (Fisher Scientific); ammonium acetate, ammonium hydroxide (Mallinckrodt); gluteraldehyde (25%) (Sigma); and ethylenediaminetetraacetic acid (EDTA) (EM Science). Stock solutions of Cd^{2+} (Inorganic Ventures); Cu^{2+} and Pb^{2+} (SCP Science) atomic absorption standards were used to prepare the 10 ppm loading solutions for the metal binding experiments. For Co^{2+}, Na^{+}, Ni^{2+} (Baker), Mn^{2+} (Matheson, Coleman & Bell) the loading solutions were prepared from standardized solutions of the reagent grade nitrate salt. A 0.5 M ammonium acetate stock solution was prepared and purified using a 100 - 200 mesh Chelex 100 (Bio-Rad) ion exchange column.

4.2.3 Immobilization

The preparation of the PLAsp-CPG and the PLGlu-CPG followed the procedure that has previously been described in the immobilization of PLHis [123]. The process was modified slightly by attaching the polyamino acid in a pH 8.0 solution. This elevated pH should enhance the efficiency of this linkage.

Elemental combustion analysis for carbon was conducted by MHW Laboratories (Phoenix, AZ), in duplicate, on the functionalized glass at various stages of the immobilization to estimate the surface coverage of the polymers on the glass.

4.2.4 Metal Binding Characteristics of PLAsp-CPG and PLGlu-CPG

The previously described flow injection analysis system was utilized in all metal binding experiments. The pumps, tubing, hollow cathode lamp and flame were warmed up for at least 15 min prior to use. After conditioning the column, unretained, acidified (pH < 1.0) metal standards were run through the column and FAA system. The absorbance values were used to prepare calibration curves.

Upon completion of the calibration curves, a 0.05 M ammonium acetate solution (pH 7.0) was pumped through the column for 2 min at 1 mL/min to recondition the column to the neutral pH and solution conditions. The metal binding solutions were prepared by dilution from the metal standards into 0.05 M ammonium acetate, diluted from the stock, and adjusted to pH 7.0 by drop wise addition of acetic acid or ammonium hydroxide. The 10 ppm ammonium acetate-metal solution was then introduced onto the column at a flow rate of 1 mL/min and the effluent concentration was detected by FAA to ultimately produce a breakthrough curve. Once the effluent concentration equaled the

influent concentration, the sample flow was stopped. Ammonium acetate was passed through the column and emptied into waste for ~10 s (i.e., 0.16 mL) to remove the remaining metal-containing solution from the lines and the column dead volume. The metals were stripped from the column by flowing 0.1 M HNO_3 for 5 min at 1 mL/min through the column and collecting the effluent in a 25 mL volumetric flask for subsequent analysis by FAA as previously described in Section 2.2.4. Breakthrough curves and strip solution data were analyzed for each of the target cations (Cd^{2+}, Co^{2+}, Cu^{2+}, Mn^{2+}, Na^{+}, Ni^{2+} and Pb^{2+}), resulting in a relative binding capacity for each of the metals. This procedure was followed on both the PLAsp-CPG column and the PLGlu-CPG column. All metal binding experiments were performed in triplicate on both columns.

In selected studies where the ICPMS was employed because of its multi-element capabilities along with its lower limits of detection, the same procedure described above was followed.

4.2.5 Evaluation of Stability Constants

Stability constants on both PLAsp and PLGlu were determined using Cd^{2+}. The on-column method of determining stability constants has been previously described [39, 40]. Determination of K_f of the stronger sites was attempted by equilibrating the PLAsp-CPG or the PLGlu-CPG with known excess concentrations of EDTA and Cd^{2+}, which lowered the free Cd^{2+} concentration and should permit evaluations without generating concerns about the loss of Cd^{2+} to the container walls because of the metal buffer provided by the Cd-EDTA system. The stability constants for Cd^{2+} and EDTA are well

documented, and binding characteristics of Cd^{2+} for PLAsp and PLGlu are experimentally measured in this study. In brief, an analytical solution of a fixed volume (25 mL), containing a known concentration of standardized EDTA and a known concentration of Cd^{2+} in 0.05 M ammonium acetate at pH 7.0 was continuously recirculated through the columns for 18 h to ensure establishment of equilibrium of mobile and bound phases. The concentration of the metal remaining in the solution and the amount of metal that was bound to the column were then determined, which permitted determination of bound and free concentrations. From knowledge of the equilibrium constant of the Cd-EDTA complex and the initial and final Cd^{2+} concentration in solution, the formation constant of the metal-peptide complex and the number of sites were determined. In addition, formation constants were also estimated by analyzing the early time baseline region of Cd^{2+} breakthrough curves in the absence of EDTA on both polymers using ICPMS. The improved sensitivity of the ICPMS permits detection of the small amounts of Cd^{2+} exiting the column even in the initial stages of flow when strong binding sites would still be available.

4.2.6 Determination of the Contribution of Unreacted Amine Functionalities to Binding the Cd:EDTA Complex

Approximately 1 g of CPG was subjected to the immobilization procedure outlined above. However, a sample of the glass was set aside after the silanization step and after the gluteraldehyde addition step. The aliquots of glass that were set aside from the immobilization procedure were used to fill columns. One column was packed with 0.0757 g of silanized (with aminopropyltriethoxysilane) glass a second column was packed with 0.0653 g of gluteraldehyde-functionalized glass. Breakthrough analysis on

these two columns, in addition to the PLAsp-CPG and the PLGlu-CPG columns, was conducted by exposing the columns to various Cd:EDTA solutions. These solutions included 10 ppm Cd^{2+} in 0.05 M ammonium acetate (pH 7), 10 ppm Cd^{2+} in 0.1 M nitric acid, 10 ppm Cd^{2+} in excess EDTA (pH 7) and 10 ppm Cd^{2+} in excess EDTA (pH 3.6).

4.2.8 Mixed Metal Solution Binding Studies

Initially mixed metal solution binding studies were conducted using a single solution containing 1 ppm each of Cd^{2+}, Cu^{2+}, Ni^{2+} and Pb^{2+} in 0.05 M ammonium acetate (pH 7.0). This solution was passed through the column and the concentration of each of the metals in the effluent was monitored simultaneously using ICPMS, generating breakthrough curves. Strip solutions were also analyzed by ICPMS for verification of the bound metals.

Mixed metal solution binding studies were also conducted using FAAS. In this case, breakthrough analysis was conducted in the same manner outlined above, only this time a single solution containing 10 ppm each of Cd^{2+}, Cu^{2+}, Ni^{2+} and Pb^{2+} in 0.05 M ammonium acetate (pH 7.0) was passed through the column and the concentration of each of the metals in the effluent was monitored sequentially using FAAS. Strip solutions were also analyzed by FAAS for verification of the bound metals. This procedure was followed on both the PLAsp-CPG column and the PLGlu-CPG column and all metal binding experiments were performed in duplicate on both columns.

4.3 RESULTS AND DISCUSSION

4.3.1 Elemental Analysis

Elemental combustion analysis yielded a %C of 3.14 ± 0.21 for the precursor gluteraldehyde functionalized CPG, 1.84 ± 0.26 for the PLAsp-CPG and 2.33 ± 0.26 for the PLGlu-CPG. This corresponds to a surface coverage of 1.40 (± 0.10) x 10^{14} gluteraldehyde residues/cm^2 of CPG, assuming a surface area of 94 m^2/g of CPG (SIGMA). Due to the variability and uncertainty associated with the chain length of the PLAsp and PLGlu, no speculation was made as to the polymer coverage, and results will be reported only as *amino acid residues*/g of support. Using the %C obtained from the elemental combustion analysis, the PLAsp coverage was determined to be 2.45 (± 0.35) x 10^{14} aspartic acid residues/cm^2 of CPG and the PLGlu coverage was determined to be 2.49 (± 0.28) x 10^{14} glutamic acid residues/cm^2 of CPG. The statistically indistinguishable coverages of the two polymers to the CPG allow a direct comparison of metal capacities to be made between these two systems without correcting for differences in coverage.

4.3.2 Metal Binding Characteristics of PLAsp-CPG and PLGlu-CPG

The PLAsp-CPG and PLGlu-CPG column capacities and breakthrough curves were obtained for Cd^{2+}, Co^{2+}, Cu^{2+}, Mn^{2+}, Na^{+}, Ni^{2+} and Pb^{2+} using separate 10 ppm influent solutions of the metal in 0.05 M ammonium acetate at pH 7.0. The influent was pumped through the column at 1.0 mL/min and the metal concentration in the effluent

was measured by FIAS-FAA as a function of influent volume. Representative breakthrough curves are shown in Figure 4.2.

Figure 4.2 Breakthrough curves on PLAsp-CPG and PLGlu-CPG for a) Cu^{2+} and b) Cd^{2+}. All solutions were 10 ppm in the respective metal and 0.05 M ammonium acetate; pH 7.0.

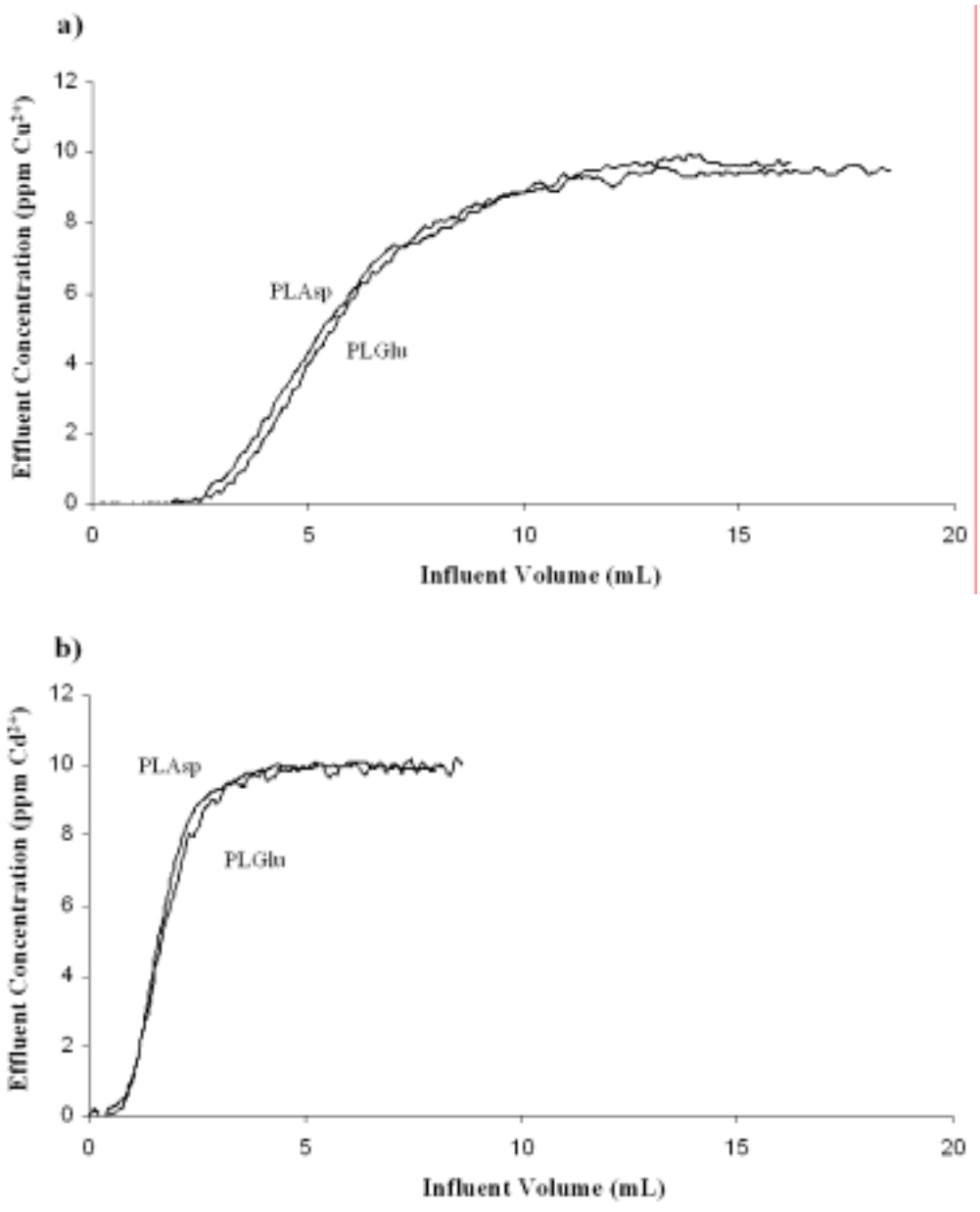

The early-time, flat baseline region present on the curves is indicative of strong metal binding. The sloped regions represent the weaker metal binding sites. By integrating the breakthrough curve, the total amount of metal retained on the column can be determined. These values are validated using the results from the stripped solutions. Since the breakthrough and strip data were in good agreement, the capacities calculated from breakthrough data and from strip data were averaged [42, 44]. Table 4.1 contains a summary of the metal binding results for PLAsp-CPG and PLGlu-CPG. As seen in this data, PLAsp-CPG and PLGlu-CPG have similar capacities for all the metals evaluated and follow a similar metal binding trend ($Cu^{2+} >> Pb^{2+} > Ni^{2+} \approx Cd^{2+} > Co^{2+} > Mn^{2+} >> Na^{+}$) as that reported by Gulumian et al. [43] for negative oxygen donors, such as carboxylates, in biological systems. It is also in good agreement with previous work on immobilized PLAsp [42, 44] and on glutamic acid-bonded silica [77].

Table 4.1 Metal-binding capacities on PLAsp-CPG and PLGlu-CPG columns determined from break through curves and strip data.[a]

Metal ion	Capacity (μmol/g CPG) on PLAsp-CPG	Capacity (μmol/g CPG) on PLGlu-CPG
Cu^{2+}	14.1 ± 1.3	13.9 ± 1.1
Pb^{2+}	6.1 ± 0.2	6.8 ± 0.2
Ni^{2+}	2.6 ± 0.2	2.7 ± 0.4
Cd^{2+}	2.2 ± 0.3	2.7 ± 0.3
Co^{2+}	1.91 ± 0.05	1.99 ± 0.06
Mn^{2+}	1.7 ± 0.1	1.59 ± 0.01
Na^{+}	0.34 ± 0.09	0.39 ± 0.08

[a] pH = 7.0, flow rate = 1 mL/min of 10 ppm influent solutions, triplicate measurements. Uncertainties expressed as sample standard deviations, reflect measurement uncertainties only.

It has been shown previously that residual functionalities from each step of the immobilization procedure do not contribute significantly to the metal binding capacity of these systems [42, 123]. Therefore this study is a direct comparison of PLAsp and PLGlu because the immobilized polymer is the main component of metal binding.

An NMR study conducted by Hikichi [124] into the specific metal-ligand interaction indicates that Cu^{2+} not only interacts with the carboxylic side chains of PLGlu but also has some interaction with the nitrogen present in the amide linkages along the backbone of the chain, while Mn^{2+} only interacts with the carboxylates. Another NMR study on the PLGlu-Co^{2+} complex suggests that Co^{2+} binds to two carboxylate groups

[125]. A polarographic study into the behavior of PLGlu-Cd^{2+} complexes indicates that two carboxylates attach to one Cd^{2+} [126]. Additionally, potentiometric studies by Imai and Marinsky [127] suggest the possibility of two different Cu^{2+}-PLGlu complexes, both of which involve the carboxylate side chains. In each of these studies the main metal binding functionality is shown to be the carboxylate side chain. As a result, all of the current metal binding studies were conducted at pH 7.0, which is significantly above the pK_as for the carboxylate side chain on PLAsp and PLGlu, which are reported to be approximately 5.4 and 4.4, respectively [42, 59, 127-129]. With pH >> pK_a maximum binding could occur since the side chain carboxylates are completely deprotonated and the chains are fully extended [44].

Structural determination has shown that PLGlu undergoes a helix-to-coil transition as the pH increases, most likely due to the deprotonation of the carboxylic acid groups [128-138]. Studies of this helix-to-coil conformational change have also considered the effects of polymer concentration [139], time [140], size of cations in solution [141], salt concentration and ionic strength [132, 142-144], and the presence of specific cations in solution [125, 126, 145-157]. Most of the studies conducted in the presence of various metals agree that the metal ions have a significant effect on the conformation of PLGlu. More specifically, the metal-PLGlu interaction shifts the helix-to-coil transition to a higher pH.

Similarly, poly (α-L-Asp) also undergoes a helix-to-coil transition [158-160]. It also exists as a compact helix at low pHs but is present as an extended random coil at higher pHs. The conformation change occurs in both of these polymers because at low pHs the H-bonds between the amide and carboxylate groups of the biopolymer stabilize

the helix and as the pH increases the carboxylates become charged, resulting in a strong electrostatic repulsion that destabilizes the helix [130, 161]. Although, it has been shown that in some instances the helix forming ability of PLAsp may be less that of PLGlu [135], Saudek and coworkers [158-160] suggest that this is due to a low helix forming ability of the β form of PLAsp. It has also been suggested that the lack of evidence of a helical form of PLAsp is due to PLAsp forming a helix at a lower degree of ionization where it also precipitates very quickly [159]. This may also be the due to the fact that the carboxylate side chains of PLAsp are shorter than those of PLGlu, resulting in a stronger electrostatic repulsion between the ionized carboxylates [159, 162]. In other words, it takes a lesser degree of ionization in PLAsp than in PLGlu to cause the same amount of repulsion. Additionally, it has been shown that due to a decrease in the hydrophobic interactions, which stabilize the helix, the helix forming ability of certain polymers decreases with a decrease in the number of CH_2 groups in the side chain [159]. In short, these studies show that PLGlu and PLAsp undergo similar -- but not identical -- conformational changes.

In addition to determining absolute capacities of the polymer functionalized CPG for various metals, these metal-binding studies provide information regarding the metal binding efficiency of the polymer chains when coupled with the polymer coverage data, calculated from the %C determined by elemental combustion analysis. The manufacturer (SIGMA) determined the degree of polymerization of PLAsp by viscosity to be ~80 and by multi-angle laser light scattering (MALLS) to be ~53. For PLGlu the degree of polymerization determined by viscosity is ~72 and by low angle laser light scattering (LALLS) it is ~38. This range in the degree of polymerization for both polymers was

used in the error analysis and, when needed, propagated as the standard deviation of the mean. Based on a degree of polymerization of PLAsp of 53 – 80 residues (SIGMA) and a Cu^{2+} capacity of 14.1 ± 1.3 μmol Cu^{2+}/g CPG for PLAsp-CPG, the number of Cu^{2+} atoms bound per chain was determined to be 2.4 ± 0.6 Cu^{2+}/chain (or 27.2 ± 2.5 aspartic acid residues/Cu^{2+} bound). The degree of polymerization for PLGlu is 38 – 72 residues (SIGMA), and with a Cu^{2+} capacity of 13.9 ± 1.1 μmol Cu^{2+}/g CPG, PLGlu-CPG binds 2.0 ± 0.7 Cu^{2+}/chain (or 28.0 ± 2.2 glutamic acid residues/Cu^{2+} bound). It is obvious from the large residue-to-metal ratios that the polymers have a large number of unused carboxylate binding functionalities that are probably not involved in coordinating the metal cations. Since it is reasonable to assume that the polymers wrap around the metal to achieve the necessary tertiary structure to bind the metal [85]; the binding similarities between PLAsp and PLGlu suggest that any differences in the chain flexibility, pK_as or steric hindrance is negligible in this application.

4.3.3 Evaluation of Conditional Stability Constants

As mentioned previously, the flat baseline region present on the breakthrough curves seen in Figure 4.2 is indicative of strong metal binding and the sloped regions represent the weaker metal binding sites. Binding studies using EDTA in solution to limit the free Cd^{2+} concentration were used for the determination and calculation of the free Cd^{2+} in solution and the amount of metal bound to the PLAsp and the PLGlu. Formation constants for Cd^{2+} binding to PLAsp-CPG and PLGlu-CPG were estimated using the relationship in Equation 4.1.

$$CdL + X \rightleftharpoons CdX + L \qquad (4.1)$$

where X is PLAsp or PLGlu and L is EDTA (Y^{4-}). The conditional stability constant for $Cd(Y)^{2-}$ (1.15×10^{13}) was based on a literature value [163].

Previous studies have used Scatchard analysis to estimate conditional stability constants for metal binding by poly-L-cysteine [40, 41]. The Scatchard function is used to determine conditional stability constants by the following expression:

$$\frac{[CdX_i]}{[Cd]} = K_i\left(n_i - [CdX_i]\right) \qquad (4.2)$$

where $[CdX_i]$ (as μmol/g resin) is the number of complexed sites of type *i*, n_i is the total concentration (as μmol/g resin) of type *i* sites and K_i is the stability constant for the i^{th} site.

However, it has been shown previously that PLAsp functionalized silica is capable of binding both cations and anions [78], and this analysis fails to consider the possibility that a negatively charged CdY^{2-} complex may bind to residual amine functionalities on the surface that remain after immobilization of the polymer chains to the CPG. Breakthrough curves were conducted on the columns containing silanized glass, gluteraldehyde glass, PLAsp-CPG and PLGlu-CPG to determine if the Cd:EDTA complex was in fact binding to the residual amines. Sample breakthrough curves from this study can be seen in Figure 4.3 and the capacities are listed in Table 4.2.

Figure 4.3 Representative breakthrough curves on a) Silanized CPG, b) Gluteraldehyde CPG, c) PLAsp-CPG, d) PLGlu-CPG; Solutions: 1) 10 ppm Cd^{2+} in 0.1M nitric acid, 2) 10 ppm Cd^{2+} in 0.05 M ammonium acetate (pH 7), 3) 10 ppm Cd^{2+} in excess EDTA (pH 7), 4) 10 ppm Cd^{2+} in excess EDTA (pH 3.6)

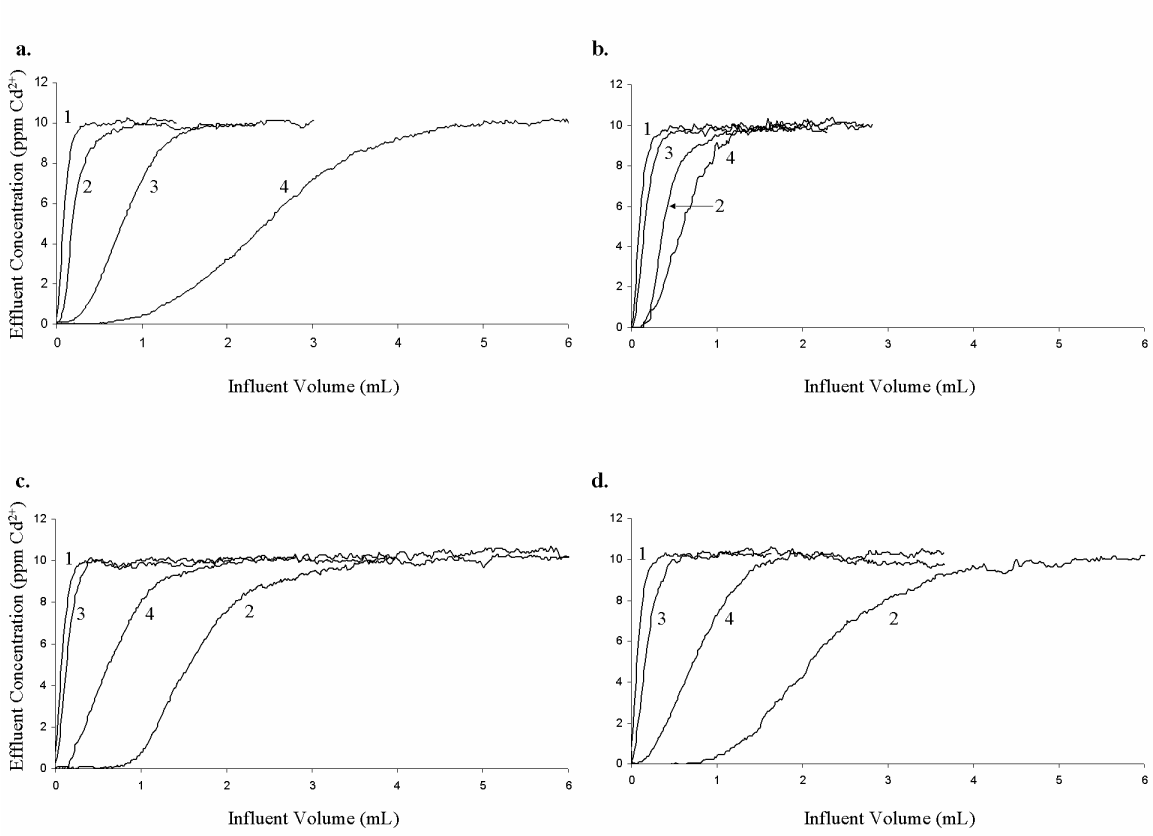

Table 4.2 Cd^{2+} Capacities from breakthrough analysis

	10 ppm Cd^{2+} Solution			
Column	Nitric acid (μmol/g CPG)	Amm. Ac. (pH 7) (μmol/g CPG)	EDTA (pH 7) (μmol/g CPG)	EDTA (pH 3.6) (μmol/g CPG)
Silanized-CPG	0.12 ± 0.02	0.29 ± 0.02	0.93 ± 0.01	2.96 ± 0.02
Gluteraldehyde-CPG	0.14 ± 0.04	0.56 ± 0.01	0.24 ± 0.02	0.87 ± 0.05
PLAsp-CPG	0.14 ± 0.01	2.20 ± 0.03	0.19 ± 0.02	0.85 ± 0.05
PLGlu-CPG	0.14 ± 0.01	2.52 ± 0.10	0.25 ± 0.02	1.19 ± 0.14

[a] Flow rate = 1 mL/min of 10 ppm influent solutions, duplicate measurements. Uncertainties expressed as sample standard deviations, reflect measurement uncertainties only.

It is interesting to note that the capacity for the Cd:EDTA complex on all of the columns is significantly higher at an acidic pH, where more of the residual, free amines will be protonated and capable of binding the negatively charged CdY^{2-}. It is obvious from this data that the unreacted amine functionalities are binding the Cd:EDTA complex. It can also be seen from this data that the addition of the polymer significantly reduces the capacity for Cd:EDTA, which would be expected considering the polymer is attaching to the free amines, essentially blocking them.

In the determination of conditional formation constants study, when the free Cd^{2+} concentration in solution is zero, Cd is still binding to the column. This is because the Cd:EDTA complex is binding. Therefore at the Y-intercept of the isotherm ([CdL] vs. $[Cd^{2+}]$), where $[Cd^{2+}] = 0$, [CdL] must be equal to the amount of Cd:EDTA that is bound because that is the only Cd species available to bind. In other words, if only free Cd^{2+}

were binding, and there was no free Cd^{2+} in solution, the amount that would be able to bind would be zero. Thus, the intercept would be 0,0.

Initially it seemed as though this may be a way to elucidate the amount of Cd:EDTA binding to the system so that the amount of free Cd^{2+} could be calculated and an accurate formation constant could be determined. Unfortunately, due to the uncertainty of the measurements we are not able to discern the free Cd^{2+} bound which prohibits us from determining the formation constant in this manner.

It was ultimately concluded that if the CdY^{2-} complex binds to the support, the *apparent amount* of bound Cd^{2+} will be higher since some of the complexed Cd is present as the CdY^{2-} species. As a result, the calculated formation constant of PLAsp and PLGlu to Cd^{2+} in the presence of EDTA is artificially high and the resulting calculated value for K can be considered the upper limit.

In order to determine the range of the actual formation constant, a minimum value of K was determined through analysis of the baseline region of the Cd^{2+} (*without EDTA)* breakthrough curves using ICPMS. Throughout this analysis Cd (111), In (115) and the argon dimer (80) were monitored. The detection limit of the ICPMS for Cd^{2+} was determined to be 0.66 ppb. Since Cd was still not detected during the flat baseline region of the breakthrough curve using the ICPMS, the free Cd^{2+} in the solution exiting the column must be less than 0.66 ppb. Substituting this information into the equilibrium expression results in the determination of $K \geq 2.0 \times 10^{8}$ for both polymers.

Thus, the calculated stability constants and site capacities for PLAsp and PLGlu are $2.0 \times 10^{8} < K < 3.8 (\pm 0.5) \times 10^{13}$, $n = 0.22 (\pm 0.04)$ μmol/g and $2.0 \times 10^{8} < K < 3.2 (\pm$

1.0) x 10^{13}, n = 0.19 (± 0.08) μmol/g, respectively. These results indicate that PLAsp and PLGlu may bind similar amounts of the Cd:EDTA complex and have the same number of sites and therefore bind equal amounts of free Cd^{2+}. This demonstrates that both polymers have similar binding capabilities for Cd^{2+}.

It is interesting to note that Lumb and Martell [164] potentiometrically determined the chelate stability constants (log K) for Cd-Asp and Cd-Glu to be 4.39 (K=2.5 x 10^4) and 3.9 (K=7.9 x 10^3), respectively, for a homogeneous solution containing the metal and amino acid monomers. With the free amino acids in solution there exists an additional carboxylate functionality at one terminus for each residue and an available amine functionality at the other terminus. In fact, they suggest a metal binding complex that utilizes both the carboxylate and amine termini on each amino acid residue.

4.3.4 Mixed Metal Solution Binding Studies

To determine how the column capacity for a specific metal is affected by the presence of other metals, a multi-metal solution was passed through the column; and breakthrough and strip analyses were conducted. Initially these studies were conducted using ICPMS due to its multi-element capabilities. However, due to the lower detection limit of the ICP compared to FAAS, the multi-metal solution contained only 1 ppm each of Cd^{2+}, Cu^{2+}, Ni^{2+} and Pb^{2+} in pH 7.0, 0.05 M ammonium acetate.

Due to the fact that all of the other metal binding studies have been done with 10 ppm metal this study was repeated using a solution that contained 10 ppm each of Cd^{2+}, Cu^{2+}, Ni^{2+} and Pb^{2+} in pH 7.0, 0.05 M ammonium acetate. In this case the metals were monitored sequentially using FAAS. Figure 4.4 contains an example of the multi-metal

breakthrough curves on PLAsp-CPG and PLGlu-CPG. The calculated capacities can be seen in Table 4.3.

Figure 4.4 Breakthrough curves on a) PLAsp-CPG and b) PLGlu-CPG from a multi-metal solution containing 10 ppm each of 1) Cd^{2+}, 2) Ni^{2+}, 3) Cu^{2+} and 4) Pb^{2+} in 0.05 M ammonium acetate, pH 7.0.

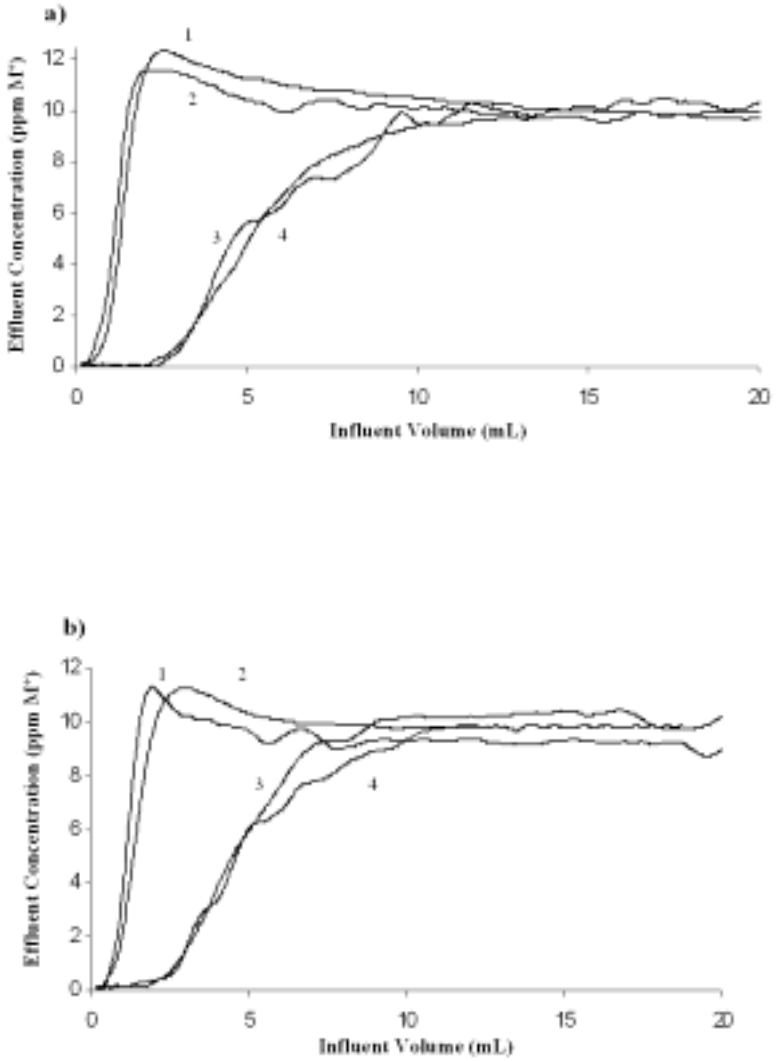

Table 4.3 Multi-metal solution binding capacities on PLAsp-CPG and PLGlu-CPG columns

Metal Ion	Capacity (μmol/g CPG) on PLAsp-CPG	Capacity (μmol/g CPG) on PLGlu-CPG
Cu^{2+}	13.0 ± 1.2	11.8 ± 2.1
Pb^{2+}	4.0 ± 0.3	4.3 ± 0.8
Ni^{2+}	1.2 ± 0.1	0.9 ± 0.1
Cd^{2+}	0.5 ± 0.1	0.75 ± 0.04

[a]10 ppm Cd^{2+}, Cu^{2+}, Ni^{2+} and Pb^{2+} in 0.05 M ammonium acetate influent, pH 7.0, flow rate = 1 mL/min, triplicate measurements

Once again, these values represent flow data and true equilibrium has likely not been achieved. As the data indicate, the binding selectivity is consistent with that determined through single metal studies and also with that previously published for carboxylate ligands [43]. The capacities were in the order $Cu^{2+} > Pb^{2+} > Ni^{2+} > Cd^{2+}$. While the calculated capacities for each metal in the multi-metal solution were lower than the capacities determined for each metal individually, the total metal binding capacity using the mixed metals solution is greater than the capacity for Cu^{2+} when run alone. (Cu^{2+} is cited since it showed the greatest individual capacity of the metals tested.) Specifically, the total amount of metal bound in the mixed metal solution is approximately 20% larger than found for the solution containing only Cu^{2+}. This is consistent with the idea that these polymers have no predetermined binding "cavity", unlike nature's metal binding proteins or traditional metal chelators such as EDTA or crown ethers. These relatively short homopolymers appear capable of adopting a different tertiary structure in the

presence of various metals, or a multi-metal solution. It may even be suggested that the formation of one metal binding cavity may instill cooperative binding to improve the likelihood of another metal binding through the new tertiary structure by altering the proximity of adjacent ligands in a favorable fashion for additional metals to bind. It is also important to note the maxima of ~12 ppm in the Cd^{2+} and Ni^{2+} curves is higher than the influent concentration of 10 ppm (Figure 4.4). Initially, when all of the sites are free, all of the metals begin to bind. Due to the selectivity sequence of carboxylate ligands, as the free sites become limited the Cu^{2+} and Pb^{2+} are able to displace the Cd^{2+} and Ni^{2+}. This supports the idea that the strong binding sites for Cu^{2+} and Pb^{2+} are stronger than the strong sites for Cd^{2+} and Ni^{2+}. Additionally, it suggests that the metal removal is not kinetically slow relative to the time scale of this experiment. Hence, the peaks in Figure 4.4 for Cd^{2+} and Ni^{2+} at approximately 3 mL of influent volume. Once Cd^{2+} and Ni^{2+} are displaced by Cu^{2+} and Pb^{2+}, their concentrations level off at 10 ppm, i.e., no additional net binding of these metals. Ritchie et al. have previously reported similar results on PLGlu with Cd^{2+} and Pb^{2+} [62].

4.4 CONCLUSION

This study showed that PLAsp-CPG and PLGlu-CPG had very similar metal binding characteristics despite the extra methylene group in the carboxylate side chain of PLGlu. These polymers are unlike nature's metal binding proteins that have a predetermined tertiary structure for metal binding. As a result, in a protein, the substitution of an asp for a glu, or vice versa, may cause a significant change in the metal

binding capabilities as might be suggested, for example, by the results of Jablonski and Morrow [165].

Metal binding experiments on PLAsp-CPG and PLGlu-CPG demonstrated that both polymers are effective metal cation chelators and exhibit similar binding selectivity for the metals tested. Both polymers possess a metal binding trend of $Cu^{2+} >> Pb^{2+} > Ni^{2+} \approx Cd^{2+} > Co^{2+} > Mn^{2+} >> Na^{+}$, with a maximum capacity for Cu^{2+} at ~ 14 μmol/g CPG. Mixed metal studies clearly demonstrated the improved selectivity of Cu^{2+} and Pb^{2+} over Cd^{2+} and Ni^{2+} for both polymers by showing that Cu^{2+} and Pb^{2+} were able to displace bound Cd^{2+} and Ni^{2+} from the columns. In general, these polymers behaved very similarly in all of the studies conducted, and should be equally suitable for trace metal preconcentration and remediation from natural and industrial waste-streams.

Chapter 5: Efforts in Developing New Immobilization Methods

5.1 INTRODUCTION

As noted previously, the immobilization procedure outlined in the previous studies (Figure 2.3) is not 100% efficient. As a result, unreacted amine functionalities remain on the surface of the CPG after immobilization of the polymer chains to the CPG. It has been shown that these residual amines contribute to anion binding and result in the inability to determine conditional formation constants using EDTA complexed metal [166]. Therefore, attempts were made to develop a method for blocking the unreacted amines or an alternate immobilization technique that utilizes a more *inert* linker. A common silane linker used to immobilize onto silica is 3-glycidoxypropyltrimethosysilane (GLYMO) [60, 62, 167-171]. Attachment of GLYMO to the silica surface results in an epoxide group on the surface to react with the amine terminus of the amino acid chain. Any residual ethoxysilane groups that remain unreacted are converted to siloxanes. Therefore, no anion reactive functionalities exist on the surface.

5.2 EXPERIMENTAL

5.2.1 Instrumentation

A Varian SpectrAA-40 flame atomic absorption (FAA) spectrophotometer with an acetylene/air flame was used for all metal determinations. Cd and Cu hollow cathode

lamps were operated at the current recommended by their manufacturers at wavelengths of 228.8 and 324.8 nm, respectively. A monochromator bandpass of 0.2 nm was used.

A simple flow injection manifold consisting of an eight-roller peristaltic pump (Ismatec minicartridge MS-REGLO) and two two-way, double inlet rotary valves (Rheodyne 5020) were used. All connections were made with 0.76 mm i.d. PTFE tubing [42].

5.2.2 Reagents

All chemicals were reagent grade unless noted; and deionized, distilled water was used to prepare solutions. All glassware was soaked in 4 M HNO_3 overnight before use. Poly-L-aspartic acid (Sigma) [DP(vis) 80, MW(vis) 11,000] and poly-L-glutamic acid (Sigma) [DP(vis) 72, MW(vis) 10,900] were used as received. The controlled pore glass (SIGMA, PG240-120) had a mean pore diameter of 22.6 nm and a mesh size of 80 - 120. Other reagents included 3-aminopropyltriethoxysilane (98%), nitric acid (Aldrich); acetic acid, toluene, acetone, sodium phosphate, ethanol, sodium hydroxide and hydrochloric acid (Fisher Scientific); ammonium acetate, ammonium hydroxide (Mallinckrodt); gluteraldehyde (25%) (Sigma); chloroacetic anhydride (97%), 1-hydroxy-1H-benzotriazol (HOBt) (98%), 3-glycidoxypropyltrimethoxysilane (GLYMO) (97%) (Acros Organics); and ethylenediaminetetraacetic acid (EDTA), N,N-Dimethylformamide (DMF), dichloromethane (DCM) (EM Science). Stock solutions of Cd^{2+} (Inorganic Ventures) and Cu^{2+} (SCP Science) atomic absorption standards were used to prepare the 10 ppm loading solutions for the metal binding experiments. A 0.5 M ammonium acetate

stock solution was prepared and purified using a 100 - 200 mesh Chelex 100 (Bio-Rad) ion exchange column.

5.2.3 N-Terminal Capping of Unreacted Amine Functionalities on CPG

The procedure previously described by Shogren-Knaak et al. was used to cap the residual unreacted amine functionalities on a portion of the silanized CPG that was set-aside during the immobilization procedure outlined previously (section 4.2.6) [172]. Approximately 0.2 g of silanized glass was allowed to react with approximately 1 mL of a 9:1 DMF:DCM solution containing 51.6 mg of chloroacetic anhydride and 40.6 mg of HOBt for 2 h with frequent mixing. A 3 mm i.d. x 25 mm long glass column with 70 mm PTFE frits (Omnifit) was packed with 0.0695 g of amine protected silanized glass. Breakthrough analysis on this column was conducted by exposing it to various Cd:EDTA solutions according to the breakthrough method used previously. These solutions included 10 ppm Cd^{2+} in 0.05 M ammonium acetate (pH 7), 10 ppm Cd^{2+} in 0.1 M nitric acid, 10 ppm Cd^{2+} in excess EDTA (pH 7) and 10 ppm Cd^{2+} in excess EDTA (pH 3.6).

5.2.4 Attempts at Immobilization Through GLYMO Linker

5.2.4.1 Method A

Initially, the CPG was activated by boiling ~1 g of the glass in 5% HNO_3 for 90 min. The solution was sonicated and placed under vacuum for several minutes in order to evacuate the pores of the glass. This step was conducted each time the CPG was placed back into solution, after being dried. The acid activated CPG was filtered in a medium

coarse, sintered glass filter, rinsed with distilled/DI H_2O, and dried overnight in an 80°C oven. Using a modification of a procedure described by Bogart et al. [170], PLAsp was immobilized to the surface of the CPG. An epoxide functionality was created on the surface of the CPG through the use of 3-glycidoxypropyltrimethosysilane (GLYMO), a silanizing agent. The acid activated glass was reacted with 50 mL of 5% GLYMO in 0.01 M ammonium acetate solution, pH adjusted to pH 5.5 – 5.8 with acetic acid, at 90°C for 6 h. After silanization, the glass was filtered in a medium coarse, sintered glass filter, rinsed with distilled/DI H_2O. 20 mg of PLAsp, dissolved in 50 mL of dH_2O at pH 8.5, was allowed to react with ~1 g of silanized CPG for 48 h at room temperature under N_2. Upon completion of the immobilization the PLAsp-CPG was rinsed, filtered, dried and packed in the microcolumn. The column required 0.0504 g of functionalized CPG. The remainder of the CPG was stored in a desiccator.

5.2.4.2 Method B

Chang et al. suggest that heating the GLYMO solution at 90°C for more than 30 min causes polymerization and loss of the functionality on the surface [167]. As a result, the same procedure as outlined in Method A was repeated, however the GLYMO solution was only heated to 90°C for 30 min. The column required 0.0684 g of functionalized CPG. The remainder of the CPG was stored in a desiccator.

5.2.4.3 Method C

An organic solvent-based procedure for the GLYMO attachment to the silica surface has also been suggested [60, 171]. Therefore, the acid activated CPG was reacted

with 50 mL of 5% GLYMO in toluene at approximately 80°C for 2 h. After silanization, the glass was filtered in a medium coarse, sintered glass filter, rinsed with distilled/DI H_2O and acetone. 20 mg of PLAsp, dissolved in 50 mL of pH 8.5, 0.01 M phosphate buffer was allowed to react with the silanized CPG for 48 h at room temperature under N_2. Upon completion of the immobilization the CPG was rinsed, filtered, dried and packed in the microcolumn. The column required 0.0801 g of CPG. The remainder of the CPG was stored in a desiccator.

5.2.4.4 Method D

Ritchie et al. also suggest that functionalization of the silica with the poly amino acid can be increased by conducting the reaction in ethanol to suppress ionization of the amine terminus on the poly amino acid chain [60]. Thus the same procedure as outline in Method C was repeated however the PLAsp attachment was conducted in a 20:30 (v/v) solution of ethanol and 0.01 M phosphate buffer at pH 8.5. The micro-column was packed with approximately 0.0828 g of CPG and the remainder was stored in a desiccator.

5.2.4.5 Method E

Ideally, the amino acid attachment in the immobilization procedure would be conducted at pH > 10, such that the amine terminus of the poly amino acid chain is deprotonated. Unfortunately, CPG cannot be subjected to pH > 8 for extended periods of time because degradation of the silica surface is possible at elevated pHs [173]. Therefore, the amino acid attachment in the current immobilization procedure cannot be

conducted at the ideal pH for optimal attachment. As a result a "reverse immobilization" procedure was investigated. Using a modification of a procedure previously outlined by Anspach, poly-L-aspartic acid was first attached to the GLYMO which in turn was attached to the CPG [169]. Approximately 0.4 g of NaOH and 0.2 g of poly-L-aspartic acid were dissolved in 100 mL of water that was cooled to approximately 5° C in an ice bath. After the solution reached the desired temperature approximately 0.5 mL of GLYMO was added. This solution was removed from the ice bath and allowed to return to room temperature and held there for approximately four hours. The solution was then heated to approximately 65° C and stirred overnight and then allowed to cool back down to room temperature. Meanwhile, approximately 0.5 g of CPG was acid activated and dried. The room temperature PLAsp-GLYMO solution was pH adjusted to 3.5 with HCl and the entire amount of acid activated glass was added. Once again the solution was sonicated and placed under vacuum for several minutes in order to evacuate the pores of the glass. This solution was stirred and heated to 95° C for approximately 3 h. The glass was then filtered in a medium coarse, sintered glass filter, rinsed with distilled/DI H_2O and allowed to dry under N_2. Once the glass was completely dry it was placed in a 150° C oven. This heating helps to ensure that any remaining ethoxysilane groups form siloxane groups [169]. The column was packed with approximately 0.0708 g of CPG and the remainder was stored in a desiccator.

5.3 RESULTS AND DISCUSSION

5.3.1 N-Terminal Capping of Unreacted Amine Functionalities on CPG

Due to the fact that it was shown that the Cd:EDTA complex was binding to the residual amines on the surface of the CPG an attempt was made to block all of the unreacted amine functionalities that may be binding the Cd:EDTA complex. Breakthrough curves were conducted on a column containing the blocked amine CPG and these curves were compared to breakthrough curves conducted on silanized glass, gluteraldehyde glass, PLAsp-CPG and PLGlu-CPG. Sample breakthrough curves from this study can be seen in Figure 5.1 and the capacities are listed in Table 5.1.

Figure 5.1 Representative breakthrough curves on a) Silanized CPG, b) Gluteraldehyde CPG, c) PLAsp-CPG, d) PLGlu-CPG, e) Amine protected silanized CPG; Solutions: 1) 10 ppm Cd^{2+} in 0.1M nitric acid, 2) 10 ppm Cd^{2+} in 0.05 M ammonium acetate (pH 7), 3) 10 ppm Cd^{2+} in excess EDTA (pH 7), 4) 10 ppm Cd^{2+} in excess EDTA (pH 3.6)

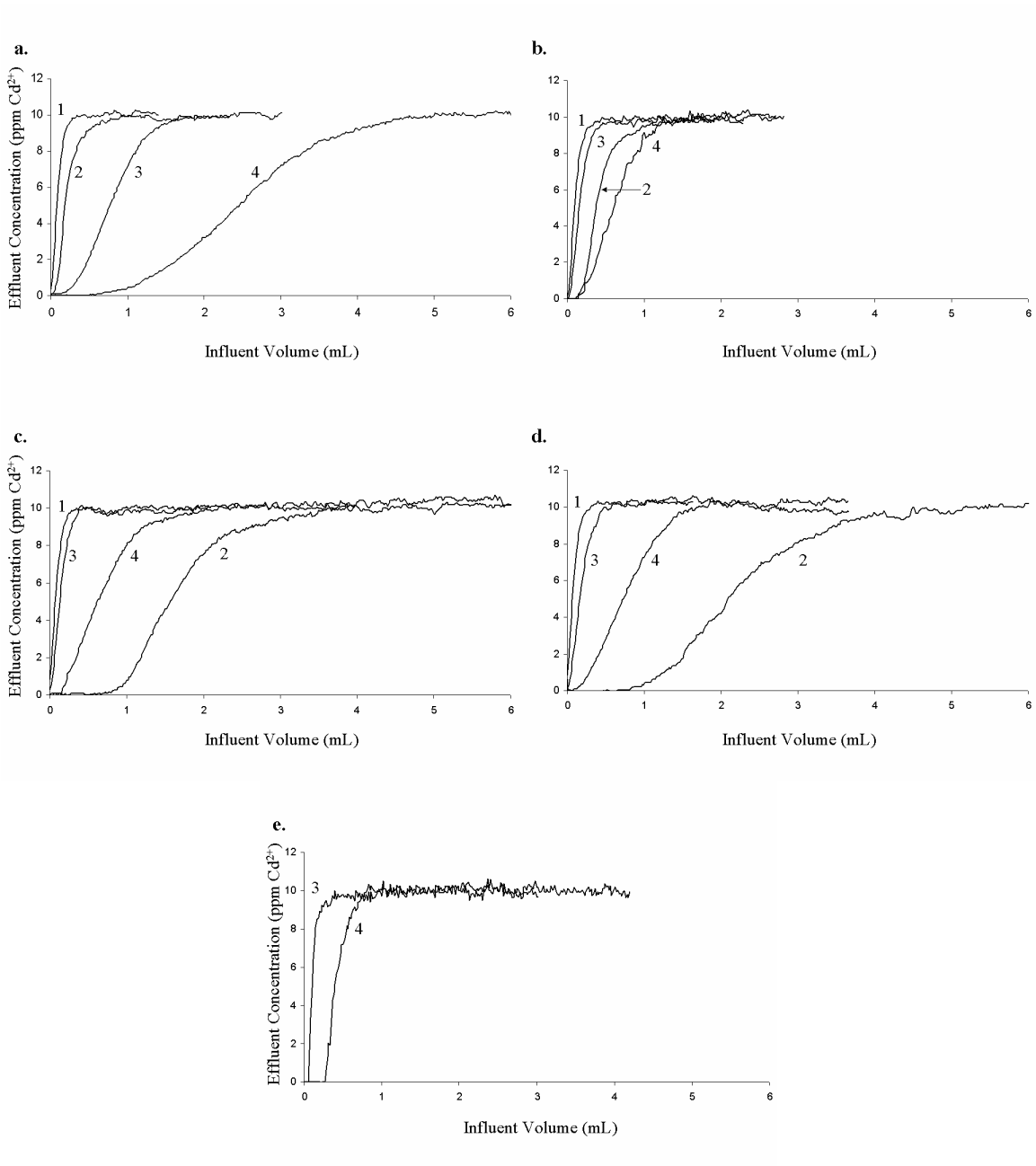

Table 5.1 Cd^{2+} capacities from breakthrough analysis[a]

	10 ppm Cd^{2+} Solution			
Column	Nitric acid (μmol/g CPG)	Amm. ac. (pH 7) (μmol/g CPG)	EDTA (pH 7) (μmol/g CPG)	EDTA (pH 3.6) (μmol/g CPG)
Silanized-CPG	0.12 ± 0.02	0.29 ± 0.02	0.93 ± 0.01	2.96 ± 0.02
Gluteraldehyde-CPG	0.14 ± 0.04	0.56 ± 0.01	0.24 ± 0.02	0.87 ± 0.05
PLAsp-CPG	0.14 ± 0.01	2.20 ± 0.03	0.19 ± 0.02	0.85 ± 0.05
PLGlu-CPG	0.14 ± 0.01	2.52 ± 0.10	0.25 ± 0.02	1.19 ± 0.14
Blocked-CPG	-------	-------	0.13 ± 0.02	0.56 ± 0.10

[a] Flow rate = 1 mL/min of 10 ppm influent solutions, duplicate measurements. Uncertainties expressed as sample standard deviations, reflect measurement uncertainties only.

It can be seen from this data that the blocking procedure significantly reduced the amount of Cd:EDTA complex binding at both pHs. However, given the capacity for Cd:EDTA that still remains on the blocked column, it is obvious that the blocking was not 100% efficient. Given that the addition of the polymer also significantly reduces the capacity for Cd:EDTA it can be concluded that if the blocking procedure were conducted on the polymer functionalized glass an even greater amount of the amines would be blocked. Unfortunately, it is likely that this would still not reach 100% efficient coverage of the free amines and Cd:EDTA would still bind. As a result, it was determined that attempting to block all of the residual free amine functionalities was not a viable approach to determining the amount of free Cd^{2+} bound by the polymer system in the presence of EDTA.

5.3.2 Alternate Immobilization Methods

As previously seen, the current immobilization procedure, using 3-aminopropyltriethoxysilane (3APS) and gluteraldehyde as an attachment for the biopolymers to a silica surface, prevents the determination of formation constants due to the anion binding capability of the unreacted amine functionalities left on the surface. As a result, several immobilization procedures were attempted using a GLYMO linker that provides an epoxide group on the surface of the CPG for linkage to the biopolymer [60, 167-171]. Although each of the techniques is slightly different they all result in the same linkage formation as seen in Figure 5.2.

Figure 5.2 GLYMO immobilization

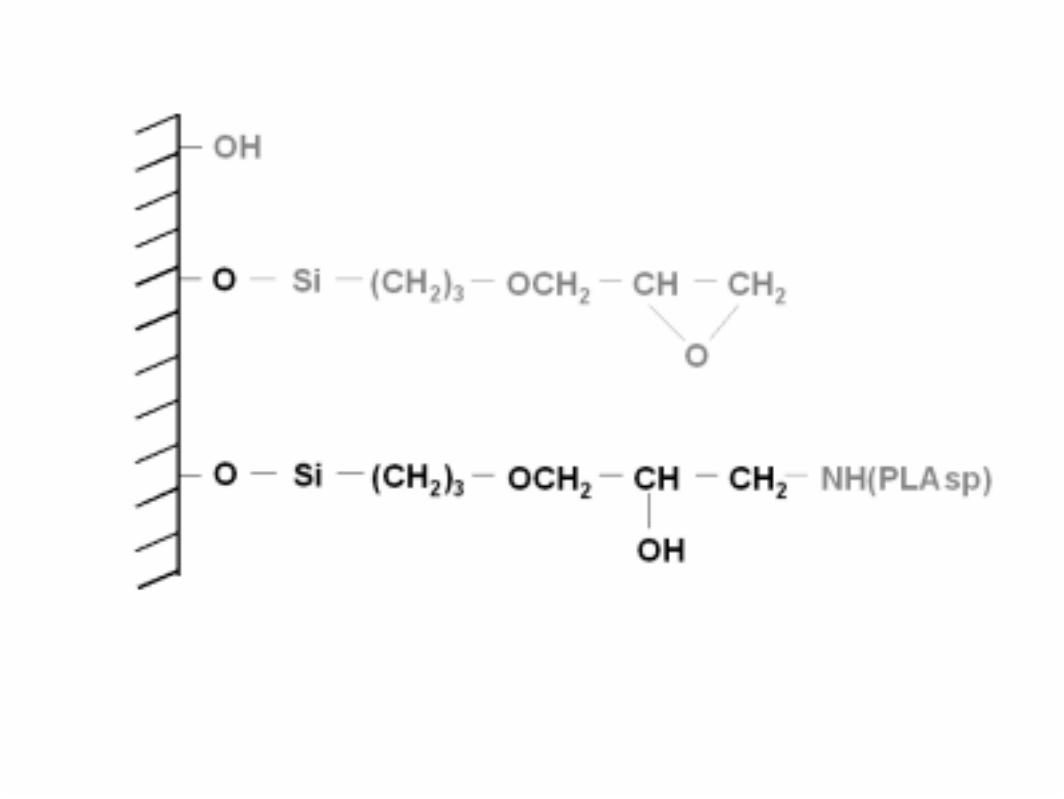

A sample of CPG from each of the immobilizations was packed into a column and breakthrough analysis was conducted with a solution of 10 ppm Cu^{2+} in 0.05 M ammonium acetate using the FIA-FAAS set-up. The capacity of each of these columns for Cu^{2+} is listed in Table 5.2.

Table 5.2 Cu^{2+} capacities from breakthrough analysis on each of the immobilizations[a]

Immobilization Procedure	**Cu^{2+} Capacity** (μmol/g CPG)
Traditional (3APS/Gluteraldehyde)	14.1 ± 1.3
Method A	3.91 ± 0.059
Method B	1.81 ± 0.11
Method C	0.56 ± 0.06
Method D	0.66 ± 0.03
Method E	2.35 ± 0.16

[a] Flow rate = 1 mL/min of 10 ppm influent solutions, duplicate measurements.

As can been seen from this data, these immobilization procedures are not as effective as the traditional method using 3APS and gluteraldehyde.

5.4 CONCLUSION

Due to the fact that the current immobilization procedure in not 100% efficient and that 3APS interferes with the determination of conditional stability constants, new immobilization methods were attempted. More specifically, an epoxide linker (3-glycidoxypropyltrimethoxysilane) was investigated. One of the advantages of this procedure lies in the fact that any unreacted epoxide groups are converted to siloxane

groups. These siloxane groups would not bind the anion complexes as seen previously. This procedure is also considerably shorter and less complex than the previous one. Unfortunately, these immobilization procedures did not produce a metal chelating system that is as effective as the previous method, as can be seen from the metal capacities determined through breakthrough analysis. However, although these immobilizations did not yield a greater Cu^{2+} capacity, some metal binding was observed, particularly with method A. Therefore, this procedure may still prove useful for not having amine functionalities when attempting the competitive binding studies with EDTA in determining conditional stability constants.

Chapter 6: The Use of Combinatorial Chemistry for the Development of Novel Metal Chelators

6.1 INTRODUCTION

Research conducted thus far has involved the study of biopolymers composed of repeating units of one amino acid residue (biohomopolymers.) Direct comparison between PLAsp and PLGlu have shown that the flexibility of the metal binding side chain on the immobilized amino acid polymers does not have a significant effect on the metal binding capabilities of the system [166]. As a result, a copolymer consisting of aspartic acid residues and glycine residues was chosen for this study in an attempt to discern if the glycine residues spaced in between the aspartic acids could alter the properties, more specifically the flexibility, of the polymer backbone and increase the metal binding capacity. However, determining the optimal ratio and sequence of aspartic acid to glycine would be difficult. Screening each of the possibilities that exist individually would take an extreme amount of time, labor and money.

Combinatorial chemistry combines a small number of chemical reagents to yield a large number of well-defined products. In fact, the pharmaceutical industry successfully uses combinatorial chemistry in compound development and drug discovery routinely [174-179]. Through the use of combinatorial chemistry a combinatorial library of peptides consisting of aspartic acid and glycine residues was designed.

It has previously been shown that micro x-ray fluorescence (MXRF) is an effective high throughput screening method for biopolymer-based libraries immobilized onto solid support beads [180]. MXRF is ideal for this type of screening because its mesoscale resolution falls between the high resolution of scanning electron microscopy (< 10 μm^2) and bulk elemental analysis by traditional x-ray fluorescence (~ 10 mm^2). Through the use of a polycapillary focusing optic on the MXRF instrument, the x-ray source can be focused to a spot size of approximately 30-50 μm in diameter.

MXRF is a nondestructive technique with minimal sample preparation. It is capable of simultaneous identification and quantification of all elements with an atomic number greater than sodium ($z \geq 11$). It also allows for single bead monitoring with a short screening time. The instrument is capable of performing single point analysis which gives spatially resolved qualitative and quantitative information; line scans which can provide concentration gradients and qualitative information; and maps or elemental imaging which covers a large area with qualitative or quantitative data. These characteristics make MXRF an ideal technique for analyzing an immobilized polypeptide library.

Through a collaboration with the Los Alamos National Laboratory Chemistry Division, MXRF will be used as a screening tool for the metal binding capabilities of a random aspartic acid/glycine library immobilized onto polymer beads. Researchers at Los Alamos have already proven MXRF successful in screening combinatorial libraries for optimizing catalytic activities [180].

6.2 EXPERIMENTAL

6.2.1 Instrumentation

An EDAX Eagle II micro x-ray fluorescence (MXRF) system was used for X-ray excitation and detection. The MXRF was equipped with a Rh target excitation source and a SiLi detector (EDAX, Mahwah, NJ). A polycapillary focusing optic was used with the X-ray source to obtain a 50 μm nominal x-ray spot size (X-ray Optical Systems, Albany, NY). The X-ray tube was operated at 35 kV and 400 μA during all analyses. The matrix chosen for each Tacky Dot image was 256x200 pixels with a 100 ms dwell time per pixel. The matrix chosen for each individual bead image was 64x50 pixels with a 100 ms dwell time per pixel. A typical imaging time for a Tacky Dot™ array of beads was 2 h. Individual beads were mapped in 10 min. The integration time of individual spectra was 100 live detector seconds. A schematic of the instrument is shown in Figure 6.1. Table 6.1 lists the element emission lines and their energies that were monitored.

Figure 6.1 Schematic of MXRF Instrument

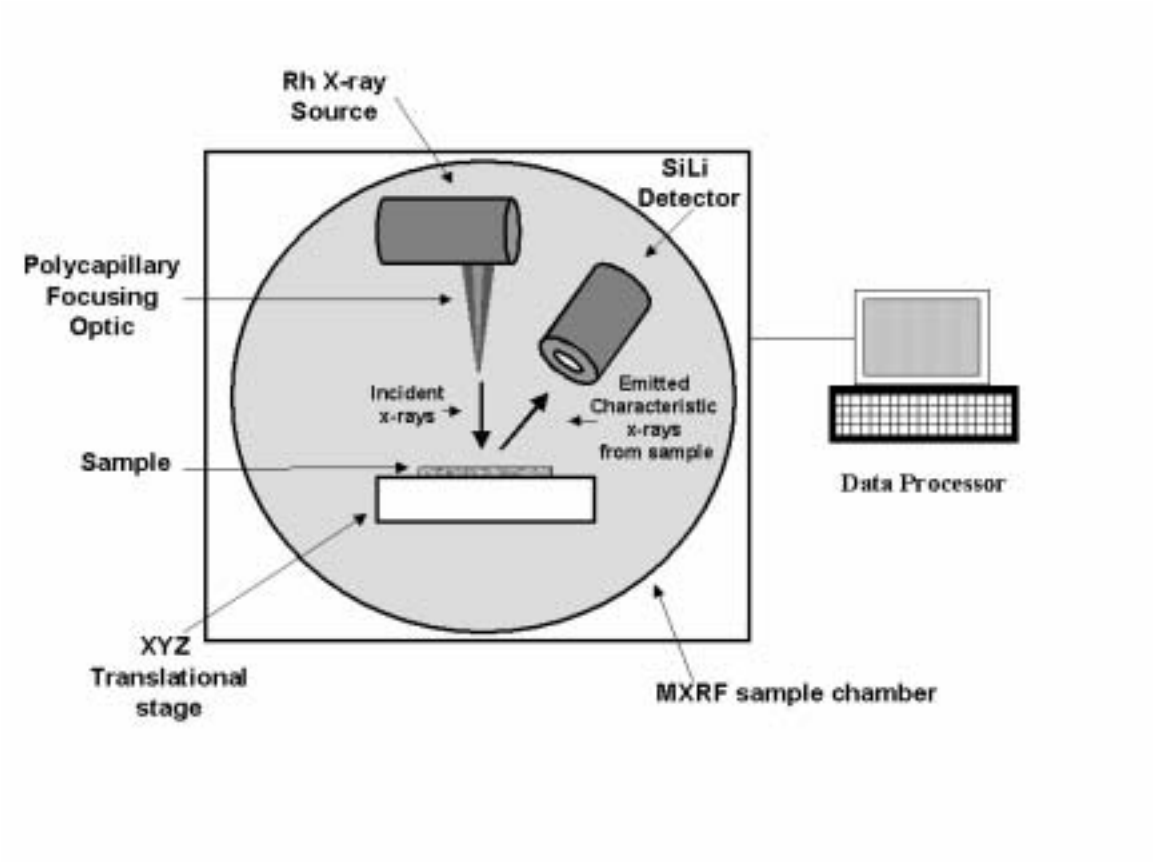

Table 6.1 Element emission lines and energies monitored in this study

Element	Emission Line	Emission Line Energy
Cl	K-$L_{2,3}$ (Kα)	2.62
S	K-$L_{2,3}$ (Kα)	2.31
Cu	K-$L_{2,3}$ (Kα)	8.05

Microscope observations were conducted on an Edman Scientific stereomicroscope. Edman degradation experiments were performed by The Institute of Cellular and Molecular Biology at The University of Texas at Austin on a PE/ABI Procise-cLc protein sequencer (Applied Biosystems, Foster City, CA).

6.2.2 Materials and Reagents

All chemicals were reagent grade unless noted; and deionized, distilled water was used to prepare solutions. All glassware was soaked in 4 M HNO_3 overnight before use. Solid-support (MBHA Resin) libraries of oligopeptides were prepared by the split and pool synthesis method (Figure 6.2), with protecting groups removed, by Biopeptide Inc., LLC (San Diego, CA). Biopeptide Inc., LLC also provided MBHA resin beads containing immobilized polyaspartic acid chains and blank MBHA resin beads. Reagents include nitric acid (Aldrich); ammonium acetate (Mallinckrodt) and trifluoroacetic acid (Fisher Scientific). A 1000 ppm stock solution of Cu^{2+} (SCP Science) atomic absorption standard was used to prepare the 10 ppm loading solutions for the metal binding experiments. A 0.5 M ammonium acetate stock solution was prepared and purified using

a 100 - 200 mesh Chelex 100 (Bio-Rad) ion exchange column. Tacky Dot™ array slides were purchased from SPI Supplies (Westchester, PA).

Figure 6.2 Split and pool library synthesis

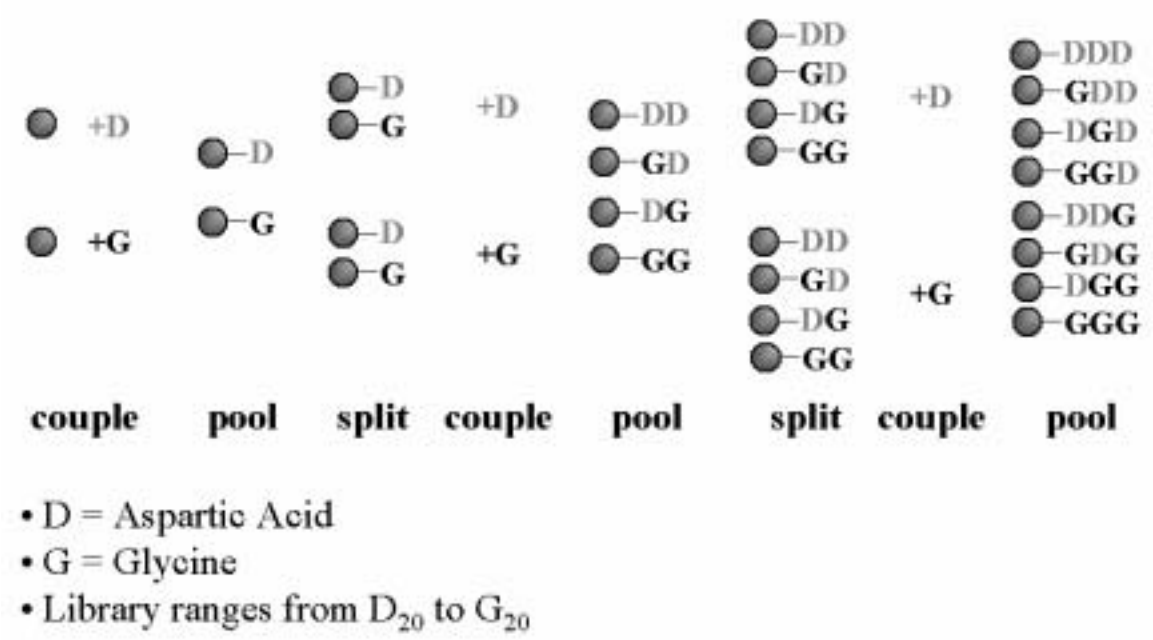

- D = Aspartic Acid
- G = Glycine
- Library ranges from D_{20} to G_{20}

6.2.3 Screening of Oligopeptide Library for Cu^{2+} Binding

Approximately 30 mg of MBHA resin-bound 20-mer oligopeptide combinatorial library was immersed in approximately 1 mL of solution containing 10 ppm Cu^{2+} in 0.05 M ammonium acetate (pH 7). Additional aliquots of library beads were exposed to dH_2O, 0.05 M ammonium acetate, 0.1 M nitric acid and 10 ppm Cu^{2+} in 0.1 M nitric acid. The polyaspartic acid beads and the blank beads were also exposed to all of the solution conditions listed above. Therefore, all three types of beads were exposed to all of the solution conditions in parallel. Figure 6.3 outlines the experimental design.

Figure 6.3 Combinatorial library experiment set-up (various blank solutions have no Cu^{2+} and included: dH_2O, 0.05 M ammonium acetate and 0.1 M nitric acid)

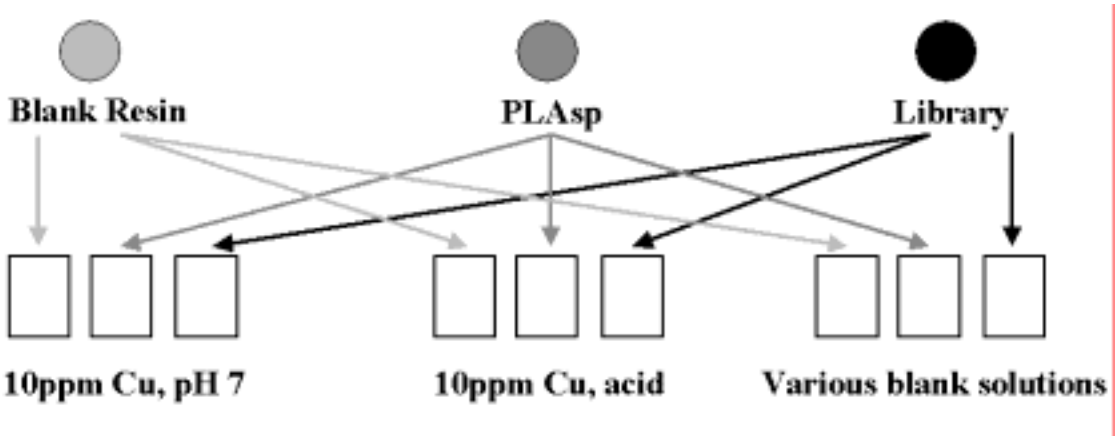

The beads were allowed to react for 24 h while being constantly mixed on an orbital rotator. The beads were then isolated by gravity filtration, rinsed 15 times with 1 mL of pH 7 dH_2O, and air dried for 24 h on filter paper. The dried beads were then immobilized onto a Tacky Dot™ slide. The Tacky Dot™ slide allows for the beads to be spatially separated and immobilized for MXRF analysis (~ 4000 beads/slide). Screening time was approximately 1 h per Tacky Dot™ plate. Specifically, the Cl Kα, Cu Kα and S Kα X-ray emission lines were monitored to detect beads that bound Cu^{2+}. Library beads that bound significantly more Cu^{2+} than the polyaspartic acid beads were isolated and their amino acid sequence determined by Edman Degradation. The Edman Degradation procedure is outlined in Figure 6.4.

Figure 6.4 Edman Degradation procedure

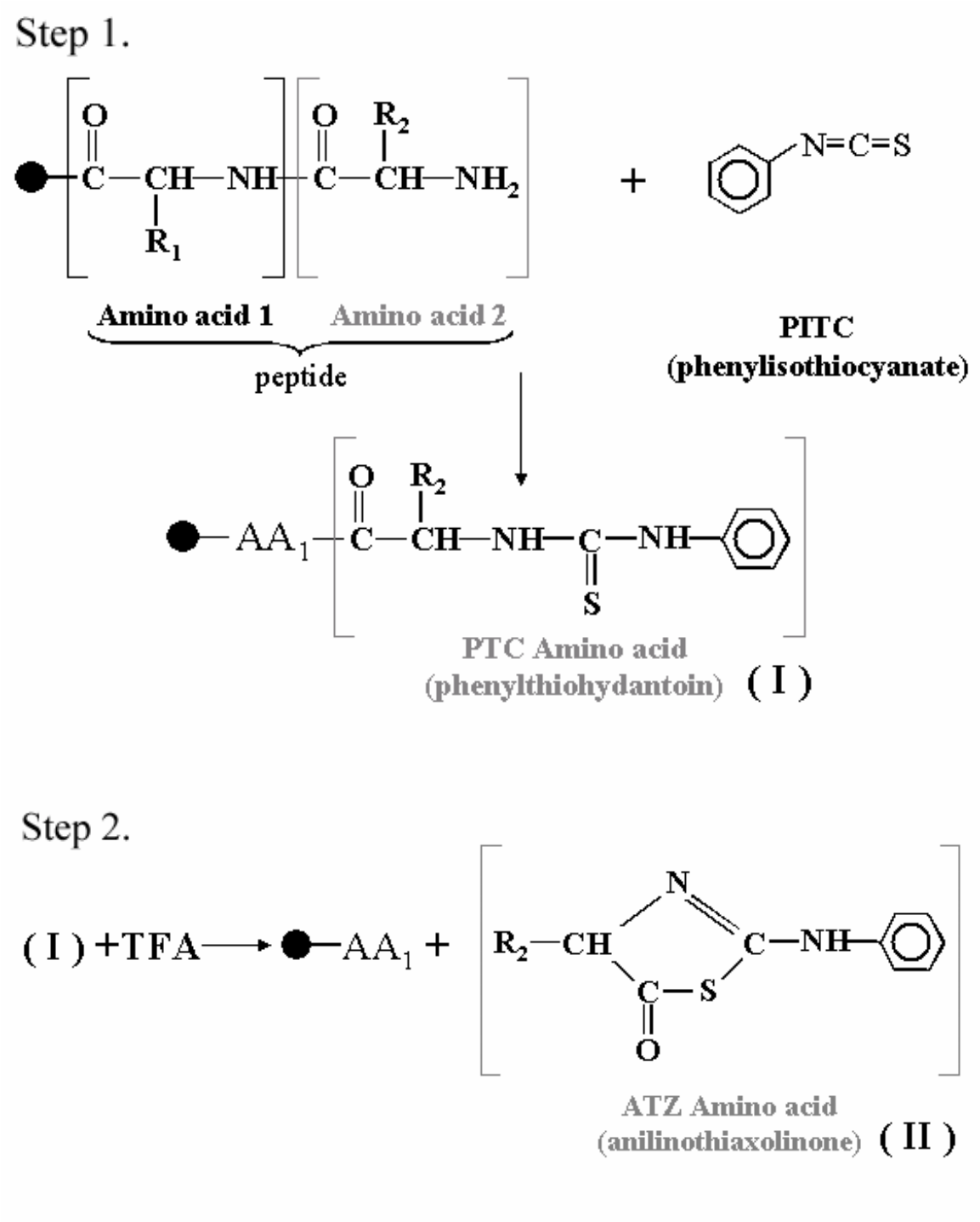

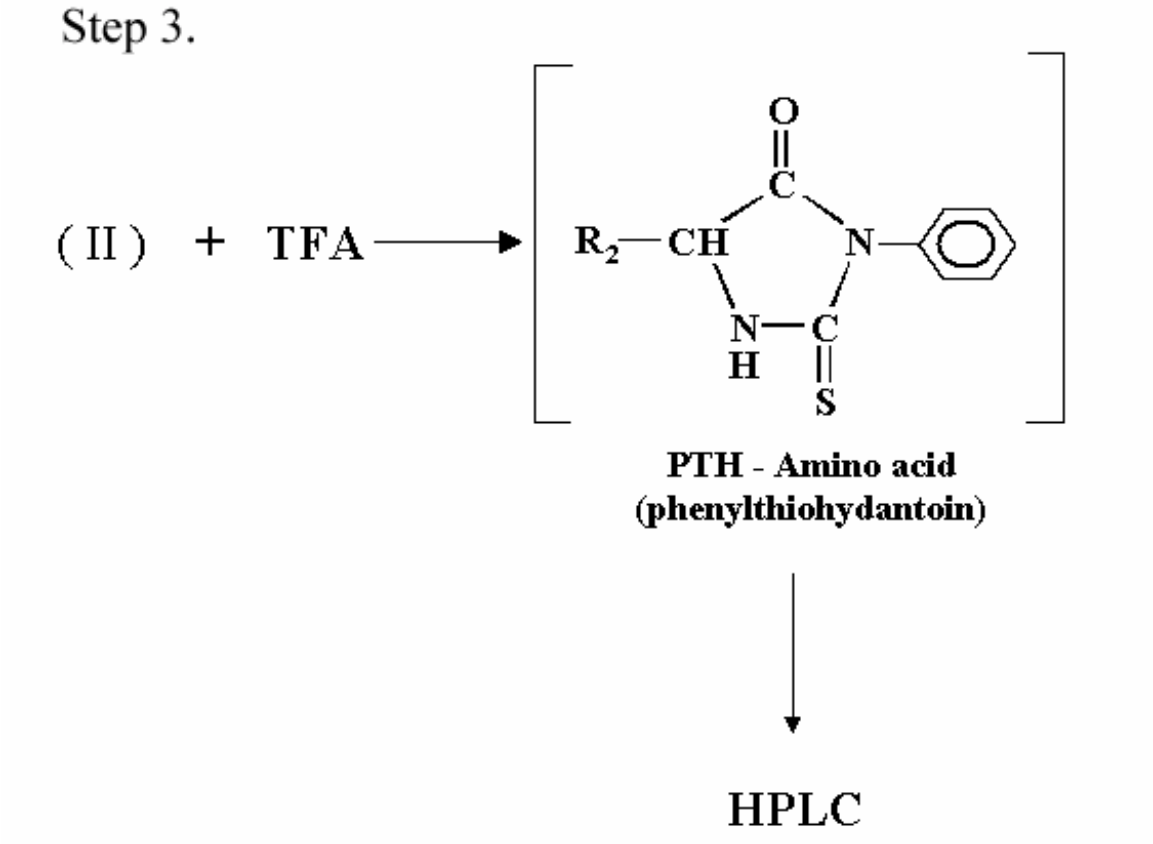

6.3 RESULTS AND DISCUSSION

6.3.1 Screening of Oligopeptide Library #1 for Cu^{2+} Binding

The initial combinatorial library, consisting of 20 amino acid residue chains (fully deblocked) immobilized onto polystyrene beads was purchased from Biopeptide Co. LLC. The peptides are immobilized onto the beads through t-Boc chemistry. These polymer chains were composed of random combinations of aspartic acid residues and glycine residues, ranging from 20 aspartic acid residues to 20 glycine residues, including all permutations in between. The glycine residues are essentially spacers between the carboxylate side chains of the aspartic acid residues and will add flexibility between the metal binding functionalities. The beads are approximately 100 μm in diameter and

should contain only one amino acid sequence per bead. The library was screened against PLAsp (n=20) beads that were treated under the exact conditions of the library to determine the effects of the glycine "spacers". A set of beads with no polymer attached was also evaluated as a "blank". Figure 6.5 displays a micrograph of a Tacky Dot™ plate with immobilized beads.

Figure 6.5 Tacky Dot™ plate

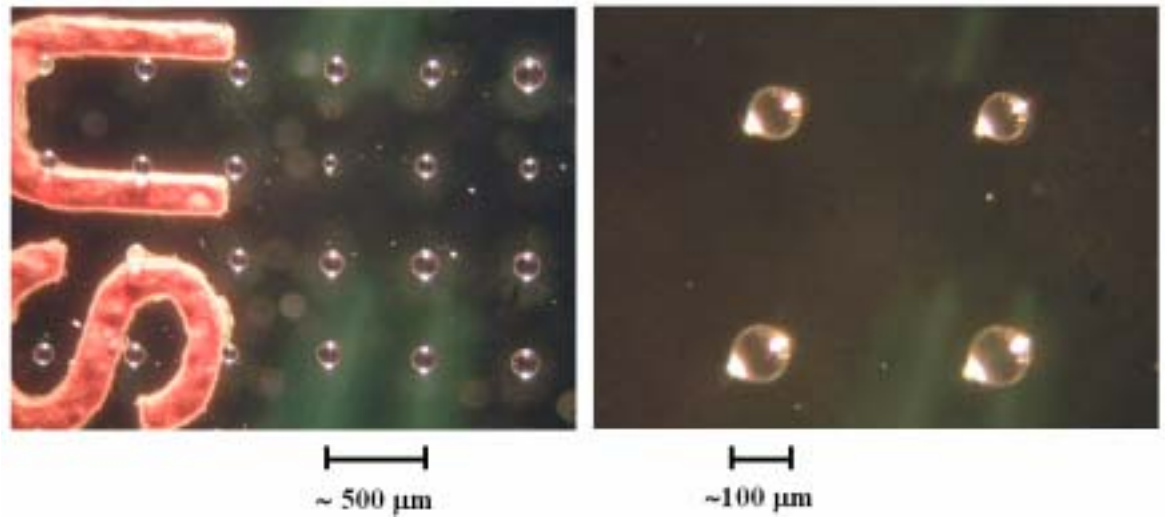

After exposure to the various solutions the library arrays were screened by MXRF for the presence of Cu^{2+}. The library arrays were compared to the PLAsp beads to locate a bead that had a significantly higher Cu^{2+} signal, thus indicating a "successful" bead. Si and Cu MXRF maps of a library array can be seen in Figure 6.6.

Figure 6.6 Si and Cu MXRF maps of a library array (exposed to 10 ppm Cu at pH 7)

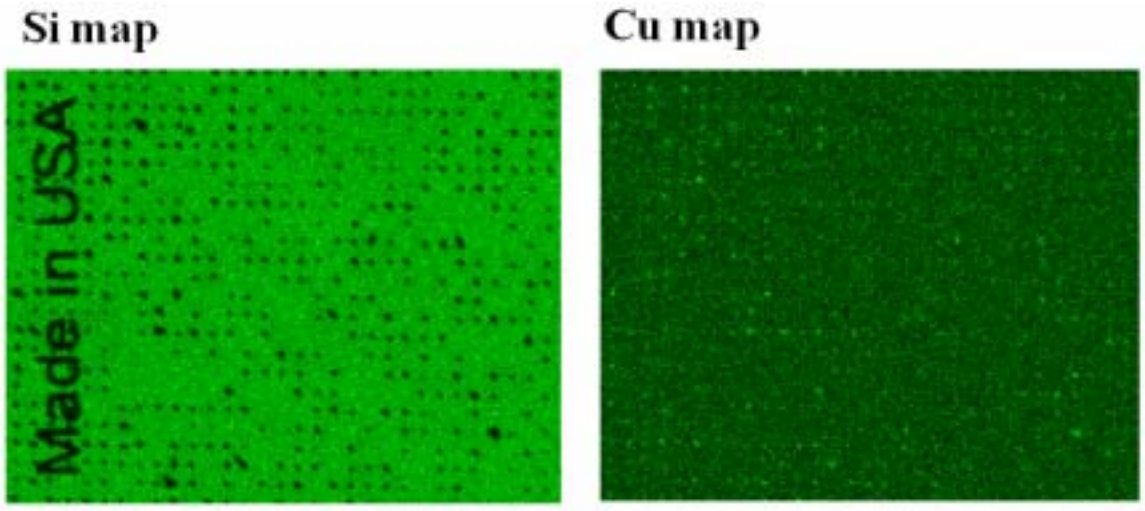

The Si map in Figure 6.6 is a negative image of the library array on the Tacky Dot™ plate. The plate is composed of Si but the beads do not have any Si. Therefore the plate gives a signal but the beads do not and they appear as dark spots on the slide. The Cu map shows a number of beads that are much brighter than the background. This indicates that these beads have a higher abundance of Cu than the surrounding areas. A micrograph of a single bead along with a high-resolution x-ray image of one of the Cu binding beads is shown in Figure 6.7.

Figure 6.7 a) Micrograph of a single bead b) High-resolution map of a single Cu binding bead

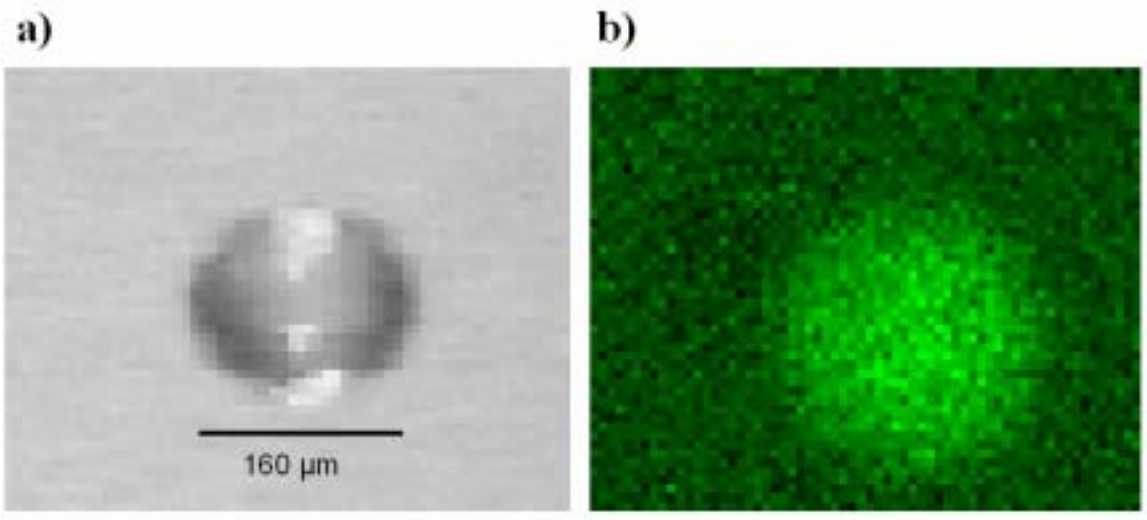

The presence of color across the bead in Figure 6.7b indicates that the Cu is binding throughout the entire bead. Figure 6.8 displays an x-ray spectrum taken from a library bead that bound Cu and one that did not. These spectra show the Cu peak present at approximately 8 keV in the bead that bound Cu but no peak is present in the non-binding bead.

Figure 6.8 X-ray spectra a) Cu binding bead b) Non-binding bead

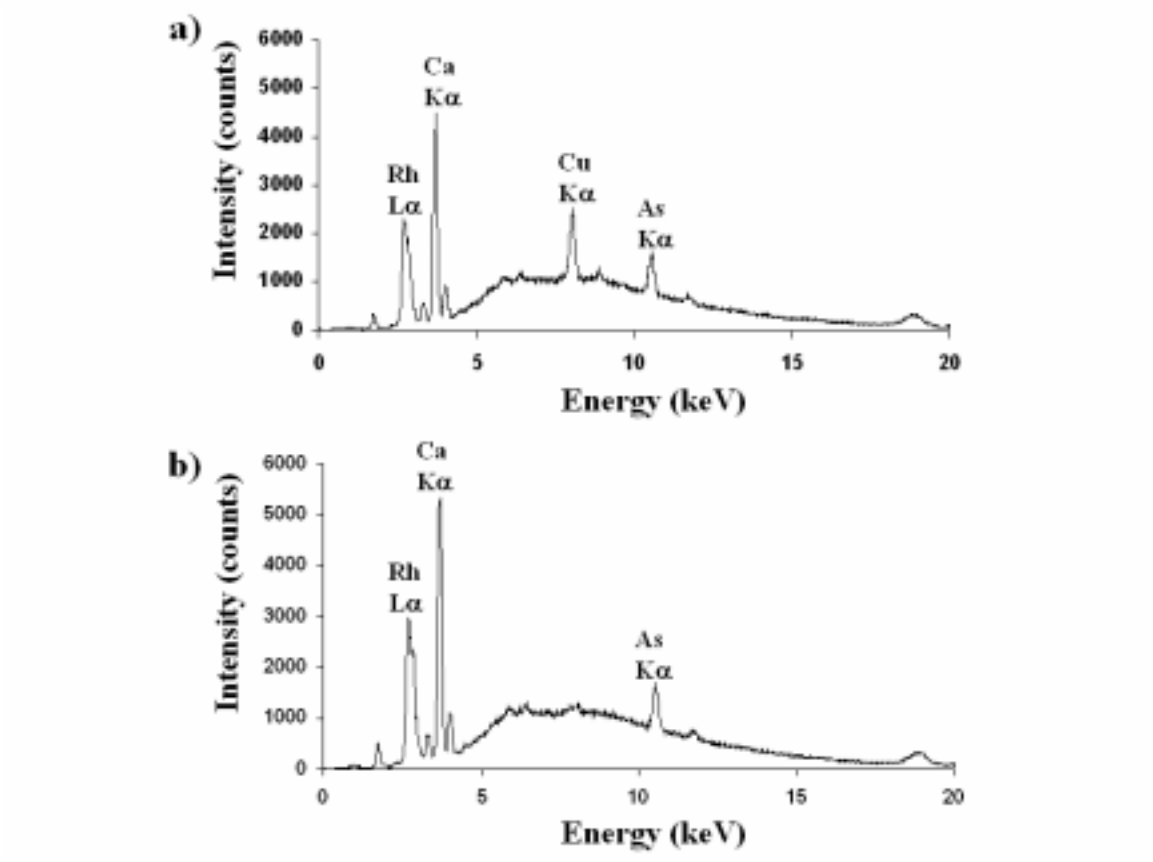

Each of the sets of beads were analyzed in this manner. Table 6.2 contains the Cu intensities for the various beads in each of the solutions tested. It is important to note that although the beads do vary slightly according to size, the Cu signal does not correlate with the size of the bead. In other words, the size of the bead is not a major determining factor in dictating the differences noted in the amount of Cu bound.

Table 6.2 Cu intensities for beads (counts per second)

	Bead		
Reaction Conditions	**Blank Resin** (n = 5)	**PLAsp** (n = 5)	**Library** (n = 5)
None	23 ± 4	25 ± 4	23 ± 2
Ammonium Acetate	43 ± 26	28 ± 5	23 ± 2
10 ppm Cu (pH 7)	51 ± 20	135 ± 25	205
			181
			200
			210
			234
			207
10 ppm Cu (acid)	62 ± 31	24 ± 2	25 ± 4

The intensities for the library beads exposed to 10 ppm Cu (pH 7) are not expressed as an average because these intensities were hand selected to show a representative sample of the highest counts obtained for library beads exposed to Cu (pH 7). The library beads that did not bind Cu had Cu intensities of 46 ± 2 cps. This data indicates that there are several library beads that bind significantly more Cu than the PLAsp beads, which had an average Cu intensity of 135 ± 25 cps. The blank beads had a Cu intensity of 51 ± 20 cps which is slightly higher than the background cps obtained from the blank solution and can be attributed to incomplete rinsing of the beads. The blank beads essentially bound no Cu (pH 7). Therefore the Cu binding on the other two sets of beads (PLAsp and library beads) can be attributed to the polymer immobilized onto the bead. Additionally, the polymers did not bind any Cu in acidic conditions,

which has previously been shown to be the case with the other systems that have been studied [39, 40, 42, 44, 82, 123, 166].

6.3.2 Edman Degradation – Round 1

The library beads that were identified by MXRF to have the greatest Cu intensity were selected for Edman Degradation. These beads were individually, hand picked off of the Tacky Dot™ plate and run. Ideally Edman Degradation will yield a single chromatograph from each cleavage step of the degradation with one clear peak indicating which amino acid residue was cleaved from the peptide. Unfortunately each chromatograph from this set of library beads had two clear peaks; one for glycine and one for aspartic acid (Figure 6.9). Initially this seemed to indicate that each bead had a mixture of sequences immobilized onto its surface.

Figure 6.9 Sample chromatograph from one cycle of Edman Degradation on a library bead

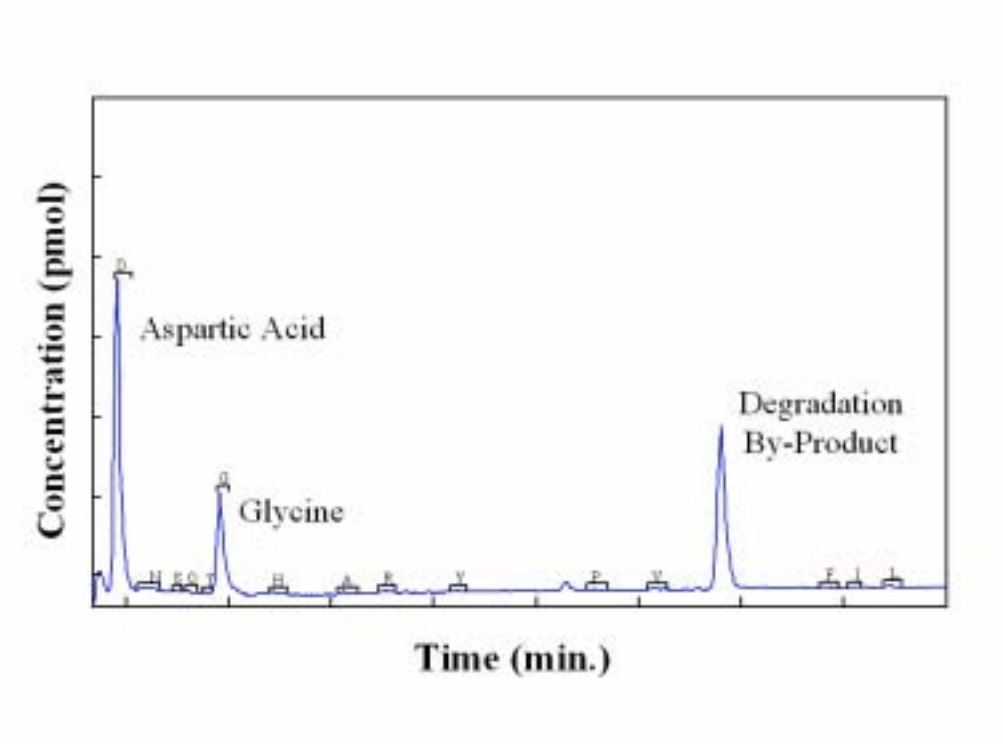

To ensure that the problem with the beads was not the sequencing procedure, library beads were sent to two other laboratory facilities capable of Edman Degradation (The Molecular Biology Core Facility at Dartmouth Medical School, and The Laboratory for Protein Sequencing and Analyses at The University of Arizona.) All of the results showed multiple peaks for each degradation step. As a result, Biopeptide Co. LLC was contacted about the possibility of mixed sequences on each bead and a second combinatorial library was provided.

6.3.3 Screening of Oligopeptide Library #2 for Cu^{2+} Binding

The second combinatorial library provided by Biopeptide Co. LLC was treated exactly as outlined in section 6.3.1. Interestingly, upon conducting MXRF analysis on the beads no Cu binding was seen on any of the beads. It was immediately suspected that the carboxylate side chain functionalities were not deblocked once peptide synthesis was complete. During peptide synthesis the carboxylate side chain on the aspartic acid residues is blocked so that the peptide bond is formed between the terminal carboxylate and the terminal amine functionality on the previous residue, not the side chain carboxylate. In order for those side chain carboxylates to be functional and capable of metal binding the protecting groups must be cleaved once synthesis is complete. Biopeptide Co. LLC acknowledged that the side chain protecting groups *may* not have been cleaved in library #2. As a result, a portion of library #2 was immersed in trifluoroacetic acid for approximately 1 h, to cleave the protecting groups, and then rinsed thoroughly with distilled/DI water.

The newly deblocked library #2 was once again treated exactly as outlined in section 6.3.1. This time the MXRF results were consistent with the first library results. Once again multiple beads exhibited Cu binding significantly greater than the PLAsp

"control" beads (Table 6.3), and once again these beads were identified and carried on for Edman Degradation.

Table 6.3 Cu intensities for beads (counts per second) exposed to 10 ppm Cu (pH 7)

Bead	Cu Intensity (cps)
Blank Resin	17 ± 2 (n = 5)
PLAsp	80 ± 5 (n = 5)
Library	293
	137
	145
	181
	125

As seen in the previous experiments with library #1, the blank beads did not show significant Cu binding and the PLAsp and the library beads only bound significant amounts of Cu in neutral solution conditions.

6.3.4 Edman Degradation – Round 2

Edman Degradation was conducted on the best performing beads selected from library #2. Unfortunately, library #2 also seemed to exhibit a mixture of sequences that was indicated by multiple peaks in each of the chromatographs.

Prior to the initiation of these studies, research on Edman Degradation revealed a possible difficulty in sequencing peptides containing glycine residues [181]. Evidently, glycine residues can be cleaved more slowly and degradation could be disrupted at glycine residues. Although this led to reservations about the feasibility of this study, personal communications with ICMB's sequencing facility operator at UT, the University

of Arizona, and Perkin Elmer technical support, affirmed that glycine residues do not pose a serious problem when sequencing by Edman Degradation. Therefore, the project was continued but with frustrating results.

Initially the multiple peaks in the chromatographs were interpreted as a mixture of sequences on each bead, which led to repeating the procedure with a new library. However, this conclusion does not explain how the library beads exhibit variable Cu binding capabilities. It would seem that if each library bead had a mixture of peptides immobilized onto the surface and participating in metal binding, then an average Cu capacity would result and each bead would look similar in terms of Cu intensity. In fact, the results show significant variation in the Cu capacity on each library bead, which indicates that each bead has a unique peptide sequence immobilized onto its surface. Ultimately the sequence of the Cu binding library beads was never determined and these observations led to the ultimate conclusion that poor Edman Degradation is the major source of complication. In fact, the presence of glycine residues in the sequences hindered the degradation process and resulted in multiple peaks in the chromatograph.

6.4 CONCLUSION

In an attempt to investigate how glycine "spacer" residues affect the metal binding capabilities of a polyaspartic acid chain a combinatorial approach was utilized. A combinatorial library of peptide sequences ranging from 20 aspartic acids to 20 glycines, and all of the sequences in between, was developed by the split and pool synthesis method. The library was screened for its Cu binding capabilities by MXRF, a high throughput elemental analysis technique. Successful library beads were determined by direct comparison to PLAsp beads. Attempts were made to sequence the beads that exhibited the greatest Cu binding by Edman Degradation. Ultimately, if these sequences

had been elucidated a polymer of the "ideal" sequence would have been synthesized, in bulk, and immobilized onto CPG and analyzed according to its metal binding capabilities.

Unfortunately the sequence of the Cu binding library beads was never determined. Due to the complex chromatography results it was initially assumed that a mixture of sequences was present on each bead. However further consideration and a closer review of the results seemed to indicate that the problem occurred in the Edman Degradation procedure due to the presence of glycine residues.

Although this experiment was not successful in establishing the relationship between the presence of glycine residues in a polyaspartic acid chain and Cu binding ability, the results were encouraging. Several beads were identified that had a significantly greater Cu binding ability than PLAsp. In addition it has been shown that the current methodology utilizing combinatorial chemistry, MXRF and Edman Degradation to investigate the metal binding capabilities of multiple sequences simultaneously was successful.

Chapter 7: On-Line, Time-Based Solution Flow Meter for Use in Flow Injection Analysis

7.1 INTRODUCTION

In recent years the use of flow injection analysis (FIA) has increased significantly [182-189]. In most FIA methods flow rate is an important parameter. The simplest means of flow rate measurement is the volumetric method [186], which involves volumetrically measuring either the system effluent or the amount of solution that is consumed over a timed interval. Although these techniques are inexpensive and simple, measuring the volume can be cumbersome and frequently requires a break in the system flow. While an interruption in the flow is acceptable in some cases, many applications benefit from the ability to measure the flow rate in-line without interrupting the flow. Commercial flow meters that measure the flow in-line are available, but are generally quite expensive.

An electronic bubble-type flow meter that is similar, in principal, to the "air-gap method" previously described by Valcarcel and Luque de Castro [186] was designed to make flow rate measurements in-line with the system flow, such that flow rate measurements can be collected while collecting data.

7.2 INSTRUMENT DESIGN AND USE

The "timed bubble flow meter" electronic circuit can be seen in Figure 7.1.

Figure 7.1 Electronic Circuit Schematic

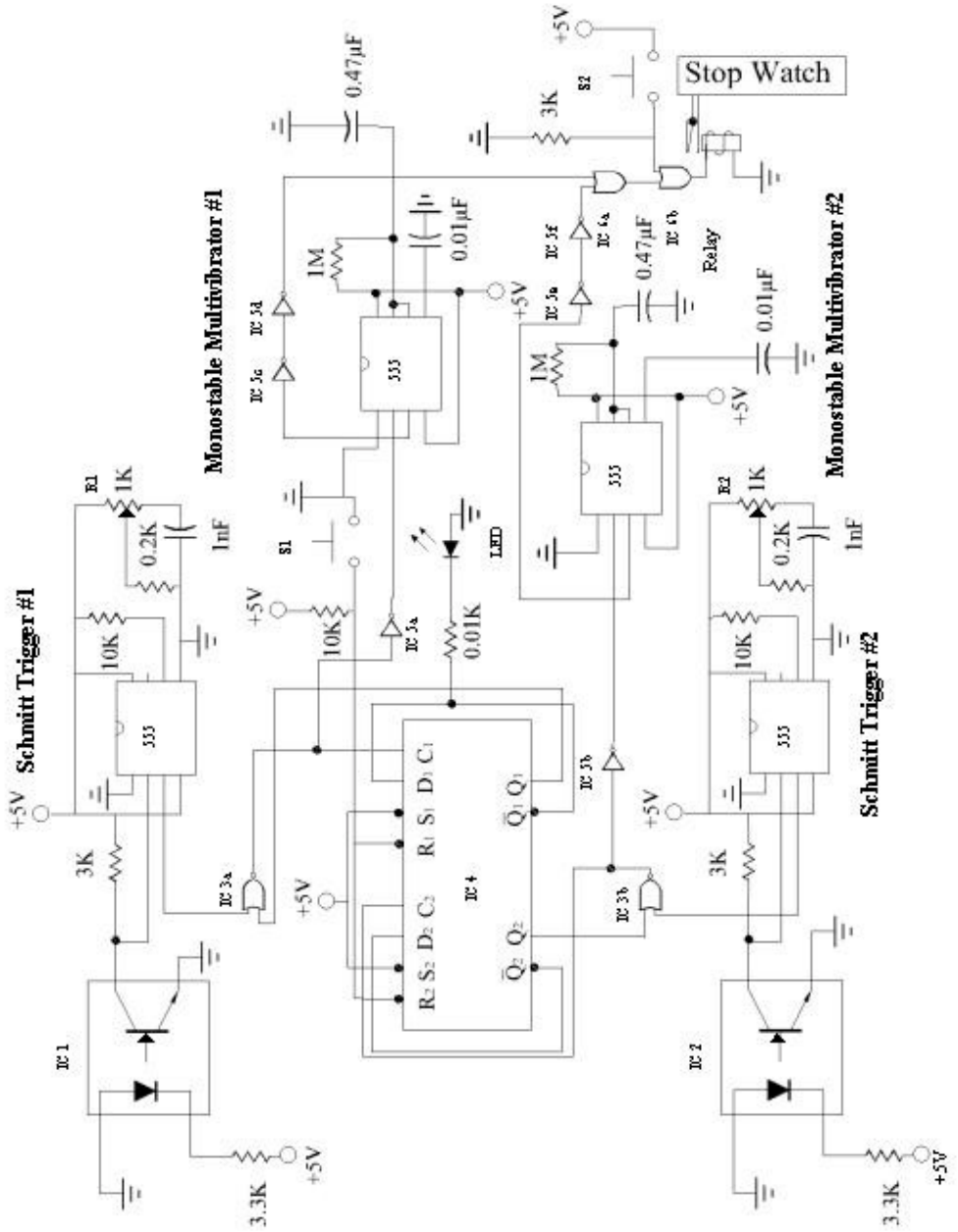

Table 7.1 contains a list of electronic components. The circuit is basically comprised of two identical Schmitt Trigger circuits that start and stop a timer as a small, injected bubble passes through the FIA tubing and past a pair of LED-photodiode sensors (Figure 7.2a). An empty 1mL syringe is teed into the effluent line of the FIA system immediately after the reaction system through the use of a Kel-F tee. After the tee, the effluent line is threaded through two photo emitter/photo diodes that are fixed approximately 22 cm apart. A small piece of plastic was machined to fit in the gap of the detector with a hole bored through it to hold the PTFE tube (0.032" ID) in place within the line of the detector (Figure 7.2b). While the system is running, the reset button (S1) is depressed and the LED lights to indicate that the system is "armed". A small air bubble is injected into the line using the syringe. When the front edge of this bubble reaches the first photo emitter/photo diode (IC 1), Schmitt Trigger #1 goes low and ultimately starts the timer. When the bubble reaches the second photo emitter/photo diode (IC 2), Schmitt Trigger #2 goes low and stops the timer.

Figure 7.2 a) “Timed bubble flow meter” device diagram, b) tube holder orientation within photo emitter/photo diode

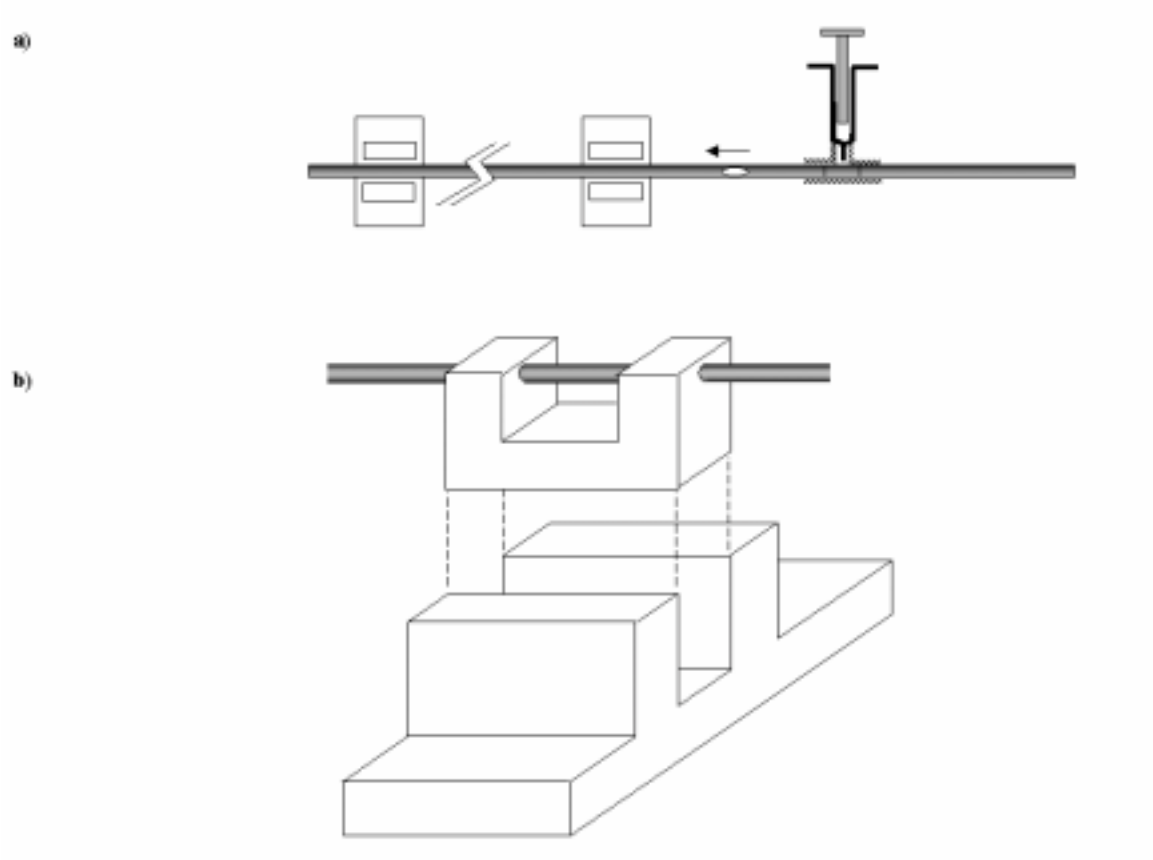

The various NOR gates, OR gates and the flip flop, FF (IC 4) are used with the multivibrator circuit to insure that retriggering of the “start” does not occur either with the back edge of the bubble or any subsequent bubble that might appear. With the RESET button (S1) pushed, the FF (IC 4) output goes low and the green LED is lit. Upon a signal from the bubble passing IC 1, IC 3a goes high and initiates the production of a single pulse (~ 0.5 sec) from the monostable multivibrator circuit (#1), which momentarily closes the relay to initiate the timing circuit of the clock. (In our case, a simple, inexpensive watch is used as the timer where the start/stop switch in the watch

has been replaced with our micro-relay.) The low-high pulse from IC 3a also turns off the green LED and disarms the FF to prevent additional signals from Schmitt #1 from passing. When the leading edge of the bubble passes the second sensor (IC 2), a similar sequence of events, involving the FF (IC 4), IC 3b and monostable multivibrator #2, once again momentarily closes the relay, which stops the timer/watch. To make another measurement, the "reset" button on the watch is depressed, the reset button (S1) of the circuit is pushed, and another small bubble injected.

While a clock display could be used, we elected to make simple modifications to an inexpensive ($2.00) AQT2 stopwatch. The start/stop button of the stopwatch was removed and the two contact leads from the relay soldered to the contacts within the watch that would normally be connected when the watch's "start" button was depressed. An accuracy of $\pm$0.01 s was available.

As mentioned previously, once the system is triggered it will not be triggered by another bubble until the RESET button (S1) is pressed and the green LED is lit. Additionally, a STOP button (S2) has been incorporated into the circuit at the OR gate (IC 6b) prior to the relay, in the event of a stray pulse that starts the timer. For example, when the system is first turned on, a pulse is sent from the FF that will accidentally start the stopwatch. The entire system is operated off of a regulated power supply and it has an on/off switch with a red LED indicating "power on".

Prior to use, the threshold on the Schmitt Triggers must be set in order to ensure that the signal from the detector will set off the trigger. This can be accomplished by injecting a bubble into the system and monitoring the output of either the FF or the 555 with an oscilloscope. If no signal is detected upon the passage of a bubble, the 1 kΩ

trim-pot (R1 and R2), within the Schmitt Trigger circuit, must be adjusted until the passage of a bubble results in an observable signal.

It is also necessary to calibrate the "timed bubble flow meter" by measuring the time it takes a bubble to flow between the two detectors. Given the relationship

$$f = V/t$$

where f is the solution flow rate, V is the tube volume between sensors and t is the time it takes a solution to traverse this volume. The recorded time for known flow rates can be used to prepare a straight line calibration curve (f versus $1/t$) that has a zero intercept and a slope that is equal to the volume of the tube between the sensors. The equation of this line can be used to convert the time read by the stopwatch into a flow rate in subsequent experiments.

Table 7.1 Components of the "timed bubble flow meter" circuit*

Label	Part number	Description
IC 1	-	Photo emitter/photo diode #1
IC 2	-	Photo emitter/photo diode #2
IC 3	7402	Dual input, quad NOR gate
IC 4	7474	Flip flop
IC 5	7404	Hex inverter
IC 6	7432	Dual input, quad OR gate
LED	-	Green LED (reset indicator)
S1	-	Momentary contact push button (reset)
S2	-	Momentary contact push button (stop)
Relay	W172DIP - 1	-

*Components labeled in Figure 7.1 as "555" are 555 timing chips wired in varying configurations to produce different functions

7.3 CONCLUSION

In summary, basic operation of the bubble flow meter involves attaching the output of the FIA flow stream to a length of tubing that is threaded through two photo emitter/photo diodes. Once the flow meter is turned on and the FIA system is operating, after pressing the RESET button, a bubble can be manually injected at any time and the time can be read directly off of the stopwatch and plugged into the equation previously determined by the calibration.

It is interesting to note that PTFE tubing is used to transport the bubble between the two detectors; and although the tubing is opaque, the passage of a bubble is capable of initiating a signal from the detector. With this in mind, it might be possible to detect more subtle changes (e.g., refractive index) in the solution with the use of transparent tubing.

It is also important to mention that this device is currently used to measure the flow of solution entering the nebulizer of a flame atomic absorption spectrophotometer (FAAS) or an inductively coupled plasma mass spectrometer (ICP-MS). In this particular application the insertion of a small air bubble into the stream does not cause any detectable perturbation in the FAAS or ICP-MS signal. However, there are applications in which the presence of a small air bubble would cause unacceptable fluctuations in the signal and this device would not be useful.

Chapter 8: Conclusions and Future Work

8.1: CONCLUSIONS

This work has involved the investigation into the utility of various immobilized biopolymers for trace metal remediation. Several of these novel metal chelators, such as poly-L-cysteine and poly-L-aspartic acid, have been investigated previously [40, 42, 44, 82]. The current studies take a closer look at improving on these systems and investigate factors that contribute to the metal binding capabilities.

The uniqueness of using these homopolymers as chelators is that the desirable free energy minimization and chelation capacity is achieved without a "preformed chelation geometry" such as that seen with crown ethers or even EDTA. Instead, strong chelation is achieved by tethering one end of the homopolymers to an immobilized substrate, permitting three degrees of freedom in tertiary structure for metal binding with the polymer tail. The result is the polymer wrapping around the metal in a three dimensional conformation, allowing it to reach a free energy minimum.

It is often desirable in chelation procedures to have the flexibility of changing the function of binding groups as well as being able to mix binding functionalities along the same chain. Unfortunately, in traditional systems while changing chain functionalities is easily achieved, having mixed functional groups on a chain is extremely difficult. Our system, using biopolymers (i.e., short chains of amino acids) provides the advantage of both of these characteristics. Additionally, the chelators are environmentally friendly when discarded.

Initially, immobilized poly-L-histidine was evaluated according to its cation metal binding capabilities. PLHis is a short chain bio homopolymer, approximately 30 – 50 residues in length. It was immobilized onto controlled pore glass using simple silane

coupling methods and characterized according to its metal binding capabilities through breakthrough analysis conducted on FIA-FAAS. Both strong and weak binding characteristics were observed for Cu^{2+}, Cd^{2+}, Co^{2+} and Ni^{2+}, while very weak to minimal binding was observed for Mn^{2+}, Ca^{2+}, Mg^{2+}, Na^{+}. The metal binding trend observed for PLHis ($Cu^{2+} >> Cd^{2+} \approx Ni^{2+} > Co^{2+} > Pb^{2+} >> Na^{+} \approx Ca^{2+} \approx Mg^{2+} \approx Cr^{3+} \approx Mn^{2+}$) resembles that published in the literature for nitrogen-based ligands [43].

PLHis is a unique metal chelator in that the imidazole side chain, which is responsible for metal binding is deprotonated in acidic pHs. Therefore this residue has been shown to be capable of binding metal oxyanions such as the chromates, arsenates and selenites in acidic conditions. Additionally PLHis demonstrates strong binding for the hexavalent form of Cr but minimal binding for the trivalent form. Cr(VI) is a much more significant environmental concern than Cr(III).

The oxyanion binding capabilities of this system are particularly relevant when considering the recent EPA announcement of the reduction of the maximum contaminant level (MCL) of arsenic in drinking water from 50 ppb to 10 ppb [107]. This ruling was made official in August 2002 and all public drinking water supplies must comply with the new standard by January 2006.

Unfortunately these oxyanions are more difficult to recover than the traditional cations from this system. As a result PLHis as a metal oxyanion remediator is not an effective preconcentrator when compared to PLHis as a metal cation remediator. Typically cations can be quantitatively recovered from PLHis in several hundred micoliters while oxyanions take up to 10 milliliters. The oxyanion binding capability of PLHis also suffers from interferences with competing anions present in solution. As a result of these difficulties it may serve as a more effective clean-up or polishing step in oxyanion removal until more efficient method for stripping the oxyanions is developed.

While previous work has focused solely on the metal binding capabilities of bio homopolymer system a direct comparison between poly-L-aspartic acid and poly-L-glutamic acid was conducted to evaluate whether subtle differences in structure had implications on remediation traits. These two amino acids differ only in that the side chain of PLGlu has an extra methylene group. In general, it was shown that these polymers behaved very similarly in all of the studies conducted, and should be equally suitable for trace metal preconcentration and remediation from natural and industrial waste-streams.

A new method of calculating approximately polymer coverage was also developed for this comparison. Successful determination of polymer coverage was conducted by carbon elemental combustion analysis. Through this analysis it was shown that the two immobilized polymer systems had statistically indistinguishable coverage values. Therefore, a direct comparison of metal capacities could be made without correcting for differences in polymer coverage. Elemental combustion analysis is also useful in the calculation of residue to metal ratios.

In further efforts to establish the relationship between the structure of the chain and the metal binding efficiency a combinatorial approach was utilized to evaluate a large number of polymer systems simultaneously. A combinatorial peptide library was designed to consist of various permutations of aspartic acid and glycine ratios. Micro x-ray fluorescence was successfully used as a screening tool to locate sequences that exhibited significant metal binding. Although the "ideal" sequence was never isolated due to complications with the Edman Degradation process, several sequences with significant metal binding were revealed. Fortunately, proof-of-concept for using the

combinatorial approach to evaluate a large number of peptides coupled with high throughput analysis was established.

Due to the importance of flow rate in FIA-FAAS breakthrough analysis an on-line, time based solution flow meter circuit was designed. The "bubble meter" essentially measures the rate of flow of a bubble passing through a tube. The circuit consists of two identical Schmitt Trigger and monostable multivibrator pairs. A timer is triggered when the bubble passes the first LED-photodiode sensor and stopped when the bubble passes the second LED-photodiode sensor. Through calibration of the system the time it takes the bubble to complete the course can be converted into a solution flow rate. The utility of this system lies in the fact that the flow rate can be measured on-line without a break in the system. Thus, the flow rate can be monitored throughout the progress of a breakthrough curve and any changes in flow rate can be compensated for.

8.2 FUTURE WORK

8.2.1 Alternate Immobilization Methods

The current immobilization procedure using 3-aminopropyltriethoxysilane and gluteraldehyde to anchor the polymers to the solid support yields favorable metal binding capacities. Unfortunately this reaction scheme has several flaws. Most significantly, due to the inefficiency of the reactions residual amine functionalities are left on the silica surface. This prevents the determination of conditional formation constants between the polymer and the metal by competitive binding experiments. Several unsuccessful attempts were made at developing a new immobilization procedure that uses 3-glycidoxypropyltimethosysilane (GLYMO), another common silane linker. GLYMO

does not provide linkage through an amine functionality. Instead, it provides an epoxide group on the surface to react with the amine terminus of the amino acid chain. It is a shorter reaction than the 3APS/gluteraldehyde reaction because no intermediate linker, such as gluteraldehyde in necessary. The amino acid attaches directly to the epoxide.

Moderate success was noted with this procedure. Further investigation into its *inertness* as a linker must be conducted to be sure that it is unreactive to the presence of anions. If it is unreactive then additional studies must also be conducted to ensure that the peptide backbone is not participating in anion binding. To make formation constant determinations through competitive binding experiments it is necessary to ensure that they only metal that is binding to the polymer is the free metal left in solution of any metal that was pulled away from the competing ligand such as EDTA, not the metal:EDTA complex.

8.2.2 Surface Plasmon Resonance Spectroscopy

Surface plasmon resonance is emerging as one of the latest "novel" chemical and biological sensors [190]. The technique is based on the concept of total internal reflection [191]. Basically, an interface is made between two materials of different refractive indicies. When plane polarized light beam in incident upon an interface between two different refractive indicies the incident light is partially reflected back into the medium with the higher refractive index and partially refracted. If the angle of incidence of the light is greater than the critical angle all of the light gets totally internally reflected. However, an electromagnetic field component penetrates a short distance (~ 10 nm) into the medium of lower refractive index. This component of the light that penetrates the surface is called the evanescent wave. When the wave vector of the

incident light (which is parallel to the surface) matches the wavelength of the surface plasmons there is a coupling of the incident light to the surface plasmons that results in a loss of energy of the reflected beam (Figure 8.1).

Figure 8.1 Surface plasmon resonance [192]

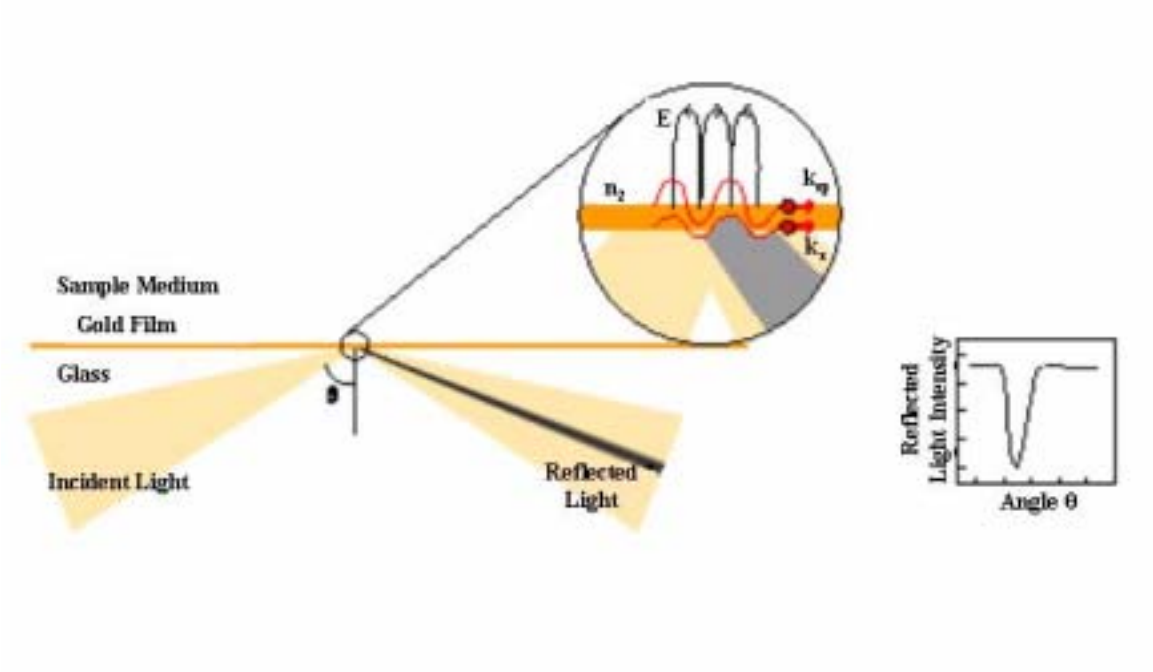

Surface plasmons are a collective oscillation of electrons in a metallic film that is coated on one surface of the interface. The utility in this technique as a sensor lies in the fact that the angle that the surface plasmon resonance phenomenon occurs is sensitive to changes in the refractive index in the layer next to the metallic film. This technology has been used for refractive index measurements [193], as a gas sensor [194, 195], as an ion sensor [196, 197] and most interestingly as an optical biosensor [198-201]. In this capacity it is capable of antibody/antigen interactions, protein/DNA interactions and protein/drug interactions. It has proven beneficial in the real-time, non-destructive, study of various receptor ligand interactions. This is possible with the flow through design by

immobilizing the biomolecules directly to the metal surface and passing a solution containing the ligand past the metal film (Figure 8.2).

Figure 8.2 Surface plasmon resonance instrument design [202]

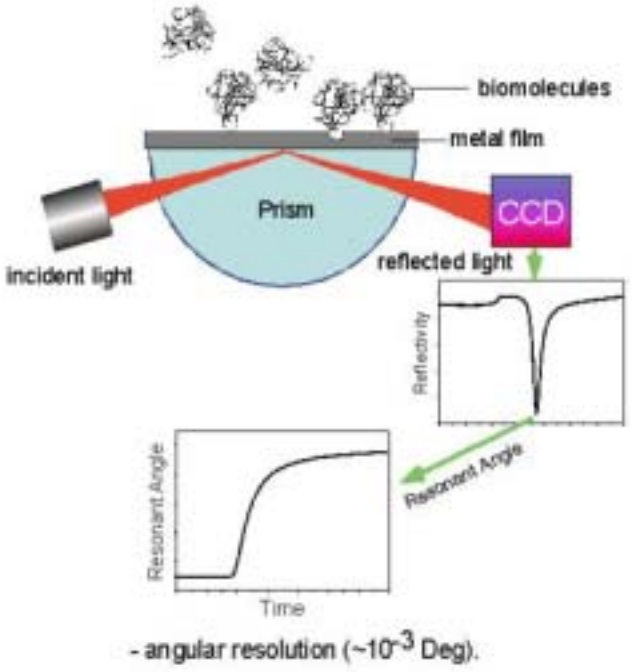

If an association occurs it will be apparent on the generated sensogram. After association the system is easily regenerated and reused making it an ideal metal ion sensor for remediation technology. Recently, Texas Instruments has come out with miniature surface plasmon resonance components [203, 204]. This Spreeta™ design is only 2 cm^3 in size [203, 205].

The current immobilized biopolymer technology can easily be applied to surface plasmon resonance in the development of a novel ion sensor. All remediation processes

require a means of evaluating the success of the system. For example, in column-type remediation techniques breakthrough is sensed with atomic spectrometric techniques. Industrial remediation sites, using precipitation and flocculation for remediation, must have a system in place to monitor the effluent stream leaving the plant to ensure compliance with environmental regulation standards. This often involves "batch" or "grab" sampling of random aliquots of the effluent stream for spectroscopic analysis. We propose an inexpensive, continuous monitoring, *in situ* probe to monitor metal concentrations in the effluent stream. An *in situ* sensor, placed after the remediation column (or downstream from a remediation pond), would give information as to when the column (or pond) has reached capacity and must be replaced or regenerated when the column is reusable. The key is to have the sensitivity to detect the metal concentrations leaving the column once capacity is reached. By utilizing the selectivity and sensitivity of biopeptides for metals remediation in conjunction with the picogram/mm^2 detection limits of surface plasmon resonance, a novel metal ion sensor is being proposed.

Preliminary studies have shown that PLAsp can be successfully immobilized onto a gold-coated cover slip by following a procedure outlined previously by Miller, et al. [45]. This gold-coated PLAsp coverslip was shown to bind ng of Cu. This translates into the possibility of immobilizing the polymer onto the surface of the surface plasmon sensor and detecting the presence of various metals in solution. Researchers have also demonstrated that the gold surface can be modified by a carboxy-methyl modified dextran which creates a larger surface area for immobilization of the peptides [206]. The extended matrix allows more molecules to interact with the solution per unit area. In addition, attachment to the flexible dextran gives a higher degree of accessibility to the

molecules as opposed to when the molecules are attached to a flat surface and may be sterically hindered. The immobilization to the extended dextran matrix may be considered if immobilization of the biopolymers is not concentrated enough to bind enough metal to generate a sufficient surface plasmon signal.

Bibliography

[1] Forstner, U.; Wittmann, G.T.W., *Metal pollution in the aquatic environment*; Springer-Verlag: New York, 1981.

[2] US EPA, http://www.epa.gov/safewater/mcl.html, 2004.

[3] Ireland, M.P., *Biological Monitoring of Heavy Metals*; Wiley: New York, 1991.

[4] Vernet, J.P., *Impact of heavy metals on the environment*; Elsevier: New York, 1992.

[5] Friber, L.; Nordberg, G.F.; Vouk, B., eds., *Handbook on the Toxicology of Metals*, Elsevier, North-Holland, Biomedical Press: Amsterdam 1979.

[6] Chen, L.H.; Chung, C.S., *Steric and Macrocyclic Effects in the Dissociation Kinetics of Cyclic and Open-Chain Tetraamine Complexes of Copper(II) in Strongly Acidic, Aqueous Media*, Inorganic Chemistry 27 (1988) p. 1880.

[7] Raymond, K.N.; Garrett, T., M.; Miller, P., W., *Highly effective 2,3-dihydroxyterephthalamides as metal ion sequestering compounds*, U.S. 5049280, 1991.

[8] Franklin, S.J.; Raymond, K.N., *Solution Structure and Dynamics of Lanthanide Complexes of the Macrocyclic Polyamino Carboxylate DTPA-dien. NMR Study and Crystal Structures of the Lanthanum(III) and Europium(III) Complexes*, Inorganic Chemistry 33 (1994) p. 5794.

[9] Hou, Z.; Sunderland, C.J.; Nishio, T.; Raymond, K.N., *Preorganization of Ferric Alcaligin, Fe2L3. The First Structure of a Ferric Dihydroxamate Siderophore*, Journal of the American Chemical Society 118 (1996) p. 5148.

[10] Hou, Z.; Raymond, K.N.; O'Sullivan, B.; Esker, T.W.; Nishio, T., *A Preorganized Siderophore: Thermodynamic and Structural Characterization of Alcaligin and Bisucaberin, Microbial Macrocyclic Dihydroxamate Chelating Agents*, Inorganic Chemistry 37 (1998) p. 6630.

[11] Raskin, I.; Ensley, B.D., *Phytoremediation of Toxic Metals: Using Plants to Clean Up the Environment*; John Wiley: New York, 2000.

[12] Tsao, D.T., ed. *Phytoremediation*; Advances in Biochemical Engineering/Biotechnology. Vol. 78, Springer: Berlin 2003.

[13] Terry, N.; Banuelos, G., eds., *Phytoremediation of Contaminated Soil and Water*, Lewis Publishers: Boca Raton 2000.

[14] Kruger, E.L.; Anderson, T.A.; Coats, J.R., eds., *Phytoremediation of Soil and Water Contaminants*; ACS Symposium Series, American Chemical Society: Washington DC 1997.

[15] Maquieira, A.; Elmahadi, H.A.M.; Puchades, R., *Immobilized Cyanobacteria for Online Trace Metal Enrichment by Flow Injection Atomic Absorption Spectrometry*, Analytical Chemistry 66 (1994) p. 3632.

[16] Maquieira, A.; Elmahadi, H.A.M.; Puchades, R., *Use of Saccharomyces cerevisiae in Flow Injection Atomic Absorption Spectrometry for Trace Metal Preconcentration*, Analytical Chemistry 66 (1994) p. 1462.

[17] Wang, J.; Martinez, T.; Darnall, D., *Uptake of Redox Couples by Algae Immobilized on Porous Cellulosic Films*, Electrochimica Acta 35 (1990) p. 1377.

[18] Gardea-Torresdey, J.; Darnall, D.; Wang, J., *Bioaccumulation and Measurement of Copper at an Alga-Modified Carbon Paste Electrode*, Analytical Chemistry 252 (1988) p. 72.

[19] Kubiak, W.W.; Wang, J.; Darnall, D., *Algae Columns with Anodic Stripping Voltammetric Detection*, Analytical Chemistry 61 (1989) p. 468.

[20] Mahan, C.A.; Holcombe, J.A., *Preconcentration of Trace Metals Using Silica-Immobilized Algae Cells in a Chromatographic Separation Procedure*, Spectrochim. Acta, Part B 47B (1992) p. 1483.

[21] Mahan, C.A.; Holcombe, J.A., *Immobilization of Algae Cells on Silica Gel and Their Characterization for Trace Metal Preconcentration*, Analytical Chemistry 64 (1992) p. 1933.

[22] Harrison, P.M., *Metalloproteins*; Verlag Chemie: Weinheim, 1985.

[23] Sigel, H.; Sigel, A., *Metal Ions in Biological Systems*; Marcel Dekker, Inc.: New York, 1989.

[24] Stillman, M.J.; Shaw, C.F.; Suzuki, K.T., eds., *Metallothioneins, Synthesis, Structure and Properties of Metallothioneins, Phytochelatins and Metal-Thiolate Comlexes*, VCH Publishers, Inc.: New York 1992.

[25] Suzuki, K.T.; Imura, N.; Kimura, M., *Metallothionein III: Biological Roles and Medical Implications*; Birkhauser Verlag: Boston, 1993.

[26] Anderson, B., *Evaluation of Immobilized Metallothionein for Trace Metal Separation and Preconcentration*; in *Chemistry and Biochemistry*. 1994, The University of Texas at Austin: Austin.

[27] Elmahadi, H.A.M.; Greenway, G.M., *Immobilized Cysteine as a Reagent for Preconcentration of Trace Metals Prior to Determination by Atomic Absorption Spectrometry*, Journal of Analytical Atomic Spectrometry 8 (1993) p. 1009.

[28] Denizli, A.; Garipcan, B.; Emir, S.; Patir, S.; Say, R., *Heavy Metal Ion Adsorption Properties of Methacrylamidocysteine-containing Porous poly(hydroxyethyl methacrylate) Chelating Beads*, Adsorption Science & Technology 20 (2002) p. 607.

[29] Denizli, A.; Garipcan, B.; Karabakan, A.; Say, R.; Emir, S.; Patir, S., *Metal-complexing Ligand Methacryloylamidocysteine Containing Polymer Beads for Cd(II) Removal*, Separation and Purification Technology 30 (2003) p. 3.

[30] Disbudak, A.; Bektas, S.; Patir, S.; Genc, O.; Denizli, A., *Cysteine-metal Affinity Chromatography: Determination of Heavy Metal Adsorption Properties*, Separation and Purification Technology 26 (2002) p. 273.

[31] George, B.; Pillai, V.N.R.; Mathew, B., *Polymer-metal complexes of N,N'-methylene-bis-acrylamide (NNMBA)-crosslinked polyacrylamide-supported glycines: effect of the degree of crosslinking on metal ion complexation and concentration*, Journal of Macromolecular Science, Pure and Applied Chemistry A35 (1998) p. 495.

[32] Vinodkumar, G.S.; Mathew, B., *Polymer-metal Complexes of Glycine Functions Supported on N,N'-methylene-bisacrylamide (NNMBA)-crosslinked Polyacrylamides: Synthesis, Characterization and Catalytic Activity*, European Polymer Journal 34 (1998) p. 1185.

[33] George, B.; Mathew, B., *Effect of the Degree of Ccrosslinking on the Metal Ion Specificity of Polyacrylamide-supported Glycines*, Journal of Macromolecular Science, Pure and Applied Chemistry A38 (2001) p. 429.

[34] George, B.; Pillai, V.N.R.; Mathew, B., *Effect of the Nature of the Crosslinking Agent on the Metal-Ion Complexation Characteristics of 4 mol % DVB- and NNMBA-Crosslinked Polyacrylamide-Supported Glycines*, Journal of Applied Polymer Science 74 (1999) p. 3432.

[35] Say, R.; Garipcan, B.; Emir, S.; Patir, S.; Denizli, A., *Preparation and Characterization of the Newly Synthesized Metal-Complexing-Ligand n-methacryloylhistidine Having PHEMA Beads for Heavy Metal Removal from Aqueous Solutions*, Macromolecular Materials and Engineering 287 (2002) p. 539.

[36] Say, R.; Birlik, E.; Ersoz, A.; Yilmaz, F.; Gedikbey, T.; Denizli, A., *Preconcentration of Copper on Ion-Selective Imprinted Polymer Microbeads*, Analytica Chimica Acta 480 (2003) p. 251.

[37] Sugii, A.; Ogawa, N.; Iinuma, Y.; Yamamura, H., *Selective Metal Sorption on Crosslinked Poly(vinylpyridine) Resins*, Talanta 28 (1981) p. 551.

[38] Masoom, M.; Townshend, A., *Determination of Glucose in Blood by Flow Injection Analysis and an Immobilized Glucose Oxidase Column*, Analytica Chimica Acta 166 (1984) p. 111.

[39] Jurbergs, H.A.; Holcombe, J.A., *Characterization of Immobilized Poly(L-cysteine) for Cadmium Chelation and Preconcentration*, Analytical Chemistry 69 (1997) p. 1893.

[40] Howard, M.; Jurbergs, H.A.; Holcombe, J.A., *Comparison of Silica-Immobilized Poly(L-cysteine) and 8-hydroxyquinoline for Trace Metal Extraction and Recovery*, Journal of Analytical Atomic Spectrometry 14 (1999) p. 1209.

[41] Miller, T.C.; Holcombe, J.A., *Characterization of Metal Ion-Exchange on Modified Surfaces of Porous Carbon*, Analytica Chimica Acta 455 (2002) p. 233.

[42] Gutierrez, E.; Miller, T.C.; Gonzalez-Redondo, J.R.; Holcombe, J.A., *Characterization of Immobilized Poly-L-aspartate as a Metal Chelator*, Environmental Science and Technology 33 (1999) p. 1664.

[43] Gulumian, M.; Hancock, R.D.; Rollin, H.B., *Handbook of Metal-Ligand Interactions in Biological Fluids: Bioinorganic Chemistry*; Handbook of Metal-Ligand Interactions in Biological Fluids: Bioinorganic Chemistry 1 Marcel Dekker Inc.: New York, 1995.

[44] Miller, T.C.; Holcombe, J.A., *Comparison and Evaluation of the Synthetic Biopolymer Poly-L-aspartic acid and the Synthetic "Plastic" Polymer Poly-acrylic acid for Use in Metal Ion-exchange Systems*, Journal of Hazardous Materials 83 (2001) p. 219.

[45] Miller, T.C.; Holcombe, J.A., *An Ion-Exchange Microcolumn Employing Gold Minigrids as Supports for the On-Line Immobilization of Poly(L-aspartate)*, Analytical Chemistry 71 (1999) p. 2667.

[46] Leggett, G.J.; Roberts, C.J.; Williams, P.M.; Davies, M.C.; Jackson, D.E.; Tendler, S.J.B., *Approaches to the Immobilization of Proteins at Surfaces for Analysis by Scanning Tunneling Microscopy*, Langmuir 9 (1993) p. 2356.

[47] Miller, T.C.; Holcombe, J.A., *Evaluation of Electroless Gold Deposited on Porous Silica for Ligand Attachment for Metal Ion-Exchange*, Analytica Chimica Acta 454 (2002) p. 37.

[48] Ho, W.S.W.; Sirkar, K.K., eds., *Membrane Handbook*, Chapman and Hall: New York 1992.

[49] Noble, R.D.; Stern, S.A., eds., *Membrane Separations Technology: Principles and Applications*, Elsevier: New York 1995.

[50] Bhattacharyya, D.; Mangum, W.C.; Williams, M.E., *Reverse Osmosis*; Kiek-Othmer Encyclopedia of Chemical Technology 21 Wiley: New York, 1997.

[51] Saito, K.; Ito, M.; Yamagishi, H.; Furusaki, S.; Sugo, T.; Okamoto, J., *Novel Hollow Fiber Membrane for the Removal of Metal Ion During Permeation: Preparation by Radiation-Induced Cografting of a Crosslinking Agent with Reactive Monomer*, Industrial & Engineering Chemistry Research 28 (1989) p. 1808.

[52] Yamagishi, H.; Saito, K.; Furusaki, S.; Sugo, T.; Ishigaki, I., *Introduction of a High-Density Chelating Group into a Porous Membrane without Lowering the Flux*, Industrial & Engineering Chemistry Research 30 (1991) p. 2234.

[53] Tsuneda, S.; Saito, K.; Furusaki, S.; Sugo, T.; Okamoto, J., *Metal Collection Using Chelating Hollow Fiber Membrane*, Journal of Membrane Science 58 (1991) p. 221.

[54] Iwata, H.; Saito, K.; Furusaki, S.; Sugo, T.; Okamoto, J., *Adsorption Characteristics of an Immobilized Metal Affinity Membrane*, Biotechnology Progress 7 (1991) p. 412.

[55] Konishi, S.; Saito, K.; Furusaki, S.; Sugo, T., *Sorption Kinetics of Cobalt in Chelating Porous Membrane*, Industrial & Engineering Chemistry Research 31 (1992) p. 2722.

[56] Sugiyama, S.; Tsuneda, S.; Saito, K.; Furusaki, S.; Sugo, T.; Makuuchi, K., *Attachment of sulfonic acid groups to various shapes of polyethylene, polypropylene and poly(tetrafluoroethylene) by radiation-induced graft polymerization*, Reactive Polymers 21 (1993) p. 187.

[57] Li, G.-Q.; Konishi, S.; Saito, K.; Sugo, T., *High Collection Rate of Pd in Hydrochloric Acid Medium Using Chelating Microporous Membrane*, Journal of Membrane Science 95 (1994) p. 63.

[58] Konishi, S.; Saito, K.; Furusaki, S.; Sugo, T., *Binary Metal-Ion Sorption During Permeation Through Chelating Porous Membranes*, Journal of Membrane Science 111 (1996) p. 1.

[59] Bhattacharyya, D.; Hestekin, J.A.; Brushaber, P.; Cullen, L.; Bachas, L.G.; Sikdar, S.K., *Novel Poly-Glutamic Acid Functionalized Microfiltration Membranes for Sorption of Heavy Metals at High Capacity*, Journal of Membrane Science 141 (1998) p. 121.

[60] Ritchie, S.M.C.; Bachas, L.G.; Olin, T.; Sikdar, S.K.; Bhattacharyya, D., *Surface Modification of Silica- and Cellulose-Based Microfiltration Membranes with Functional Polyamino Acids for Heavy Metal Sorption*, Langmuir 15 (1999) p. 6346.

[61] Hestekin, J.A.; Bachas, L.G.; Bhattacharyya, D., *Poly(amino acid)-Functionalized Cellulosic Membranes: Metal Sorption Mechanisms and Results*, Industrial & Engineering Chemistry Research 40 (2001) p. 2668.

[62] Ritchie, S.M.C.; Kissick, K.E.; Bachas, L.G.; Sikdar, S.K.; Parikh, C.; Bhattacharyya, D., *Polycysteine and Other Polyamino Acid Functionalized Microfiltration Membranes for Heavy Metal Capture*, Environmental Science and Technology 35 (2001) p. 3252.

[63] Denizli, A.; Say, R.; Patir, S.; Arica, Y., *Synthesis and Ddsorption Properties of Poly(2-hydroxyethylmethacrylate-co-methacrylamidophenylalanine) Membranes for Copper Ions*, Reactive & Functional Polymers 46 (2000) p. 157.

[64] Denizli, A.; Say, R.; Patir, S.; Arica, Y., *Heavy Metal Separation Capacity of a Porous Methacrylamidophenylalanine Containing Membrane Based on a Polyhydroxyethyl Methacrylate Matrix*, Separation Science and Technology 36 (2001) p. 2213.

[65] Kiyohara, S.; Sasaki, M.; Saito, K.; Sugita, K.; Sugo, T., *Radiation-Induced Grafting of Phenylalanine-Containing Monomer onto a Porous Membrane*, Reactive & Functional Polymers 31 (1996) p. 103.

[66] Terashima, M.; Oka, N.; Sei, T.; Yoshida, H., *Adsorption of Cadmium Ion and Gallium Ion to Immobilized Metallothionein Fusion Protein*, Biotechnology Progress 18 (2002) p. 1318.

[67] Bae, W.; Chen, W.; Mulchandani, A.; Mehra, R.K., *Enhanced Bioaccumulation of Heavy Metals by Bacterial Cells Displaying Synthetic Phytochelatins*, Biotechnology and Bioengineering 70 (2000) p. 518.

[68] Xu, Z.; Bae, W.; Mulchandani, A.; Mehra, R.K.; Chen, W., *Heavy Metal Removal by Novel CBD-EC20 Sorbents Immobilized on Cellulose*, Biomacromolecules 3 (2002) p. 462.

[69] Gubitz, G.; Jellenz, W.; Santi, W., *Separation of the Optical Isomers of Amino Acids by Ligand-Exchange Chromatography Using Chemically Bonded Chiral Phases*, Journal of Chromatography 203 (1981) p. 377.

[70] Bacold, M.D.; Rassi, X.E., *High-Performance Metal Chelate Interaction Chromatography of Proteins with Silica-Bound Ethylenediamine-N,N'-diacetic Acid*, Journal of Chromatography 512 (1990) p. 237.

[71] Gaida, A.V.; Monastyrskii, V.A.; Magerovskii, Y.V.; Staroverov, S.M.; Lisichkin, G.V., *Affinity chromatography of human thrombin on modified silica*, Journal of Chromatography 424 (1988) p. 385.

[72] Nesterenko, P.N., *Silica-Bonded L-hydroxyproline and its Application to the Separtation of Inorganic Anions*, Journal of High Resolution Chromatography 14 (1991) p. 767.

[73] Nesterenko, P.N., *Application of Amino Acid-Bonded Silicas as Ion Exchangers for the Separation of Anions by Single-Column Ion Chromatography*, Journal of Chromatography 605 (1992) p. 199.

[74] Nesterenko, P.N.; Shpigun, O.A.; Zolotov, Y.A., *Bipolar ion-exchangers and new prospects in ion chromatography*, Doklady Akademii Nauk 324 (1992) p. 107.

[75] Nesterenko, P.N.; Kopylov, R.V.; Tarasenko, D.A.; Shpigun, O.A.; Zolotov, Y.A., *Simultaneous separation of anions and cations by single-column ion chromatography*, Doklady Akademii Nauk 326 (1992) p. 838.

[76] Nesterenko, P.N.; Elefterov, A.I.; Tarasenko, D.A.; Shpigun, O.A., *Selectivity of Chemically Bonded Zwitterion-Exchange Stationary Phases in Ion Chromatography*, Journal of Chromatography A 706 (1995) p. 59.

[77] Elefterov, A.I.; Kolpachnikova, M.G.; Nesterenko, P.N.; Shpigun, O.A., *Ion-Exchange Properties of Glutamic Acid-Bonded Silica*, Journal of Chromatography, A 769 (1997) p. 179.

[78] Kiseleva, M.G.; Kebets, P.A.; Nesterenko, P.N., *Simultaneous Ion Chromatographic Separation of Anions and Cations on Poly(aspartic acid) Functionalized Silica*, Analyst 126 (2001) p. 2119.

[79] Liu, C.Y.; Sun, P.J., *Preparation and Analytical Properties of a Chelating Resin Containing Cysteine Groups*, Analytica Chimica Acta 132 (1981) p. 187.

[80] Liu, C.Y.; Sun, P.J., *Separation and Concentration of Molybdenum(VI) and Tungsten(VI) with Chelating Ion-Exchange Resins Containing Sulfur Ligands*, Talanta 31 (1984) p. 353.

[81] Bektas, S.; Disbudak, A.; Denizli, A.; Genc, O., *Cd(II) Removal from Human Plasma by Cysteine-Immobilized PHEMA Microspheres*, Trace Elements and Electrolytes 19 (2002) p. 26.

[82] Howard, M.; Jurbergs, H.A.; Holcombe, J.A., *Effects of Oxidation of Immobilized Poly(L-Cysteine) on Trace Metal Chelation and Preconcentration*, Analytical Chemistry 70 (1998) p. 1604.

[83] Kolpachnikova, M.G.; Penner, N.A.; Nesterenko, P.N., *Effect of Temperature on Retention of Alkali and Alkaline-Earth Metal Ions on Some Aminocarboxylic Acid Functionalized Silica Based Ion Exchangers*, Journal of Chromatography, A 826 (1998) p. 15.

[84] Kebets, P.A.; Kuz'mina, K.A.; Nesterenko, P.N., *The heats of adsorption of metal cations on silica gel with covalently attached polyaspartic acid*, Zhurnal Fizicheskoi Khimii 76 (2002) p. 1639.

[85] Miller, T.C.; Kwak, E.-S.; Howard, M.E.; Vanden Bout, D.A.; Holcombe, J.A., *An in Situ Study of Metal Complexation by an Immobilized Synthetic Biopolymer Using Tapping Mode Liquid Cell Atomic Force Microscopy*, Analytical Chemistry 73 (2001) p. 4087.

[86] Autry, H.; Holcombe, J.A., *Cadmium, copper and zinc complexes of poly-L-cysteine*, Analyst 120 (1995) p. 2643.

[87] Miller, T.C., *Development of novel bonded-phase ion exchange systems for the preconcentration and recovery of trace metals from aqueous systems*. 2001, University of Texas, Austin.

[88] Howard, M.E.; Holcombe, J.A., *Effective trace-metal separation and preconcentration using immobilized biopolymers*, Book of Abstracts, 218th ACS National Meeting, New Orleans, Aug. 22-26 (1999).

[89] Sahni, S.K.; Driessen, W.L.; Reedijk, J., *Synthesis and Characterization of Chelating Ion-Exchange Resins: A Spectral Study of Copper(II) Complexes of Chelating Ion-Exchange Resins Containing Multidentate Imidazole Moieties*, Inorganica Chimica Acta 154 (1988) p. 141.

[90] Moreira, J.C.; Gushikem, Y., *Preconcentration of Metal Ions on Silica Gel Modified with 3(1-imidazolyl)propyl Groups*, Analytica Chimica Acta 176 (1985) p. 263.

[91] Edsall, J.T.; Felsenfeld, G.; Goodman, D.S.; Gurd, F.R.N., *The Association of Imidazole with the Ions of Zinc and Cupric Copper*, Journal of the American Chemical Society 76 (1954) p. 3054.

[92] Gurd, F.R.N.; Goodman, D.S., *Preparation and Properties of Serum and Plasma Proteins. XXXII. The Interaction of Human Serum Albumin with Zinc Ions*, Journal of the American Chemical Society 74 (1952) p. 670.

[93] Tanford, C., *The Effect of pH on the Combination of Serum Albumin with Metals*, Journal of the American Chemical Society 74 (1952) p. 211.

[94] Tanford, C.; Wagner, M.L., *The Consecutive Constants for the Association of Cadmium with Imidazole*, Journal of the American Chemical Society 75 (1953) p. 434.

[95] McCurdie, M.P.; Belfiore, L.A., *Solid-State Complexes of Poly(L-Histidine) with Metal Chlorides from the First Row of the d-Block*, Journal of Polymer Science, Part B: Polymer Physics 37 (1999) p. 301.

[96] Patchornik, A.; Berger, A.; Katchalski, E., *Poly-L-histidine*, Journal of the American Chemical Society 79 (1957) p. 5227.

[97] Tanford, C., *Preparation and properties of serum and plasma proteins. XXIII. Hydrogen-ion equilibria in native and modified human serum albumins*, Journal American Chemical Society 72 (1950) p. 441.

[98] Levitzki, A.; Pecht, I.; Berger, A., *Copper-Poly-L-histidine Complexes. II. Physicochemical Properties*, Journal of the American Chemical Society 94 (1972) p. 6844.

[99] Pecht, I.; Levitzki, A.; Anbar, M., *Copper-Poly-L-histidine Complex. I. The Environmental Effect of the Polyelectrolyte on the Oxidase Activity of Copper Ions*, Journal of the American Chemical Society 89 (1967) p. 1587.

[100] Palumbo, M.; Cosani, A.; Terbojevich, M.; Peggion, E., *Metal Complexes of Poly(alpha-aminoacids). Conformational Aspects of the Interaction Between Cupric Ions and Poly(L-Histidine)*, Macromolecules 11 (1978) p. 1271.

[101] Beychok, S.; Pflumm, M.N.; Lehmann, J.E., *Sense of Helix of Poly-L-Histidine*, Journal of the American Chemical Society 87 (1965) p. 3990.

[102] Norland, K.S.; Fasman, G.D.; Katchalski, E.; Blout, E.R., *Some Optical Properties of Poly-1-benzyl-L-histidine and Poly-L-histidine*, Biopolymers 1 (1963) p. 277.

[103] Muehlinghaus, J.; Zundel, G., *Infrared Investigation of Poly-L-Histidine Structure Dependent on Protonation*, Biopolymers 10 (1971) p. 711.

[104] Myer, Y.P.; Barnard, E.A., *Structure-Reactivity Relations of Imidazole in Polypeptides. II. Structural Transitions and a Beta-Structure in Poly-L-Histidine Solutions*, Archives of Biochemistry and Biophysics 143 (1971) p. 116.

[105] Peggion, E.; Cosani, A.; Terbojevich, M.; Scoffone, E., *Solution Properties of Synthetic Polypeptides. Circular Dichroism Studies on Poly-L-Histidine and on Random Copolymers of L-Histidine and L-Lysine in Aqueous Solution*, Macromolecules 4 (1971) p. 725.

[106] US EPA, http://www.epa.gov/ogwdw/ars/arsenic_finalrule.html, 2004.

[107] EPA, http://www.epa.gov/safewater/arsenic.html, 2004.

[108] Adeel, Z.; Ali, M.A., A Comparative Evaluation and Field Implementation of Treatment Technologies for Arsenic Removal from Groundwater, www.unu.edu/env/Arsenic/Adeel%20KJIST%20Paper.doc.

[109] US EPA, http://www.epa.gov/safewater/ars/ars_rule_factsheet.html, 2001.

[110] US EPA, Technologies and Costs for Removal of Arsenic from Drinking Water, http://www.epa.gov/safewater/arsenic.html, 2000.

[111] Johnston, R.; Heijnen, H., Safe Water Technology for Arsenic Removal, www.unu.edu/env/Arsenic/Han.pdf.

[112] Chen, H.W.; Frey, M.M.; Clifford, D.; McNeill, L.S.; Edwards, M., *Arsenic Treatment Considerations*, Journal of the American Water Works Association 91 (1999) p. 74.

[113] Clifford, D.A., *Ion Exchange and Inorganic Adsorption*, in *Water Quality and Treatment*, Letterman, R.D., Editor. 1999, McGraw-Hill Inc.: New York. p. 9.1.

[114] Richard, F.C.; Bourg, A.C.M., *Aqueous Geochemistry of Chromium: A Review*, Water Research 25 (1991) p. 807.

[115] Santiago, I., *Removal of Hexavalent Chromium From Water Using Tailored Zeolites*. 1996, New Mexico State University, Las Cruces.

[116] Gang, D.; Banerji, S.K.; Clevenger, T.E., *Factors Affecting Chromium(VI) Removal by Modified Poly(4-vinylpyridine) Coated Silica Gel*, Practice Periodical of Hazardous, Toxic, and Radioactive Waste Management 5 (2001) p. 58.

[117] Owens, D.L., *Practical Principles of Ion Exchange Water Treatment*; 1st Tall Oaks Publishing, Inc.: New Jersey, 1985.

[118] Pontius, F.W., *Water Quality and Treatment*; 4th McGraw-Hill, Inc.: New York, 1991.

[119] Sengupta, A.K.; Clifford, D., *Important Process Variables in Chromate Ion Exchange*, Environmental Science and Technology 20 (1986) p. 149.

[120] Zhao, D.; SenGupta, A.K.; Stewart, L., *Selective Removal of Cr(VI) Oxyanions with a New Anion Exchanger*, Industrial & Engineering Chemistry Research 37 (1998) p. 4383.

[121] Leyden, D.E.; Luttrell, G.H.; Nonidez, W.K.; Werho, D.B., *Preconcentration of Certain Anions Using Reagents Immobilized via Silylation*, Analytical Chemistry 48 (1976) p. 67.

[122] Styles, P.M.; Chanda, M.; Rempel, G.L., *Sorption of Arsenic Anions onto Poly(ethylene mercaptoacetimide)*, Reactive & Functional Polymers 31 (1996) p. 89.

[123] Malachowski, L.; Holcombe, J.A., *Immobilized Poly-l-histidine for Chelation of Metal Cations and Metal Oxyanions*, Analytica Chimica Acta 495 (2003) p. 151.

[124] Hikichi, K.; Tanaka, H.; Konno, A., *Nuclear Magnetic Resonance Study of Poly(gamma-glutamic acid)-Copper(II) and Manganese(II) Complexes*, Polymer Journal 22 (1990) p. 103.

[125] Iwaki, O.; Hikichi, K.; Kaneko, M.; Shimizu, S.; Maruyama, T., *An NMR Study of a Poly(glutamic acid) Metal Complex*, Polymer Journal 4 (1973) p. 623.

[126] Kurotu, T., *Polarographic Behavior of Cadmium(2+) and Zinc(2+)-PGA Complexes. Polarographic and Circular Dichroism Spectroscopic Studies on the Cd2+ and/or Zn2+-Poly(alpha-L-glutamic acid) Complex in Aqueous Solution*, Inorganica Chimica Acta 191 (1992) p. 141.

[127] Imai, N.; Marinsky, J.A., *Copper(II) Ion Binding in Poly(glutamic acid)*, Macromolecules 13 (1980) p. 275.

[128] Olander, D.S.; Holtzer, A., *The Stability of the Polyglutamic Acid alpha Helix*, Journal of the American Chemical Society 90 (1968) p. 4549.

[129] Paoletti, S.; Cesaro, A.; Arce Samper, C.; Benegas, J.C., *Conformational Transition of Poly(alpha-L-glutamic acid). A Polyelectrolytic Approach*, Biophysical Chemistry 34 (1989) p. 301.

[130] Doty, P.; Wada, A.; Yang, J.T.; Blout, E.R., *Polypeptides. VIII. Molecular Configurations of Poly-L-glutamic Acid in Water-Dioxane Solution*, Journal of Polymer Science, Part B: Polymer Physics 23 (1957) p. 851.

[131] Idelson, M.; Blout, E.R., *Polypeptides. XXI. High Molecular-Weight Poly(alpha,L-glutamic acid): Preparation and Optical Rotation Changes*, Journal of the American Chemical Society 80 (1958) p. 4631.

[132] Nagasawa, M.; Holtzer, A., *The Helix-Coil Transition in Solutions of Polyglutamic Acid*, Journal of the American Chemical Society 86 (1964) p. 538.

[133] Fasman, G.D.; Lindblow, C.; Bodenheimer, E., *Conformational Studies on Synthetic Poly-alpha-amino Acids. Factors Influencing the Stability of the Helical Conformation of Poly-L-glutamic Acid and Copolymers of L-glutamic Acid and L-leucine*, Biochemistry 3 (1964) p. 155.

[134] Snipp, R.L.; Miller, W.G.; Nylund, R.E., *The Charge-Induced Helix-Random Coil Transition in Aqueous Solution*, Journal of the American Chemical Society 87 (1965) p. 3547.

[135] McDiarmid, R.; Doty, P., *The Spectrophotometric Titration of Polyacrylic, Poly-L-aspartic, and Poly-L-glutamic Acids*, Journal of Physical Chemistry 70 (1966) p. 2620.

[136] Kidera, A.; Nakajima, A., *Thermodynamic Study on Charge-Induced Helix-Coil Transition of Ionizable Polypeptide. 2. Potentiometric Titration of Poly(L-glutamic acid) and Copolypeptides of L-glutamic Acid with L-alanine or L-valine*, Macromolecules 14 (1981) p. 640.

[137] Pefferkorn, E.; Schmitt, A.; Varoqui, R., *Helix-Coil Transition of Poly(alpha,L-glutamic acid) at an Interface: Correlation with Static and Dynamic Membrane Properties*, Biopolymers 21 (1982) p. 1451.

[138] Holtzer, A.; Hawkins, R.B., *The State of Aggregation of alpha-helical Poly(L-glutamic acid) in Aqueous Salt Solutions*, Journal of the American Chemical Society 118 (1996) p. 4220.

[139] Nitta, K.; Yoneyama, M.; Ohno, N., *Polymer Concentration Dependence of the Helix to Random Coil Transition of a Charged Polypeptide in Aqueous Salt Solution*, Biophysical Chemistry 3 (1975) p. 323.

[140] Morcellet, M.; Loucheux, C., *Time Dependent Phenomena During the Solvent Induced Coil to Helix Transition of Poly(alpha-L-glutamic acid) in Aqueous Mixed Solvents*, European Polymer Journal 14 (1978) p. 697.

[141] Daoust, H.; St-Cyr, D., *Effect of the Cation Size and of the Solvent Composition on the Conformation of Poly(L-glutamic acid) Alkaline Metal Salts*, Polymer Journal 14 (1982) p. 831.

[142] Satoh, M.; Komiyama, J.; Iijima, T., *Dependence on Ionic Strength of Charge-Induced Coil-Helix Transition of Sodium Poly(L-glutamate) in Aqueous Solution*, Biophysical Chemistry 14 (1981) p. 347.

[143] Nilsson, S.; Zhang, W., *Helix-Coil Transition of a Titrating Polyelectrolyte Analyzed within the Poisson-Boltzmann Cell Model: Effects of pH and Salt Concentration*, Macromolecules 23 (1990) p. 5234.

[144] Zhang, W.; Nilsson, S., *Helix-Coil Transition of a Titrating Polyelectrolyte Analyzed within the Poisson-Boltzmann Cell Model. Effects of pH and Counterion Valency*, Macromolecules 26 (1993) p. 2866.

[145] Jacobson, A.L., *Effect of a Helix-Coil Transformation on Magnesium Binding to alpha-poly-L-glutamic Acid*, Biopolymers 1 (1963) p. 269.

[146] Jacobson, A.L., *Specific Cationic Effects on the Conformation of alpha-poly-L-glutamic Acid*, Biopolymers 2 (1964) p. 207.

[147] Jacobson, A.L., *Salt Effects on the Conformation of alpha-poly-L-glutamic Acid*, Biopolymers 2 (1964) p. 237.

[148] Iizuka, E.; Yang, J.T., *Effect of Salts and Dioxane on the Coiled Conformation of Poly-L-glutamic Acid in Aqueous Solution*, Biochemistry 4 (1965) p. 1249.

[149] Kono, N.; Ikegami, A., *Potentiometric Titration of Poly(L-glutamic acid) in Aqueous Solutions and Binding of Bivalent Cations*, Biopolymers 4 (1966) p. 823.

[150] Yamaoka, K.; Masujima, T., *Equilibrium Dialysis Study of the Interaction Between Poly(alpha-L-glutamic acid) and Transition Metal Ions in the Helix-Coil Transition Region*, Polymer Journal (Tokyo, Japan) 11 (1979) p. 889.

[151] Yamaoka, K.; Masujima, T., *The Visible-UV Absorption and Circular Dichroism Studies of Poly(alpha-L-glutamic acid)-Copper(II) Complexes with Emphasis on the Extrinsic Cotton Effect*, Bulletin of the Chemical Society of Japan 52 (1979) p. 1286.

[152] Masujima, T., *Conformational Changes of the Poly(alpha-L-glutamic acid)-Copper(II) Macromolecular Complexes in the pH Range of 4-7. A Light Scattering Study with Emphasis on Aggregation and Helix-Coil Transitions*, Bulletin of the Chemical Society of Japan 56 (1983) p. 838.

[153] Maeda, H.; Hiramatsu, T.; Ikeda, S., *Effects of Bivalent Metal Cations on the Conformation and Aggregation of Poly(L-glutamic acid)*, Bulletin of the Chemical Society of Japan 59 (1986) p. 587.

[154] Huh, Y., II; Inamura, T.; Satoh, M.; Komiyama, J., *Counterion-Specific Helix Formation of Poly(L-glutamic acid) in a Crosslinked Membrane*, Polymer 33 (1992) p. 3262.

[155] Huh, Y.I.; Kotake, N.; Satoh, M.; Komiyama, J., *Counterion-Specific Swelling Behavior of Crosslinked Poly(L-glutamic acid) Membranes in Aqueous Alcohols*, Journal of Membrane Science 81 (1993) p. 253.

[156] Satoh, M.; Fujiwara, T.; Komiyama, J., *Helix Formation of Poly (L-glutamic acid) in the Presence of Alkaline Earth Metal Cations in Aqueous Alcohol Solutions*, Biophysical Chemistry 53 (1995) p. 207.

[157] Asano, A.; Sullivan, C.M.; Yanagisawa, A.; Kimoto, H.; Kurotsu, T., *Polarographic Study on Poly alpha-L-glutamic Acid-Cd2+,Co2+ Complexes in the Helix-Coil pH Region*, Analytical and Bioanalytical Chemistry 374 (2002) p. 1250.

[158] Saudek, V.; Stokrova, S.; Schmidt, P., *Conformational study of poly(alpha,beta-L-aspartic acid)*, Biopolymers 21 (1982) p. 2195.

[159] Saudek, V.; Stokrova, S.; Schmidt, P., *Conformational study of poly(.alpha.-L-aspartic acid)*, Biopolymers 21 (1982) p. 1011.

[160] Pivcova, H.; Saudek, V., *Carbon-13 NMR Relaxation Study of Poly(aspartic acid)*, Polymer 26 (1985) p. 667.

[161] Tanaka, S.; Nakajima, A., *Conformational Aspects of Polypeptides Containing Ionizable Side Chains*, Polymer Journal 1 (1970) p. 505.

[162] Fasman, G.D., *Poly-.alpha.-Amino Acids, Protein Models for Conformational Studies*; Biological Macromolecules Vol. 1, 1967, p. 764 pp.

[163] Martell, A.E.; Smith, R.M., eds., *Amino Acids*; Critical Stability Constants. Vol. Vol. 1 1974.

[164] Lumb, R.F.; Martell, A.E., *Metal-Chelating Tendencies of Glutamic and Aspartic Acids*, Journal of Physical Chemistry 57 (1953) p. 690.

[165] Jablonski, S.A.; Morrow, C.D., *Mutation of the Aspartic Acid Residues of the GDD Sequence Motif of Poliovirus RNA-Dependent RNA Polymerase Results in Enzymes with Altered Metal Ion Requirements for Activity*, Journal of Virology 69 (1995) p. 1532.

[166] Malachowski, L.; Holcombe, J.A., *A Comparison of Immobilized Poly-L-Aspartic Acid and Poly-L-Glutamic Acid for Chelation of Metal Cations*, Analytica Chimica Acta 517 (2004) p.187.

[167] Chang, S.H.; Gooding, K.M.; Regnier, F.E., *Use of Oxiranes in the Preparation of Bonded Phase Supports*, Journal of Chromatography 120 (1976) p. 321.

[168] Anspach, F.B., *Silica-Based Metal Chelate Affinity Sorbents. II. Adsorption and Elution Behavior of Proteins on Iminodiacetic Acid Affinity Sorbents Prepared via Different Immobilization Techniques*, Journal of Chromatography, A 676 (1994) p. 249.

[169] Anspach, F.B., *Silica-Based Metal Chelate Affinity Sorbents. I. Preparation and Characterization of Iminodiacetic Acid Affinity Sorbents Prepared via Different Immobilization Techniques*, Journal of Chromatography, A 672 (1994) p. 35.

[170] Bogart, G.R.; Leyden, D.E.; Wade, T.M.; Schafer, W.; Carr, P.W., *Spectroscopic Investigation of the Hydrolysis of g-glycidoxypropylsilane Bound to Silica Surfaces*, Journal of Chromatography 483 (1989) p. 209.

[171] Ernst-Cabrera, K.; Wilchek, M., *Coupling of Ligands to Primary Hydroxyl-Containing Silica for High-Performance Affinity Chromatography. Optimization of Conditions*, Journal of Chromatography 397 (1987) p. 187.

[172] Shogren-Knaak, M.A.; McDonnell, K.A.; Imperiali, B., *alpha-Chloroacetyl Capping of Peptides: An N-terminal Capping Strategy Suitable for Edman Sequencing*, Tetrahedron Letters 41 (2000) p. 827.

[173] Unger, K.K., *Porous Silica*; Journal of Chromatography Library 16 Elsevier Scientific Publishing Company: Amsterdam, 1979.

[174] Wilson, S.R.; Czarnik, A.W., eds., *Combinatorial Chemistry: Synthesis and Application*, Wiley: New York 1997.

[175] Mierus, S.; Fassina, G., eds., *Combinatorial Chemistry and Technology: Principles, Methods, and Applications*, Marcel Dekker: New York 1999.

[176] Gordon, E.M.; Kerwin, J.F., eds., *Combinatorial Chemistry and Molecular Diversity in Drug Discovery*, Wiley-Liss: New York 1998.

[177] Bannwarth, W.; Felder, E., eds., *Combinatorial Chemistry: A Practical Approach*; Methods and Principles in Medicinal Chemistry. Vol. 9, Wiley-VCH: Weinheim 2000.

[178] Terrett, N., *Combinatorial Chemistry*; Oxford Chemistry Masters 2 Oxford University Press: Oxford, 1998.

[179] Abelson, J.N., ed. *Combinatorial Chemistry*; Methods in Enzymology. Vol. 267, Academic Press: San Diego 1996.

[180] Miller, T.C.; Mann, G.; Havrilla, G.J.; Wells, C.A.; Warner, B.P.; Baker, R.T., *Micro-X-ray Fluorescence as a General High-Throughput Screening Method for Catalyst Discovery and Small Molecule Recognition*, Journal of Combinatorial Chemistry (2003) p.

[181] The University of Iowa, http://www.medicine.uiowa.edu/maf/services/proteinseq/htm, 2004.

[182] Ruzicka, J.; Hansen, E.H., *Flow Injection Analysis*; Chemical Analysis 62 John Wiley & Sons: New York, 1988.

[183] Fang, Z., *Flow Injection Separation and Preconcentration*; VCH: Weinheim, 1993.

[184] Fang, Z., *Flow Injection Atomic Absorption Spectometry*; John Wiley & Sons: Chichester, 1995.

[185] Sanz-Medel, A., ed. *Flow Analysis with Atomic Spectrometric Detectors*; Analytical Spectroscopy Library. Vol. 9, Elsevier: Amsterdam 1999.

[186] Valcarcel, M.; Castro, M.D.L.d., *Flow-Injection Analysis - Principles and Applications*; Ellis Horwood Series in Analytical Chemistry Ellis Horwood Limited: Chichester, 1987.

[187] Karlberg, B.; Pacey, G.E., *Flow Injection Analysis - A Practical Guide*; Techniques and Instrumentation in Analytical Chemistry 10 Elsevier: Amsterdam, 1989.

[188] Trojanowicz, M.; Editor, *Flow Injection Analysis: Instrumentation and Applications*, 1996.

[189] Burguera, J.L., ed. *Flow Injection Atomic Spectroscopy*; Practical Spectroscopy Series, ed. Edward G. Brame, J. Vol. 7, Marcel Dekker, Inc.: New York 1989.

[190] Homola, J.; Yee, S.S.; Gauglitz, G., *Surface Plasmon Resonance Sensors: Review*, Sensors and Actuators, B: Chemical B54 (1999) p. 3.

[191] Burstein, E.; Chen, W.P.; Chen, Y.J.; Hartstein, A., *Surface Polaritons. Propagating Electromagnetic Modes at Interfaces*, Journal of Vacuum Science and Technology 11 (1974) p. 1004.

[192] Biacore, http://info.bio.cmu.edu/Courses/03438/!PCB02/BIAcore-Discussion-3/TN_1.pdf.

[193] Jorgenson, R.C.; Jung, C.; Yee, S.S.; Burgess, L.W., *Multi-Wavelength Surface Plasmon Resonance as an Optical Ssensor for Characterizing the Complex Refractive Indices of Chemical Samples*, Sensors and Actuators, B: Chemical 14 (1993) p. 721.

[194] Liedberg, B.; Nylander, C.; Lundstroem, I., *Surface Plasmon Resonance for Gas Detection and Biosensing*, Sensors and Actuators 4 (1983) p. 299.

[195] Miwa, S.; Arakawa, T., *Selective Gas Detection by Means of Surface Plasmon Resonance Sensors*, Thin Solid Films 281-282 (1996) p. 466.

[196] Yang, X.L.; Dutta, P.; Wong, G.K.; Anderson, J.B., *Surface Plasmon Resonance as a Probe of the Complexing Process of Valinomycin Langmuir-Blodgett Films by Potassium Ions*, Thin Solid Films 219 (1992) p. 210.

[197] Ideta, K.; Arakawa, T., *Surface Plasmon Resonance Study for the Detection of Some Chemical Species*, Sensors and Actuators, B: Chemical 13 (1993) p. 384.

[198] Kooyman, R.P.H.; Kolkman, H.; Van Gent, J.; Greve, J., *Surface Plasmon Resonance Immunosensors: Sensitivity Considerations*, Analytica Chimica Acta 213 (1988) p. 35.

[199] Daniels, P.B.; Deacon, J.K.; Eddowes, M.J.; Pedley, D.G., *Surface Plasmon Resonance Applied to Immunosensing*, Sensors and Actuators 15 (1988) p. 11.

[200] Jonsson, U.; Fagerstam, L.; Ivarsson, B.; Johnsson, B.; Karlsson, R.; Lundh, K.; Lofas, S.; Persson, B.; Roos, H.; Ronnberg, I., *Real-Time Biospecific Interaction Analysis Using Surface Plasmon Resonance and a Sensor Chip Technology*, BioTechniques (1991) p. 620.

[201] Liedberg, B.; Nylander, C.; Lundstrom, I., *Biosensing With Surface Plasmon Resonance--How It All Started*, Biosensors & bioelectronics 10 (1995) p. i.

[202] Arizona State University, www.public.asu.edu/NTAO1/spr.HTM.

[203] Melendez, J.; Carr, R.; Bartholomew, D.U.; Kukanskis, K.; Elkind, J.; Yee, S.; Furlong, C.; Woodbury, R., *A Commercial Solution for Surface Plasmon Sensing*, Sensors and Actuators, B: Chemical B35 (1996) p. 212.

[204] Melendez, J.; Carr, R.; Bartholomew, D.; Taneja, H.; Yee, S.; Jung, C.; Furlong, C., *Development of a Surface Plasmon Resonance Sensor for Commercial Applications*, Sensors and Actuators, B: Chemical B39 (1997) p. 375.

[205] Texas Instruments, www.ti.com/sc/docs/products/msp/control/spreeta/refract.htm.

[206] Jonsson, U.; Malmqvist, M., *Real Time Biospecific Interaction Analysis*, in *Advances in Biosensors*. 1992, JAI Press: London. p. 291.

Vita

Lisa Lyn Malachowski, daughter of David and Sharon Malachowski was born in Buffalo, New York on February 17, 1974 and raised in Sardinia, New York. She attended Pioneer Central High School and graduated in 1992. Lisa earned a Bachelors of Science degree in Biochemistry from Roberts Wesleyan College (Rochester, New York) in 1996. While there she conducted a research project and internship at The Monroe County Forensic Science Laboratory. Upon graduation she enrolled at John Jay College of Criminal Justice (Manhattan, New York) and began work on a Masters of Science degree in Forensic Science. During this time she began an internship and eventual employment at The Westchester County Forensic Science Laboratory in both the DNA and Trace Evidence sections. She entered graduate school in analytical chemistry at The University of Texas at Austin in the fall of 2000. She joined the research lab of Dr. James A. Holcombe that fall.

Permanent Address: 12950 Deerfield Drive, Sardinia, NY 14134

This dissertation was typed by the author.